NBK 2000

presents

Excerps From

Fundamentals of Shape Charges

Compiled by Festergrump

14.7. SHAPED CHARGE JET COLLISIONS

Figure 82 depicts a shaped charge jet overtaking and colliding with the tail of another shaped charge jet.

Finally, in a classic experiment, Pernick (1965) [also Lukasik and Pernick (1965)] obtained a framing camera record for two shaped charge jets colliding head-on in air. The direction of jet motion was vertical, and a conventional argon bomb was used to provide back lighting for the camera. As shown in Figure 83 the approaching jets first appear from behind the expanding detonation products in the second frame. In Figure 83, the time increases from left to right and top to bottom with 1.4 μs per frame. The jet tips are highly luminous and cometlike in appearance. The highly luminous collision is first observed in the fourteenth frame. The collision region expands in time, and its extreme brightness persists for the duration of the film record. Growing dark areas appear in the last three frames and are probably due to expansion cooling and interaction with the encroaching detonation products (Pernick 1965).

Figure 84 is a streak camera record of a shaped charge jet collision in air. On the left side of the figure is an image of a marker scale located between the two shaped charges. This scale provides a calibration between spatial position at the explosive event and transverse distance on film. The time scale calibration follows from the streak camera rotational speed. The direction of increasing time is from left to right. The camera entrance slit is oriented in the

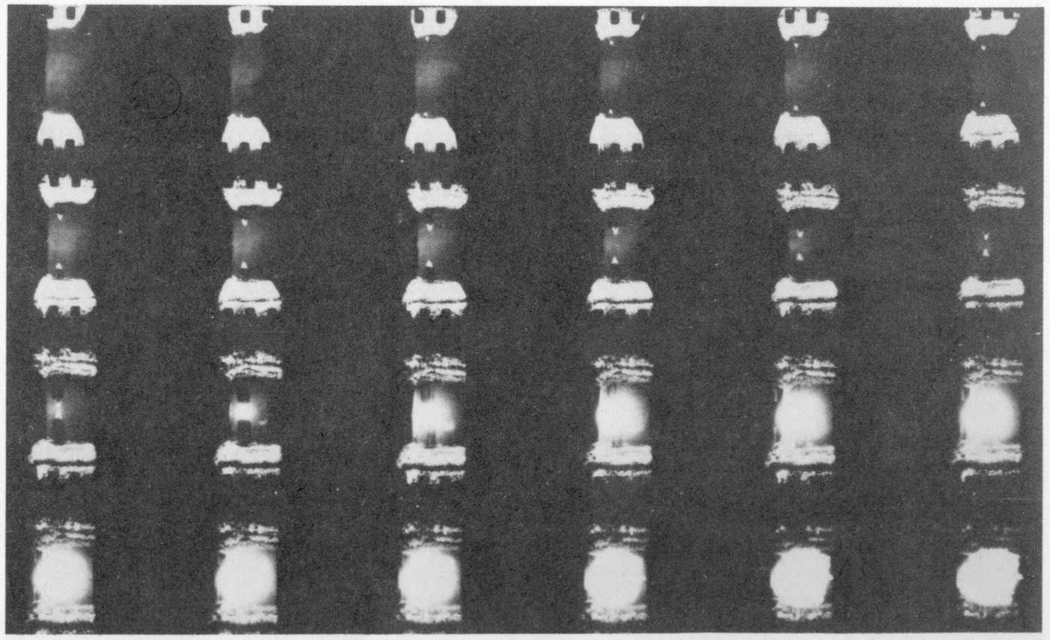

Figure 83. Framing camera record of jet collision in air (courtesy of B. J. Pernick 1965).

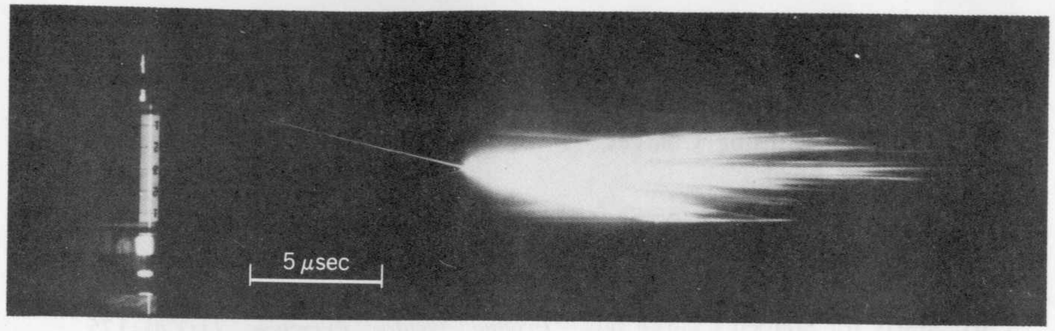

Figure 84. Streak camera record of two copper jets before and after collision in air (courtesy of B. J. Pernick 1965).

direction of jet motion. The two narrow light trails on the left side of the figure represent the approaching jets. The light comes from the luminous jet tips. Jet collision is characterized by the intersection of these trails and subsequent exposure that lasts for about 50 μs. A region of intense luminosity, centered about the impact point, remains roughly localized for the length of the camera record. Aside from the initial jet velocity data contained in a streak record, the extremely high light intensity of the collision products is apparent, even when viewed through a narrow streak camera entrance slit. Pernick (1965) provides additional data on head-on shaped charge jet collisions and the resulting plasma production.

REFERENCES

AMCP (1964), "Ammunition Series Section 2, Design for Terminal Effects," Army Materiel Command Pamphlet, AMCP 706-245, July.

Arvidsson, B., and Ohlsson, H. G. (1984), "Investigation of Liners For Shaped Charges Manufactured from Cu-Powder by X-ray Diffraction and Ultrasonic Techniques," *Proc. 8th Int. Symp. on Ballistics*, Orlando, Florida, 23–25 October.

Chanteret, P. Y., and Jamet, F. (1984), "Quasi Non-Stretching Hypervelocity Jets," *8th Int. Symp. on Ballistics*, Orlando, Florida, 23–25 October.

Chou, P. C., Ciccarelli, R. D., and Walters, W. P. (1983), "The Formation of Jets from Hemispherical-Liner Warheads," *Proc. 7th Int. Symp. on Ballistics*, The Hague, Netherlands, 19–21 April.

Chou, P. C., Walters, W. P., Ciccarelli, R. D., and Weaver, G. W. (1985), "Jet Formation Mechanics of Hemispherical Warheads," Ballistic Research Laboratory Contractor Report, ARBRL-CR-545, October.

Cook, M. A. (1958), *The Science of High Explosives*, New York: Reinhold Publishing.

Davison, D. K., and Arvidsson, B. K. (1985), "Optimization of a 90 mm Shaped Charge Warhead," *2nd Symp. on the Interaction of Non-Nuclear Munitions with Structures*, Panama City Beach, Florida.

Geiger, W., and Honcia, G. (1977), "Shaped Charges with Pyramidal Liners," *3rd Int. Symp. on Ballistics*, Karlsruhe, West Germany, 23–25 March.

b. Computational Results

Numerous results of simulations with TOODY have been published in journal articles and government reports. For a classic application see:

Bertholf, L. D. et al. (1975), "Damage in Steel Plates from Hypervelocity Impact: Part II—Numerical Results and Spall Measurement," *J. Appl. Phys.*, *46*(9):3776–3783.

ZEUS

____ (1987), "ZEUS Technical Description and User's Manual," Computational Mechanics Consultants, Inc.

CHAPTER 13

SHAPED CHARGE GENERALITIES

In this chapter, the various variables and parameters that govern the formation and performance of lined cavity charges are discussed. Simple analytical models and computer codes used in these studies are presented.

13.1. SHAPED CHARGE VARIABLES

The Liner

Probably, the most important shaped charge design element is the metallic (or nonmetallic) liner. The variables associated with the liner are the liner material and the liner geometry. The liner geometry can consist of a multitude of arcuate devices. The most popular are the cone, hemisphere, tulip, trumpet, the dual-angle cone (also called the biconic liner), Misznay–Schardin liners or ballistic discs or P charge liners (also known as self-forging fragments or explosively formed penetrators), tandem devices, and combinations of all these, such as a cone attached to the open apex of a hemisphere (i.e., a hemi-cone).

Once the geometric configuration is established, a pertinent variable is the liner diameter, where the term *liner diameter* refers to the outer diameter of the liner, in shaped charge notation. In general, the bigger the liner, the longer the jet and the greater the penetration capability, that is, the bigger, the better. (Recall the discussion on scaling.)

In general, liner diameters range from the 1 to 2 in. size used in research devices or bomblets up to 12 in. or so as used in torpedos. However, larger and smaller shaped charges have been employed for special applications. Smaller charges (1–2 in. or less) are difficult to fabricate to the required tolerances.

Large liners are also difficult to fabricate because of their size, and are also difficult to load. Loading is difficult due to the large height and diameter of the explosive fill, which may exceed the capabilities of the explosive pressing or casting facilities. In this case, loading is carried out in stages. In addition, for very large or very small liners, control of the metallurgical and mechanical properties of the liner material is difficult. Usually, army designers and their contractors deal with diameters ranging from about 2.5 in. (light antitank weapons) to 7 in. (heavy antitank weapons). Army rounds sometimes are required to be man portable. This requires the warhead weight (or diameter) to be as small as feasible.

The Liner Wall Thickness

Another critical liner design variable is the wall thickness. Typically, uniform wall thicknesses range from about 1 to 4 % of the charge diameter. However, liner wall thicknesses of up to 8% or so have been used. The charge diameter is the outer diameter of the explosive fill and is, of course, always greater than or equal to the liner diameter. The charge diameter will be discussed later in this chapter. The wall thickness chosen depends on the liner geometry, the liner material, and the required properties of the jet in reference to its intended application. Note that an optimum charge design, fabrication method, or geometry does not exist. The design is governed by the intended application and the imposed constraints. A unique solution or design for any particular problem seldom exists.

In addition, the wall thickness contour need not be uniform but may be tapered. A smooth taper, where the liner is thick at its pole or apex and thin at its equator or base, is simply called a taper. If the smooth taper results in a liner that is thin at its pole or apex and thick at its equator or base, the liner is said to have an inverse taper. The taper, in either direction, does not have to be smooth, but care should be taken to avoid sharp discontinuities or sharp thickness variations in the liner. Otherwise, the liner may particulate early according to the location of these discontinuities resulting in a poorly formed jet. The resulting jet then may not be an effective penetrator. The taper usually occurs on the inside (or air side) of the liner, away from the side of the liner in contact with the explosive, although this is not always the case. Basically, tapering the liner allows the designer to control the jet velocity gradient, jet length, and to an extent, the breakup time. In general, thin walled liners can be accelerated to higher velocities than thick walled liners. As examples, Aseltine et al. (1978) and Arbuckle et al. (1980) present studies of tapered hemispherical liners and Klamer (1964) discusses tapered conical liners.

The Liner Apex Angle

The other pertinent variable necessary to describe the liner is the liner apex angle (in the case of conical-like liners) or the altitude (or depth) for other

geometric shapes. For a cone, the smaller the apex angle, within reason, the faster the jet tip velocity and the lower the jet mass. Liners with a wide apex angle have a slower tip velocity and are more massive. Very wide apex angle cones begin to approximate hemispherical liners or arcuate devices such as explosively formed penetrators. A large depth or altitude of a nonconical liner implies more liner material available and a greater surface area in contact with the high explosive. This should result in a greater length of penetrator and hence a deeper penetration than a device with a shallower depth. Klamer (1964) discusses the effect of liner apex angle.

If one considers the various altitudes, diameters, wall thicknesses, and wall contour tapers that are possible for each of the arcuate geometries mentioned earlier, a multitude of geometric designs are possible. However, the various geometric designs have a different mode of collapse and jet formation, and this can greatly influence the resulting properties of the jet. See, for example, Kolsky et al. (1949), Evans (1950), Evans and Ubbelohde (1950a, 1950b), Kolsky (1949), Kiwan and Arbuckle (1977), and Pugh et al. (1946).

The conical shaped charge liners collapse, form, and breakup in the manner discussed in the earlier chapters. For narrow-angle (low apex angle) cones, the tip velocity and stretch rate are higher than for wide-angle cones. In fact, cylindrical liners, usually tapered to simulate a small apex angle cone, are capable of producing very fast jets. For example, George (1945), Kolsky et al. (1949), Evans (1950), and Evans and Ubbelohde (1950a, 1950b) describe the collapse of various shaped charge liners. Except for cylindrical charges, conical apex angles of 30° to 120°, depending on the liner material, are popular. Variations to the conical liner geometry, other than those already mentioned, include alteration of the conical apex region. The apex may be sharp, rounded, or blunt with a truncated cone. These variations affect the lead particle of the jet, the jet tip velocity, the jet tip mass, and the jet velocity gradient and mass distribution. Carleone et al. (1977) discuss jet formation and the origin of the jet tip for a conical shaped charge.

Nonconical Liners

The tulip and trumpet liners collapse similar to a conical liner, although the tulip liner, or elliptical liner, may behave like a hemispherical liner depending on its overall warhead configuration design. Also, trumpet liners typically have a high tip velocity and do not possess the inverse velocity gradient characteristic of conical liners. The hemispherical liners exhibit an entirely different mode of collapse than conical liners. The hemispherical liner is inverted from the pole or turned inside out. This results in a lower strain rate, less severe deformation process than the violent collision on the axis that conical liners undergo (Aseltine et al. 1978; Arbuckle et al. 1980; Kolsky 1949; Kiwan and Arbuckle 1977; Chou et al. 1981, 1983). Thus, the design of hemispherical and tulip-type liners must take into account the nature of the formation process (Aseltine et al. 1978; Arbuckle et al. 1980; Kolsky 1949; Kiwan and Arbuckle

1977; Chou et al. 1981, 1983, 1985, 1986; Perez et al. 1977). The collapse and formation of the jet from a hemispherical shaped charge liner was studied analytically by Chou et al. (1985). Walters and Golaski (1987) experimentally verified the jet collapse and formation mechanisms depicted by Chou et al. (1985).

For explosively formed penetrators (EFPs), self-forging fragments, P charges, dish-shaped devices, spherical caps, Misznay–Schardin devices, or the like, the collapse and formation depend to a large extent on the explosive geometry, the confinement geometry, and the metallic liner geometry. For example, under the proper conditions, one can form a projectile from a rearward-folding device (pole or apex of the liner emerges first) or a forward-folding device (tail or wings or base of the liner emerge first) or a W-fold device (where the liner forms into a W shape and collapses upon itself). Each of these devices may be generated by various tapers of the liner wall thickness and a confining body. A point focus device employs a uniform wall thickness liner and attempts to focus all liner material into a single point. The W-fold device and the point focus device are used to produce compact spheres or oblate spheroids. Forward- and rearward-folding devices are used to produce continuous rods or projectiles, which hopefully will stretch and elongate, but will not particulate, or if they do break, they will consist of only two or three segments. For the short EFP slugs, the initial stretching rate is much less than for a shaped charge. Thus, the effect of the free ends can propagate through the slug before actual breakup occurs. Therefore, the EFP breakup is more sensitive to small changes in material strength than the breakup of shaped charge jets. In addition to spheres and long rods, other shapes can be formed including hollow caps and rods with a flared, conical base to provide aerodynamic stability.

EFPs typically are low-velocity devices (as compared to shaped charges) and yield a tip velocity of 2–3 km/s. However, they generate large diameter, high mass projectiles and produce large holes in the target material. The penetration does not diminish rapidly over a long standoff (tens of meters) if the projectile is aerodynamically stable. Air drag and tumbling, if the projectile is unstable, are the main causes of degradation of penetration with standoff. At short standoff distances the performance is poor since the penetrator must have time, and hence distance, to form. Optimal penetration (at the appropriate standoff) is usually about one to two charge diameters into steel. Again, confinement effects and explosive geometry also influence the formation and performance. Increasing the L/CD of the EFP warhead increases the jet kinetic energy.

The collapse and formation of a typical EFP configuration is illustrated in the chapter on example applications. Carleone (1987) presents a detailed description of EFP charges.

Combinations of spherical caps or hemispherical liners and conical liners are possible. Such devices are constructed by removing the apex region of a hemispherical liner and covering the opening with a cone or another hemisphere, or using a conical liner with a hemispherical apex region as in Pugh et al. (1946). These devices can be contoured to form continuous jets or to form two distinct jets where one jet leads the other in space and time. Shaped charge devices of this type are useful in producing a "prejet," or precursor jet, to remove elements positioned between the warhead and the target, such as a seeker or guidance package on the missile carrying the shaped charge. (Recall the discussion by Kennedy on the origin of the trumpet liner given in Chapter 3.)

For combinations of charges such as conical–spherical, conical–conical, and so on, the two liners may be blended together to form a smooth transition between them or they may be joined by a sharp geometric discontinuity. If the charges are carefully blended together to form a continuous jet a new geometric configuration may result, for example, the trumpet liner. The old Carnegie group (Pugh et al. 1946) experimented with some of these geometric combinations.

If the apex region of a conical liner is removed and replaced by another conical liner, the resulting liner is called a dual-angle or biconic liner. Note that in the literature, devices of this type are sometimes called tandem liners.

However, in this text, a tandem liner is defined to be two distinct and separate liners that are not in contact. The intent of this device is to provide a one-two punch against the target, that is, one jet followed by another. The tandem liner concept, that is, a series of coaxial shaped charges, was first proposed by Tuck (1943).

Other shaped charge geometries consist of fluted conical liners, as discussed in Chapter 3. A fluted liner contains grooved pleats on the inside (air side) surface of the liner which extend from the apex to the base. The flutes cause the jet to rotate, the idea being to counterbalance the rotation of the warhead in flight. Warheads are often spun in flight to provide aerodynamic stability. If a jet forms while the warhead is spinning, the jet may disperse in a radial direction if the spin rate is high enough. A jet that is spinning as it forms (via flutes, as one example) can be designed to counterbalance the missile spin and avoid radial dispersion of the jet. Such liners are termed spin compensated. Other techniques for spin compensation involve the metallurgical control of the liner material. Thomas (1951) discussed fluted liners and Weickert (1986) used hydrocodes to analyze the effect of the flutes on the liner collapse.

Of course, many other liner shapes and contour variations are possible. Only some of the more popular liner shapes have been described here.

13.2. THE EXPLOSIVE FILL AND INITIATION MODE

The next design variable to be addressed is the explosive fill. Usually, more energetic explosive fills yield faster jets, a greater jet kinetic energy, and deeper penetration. Table 1 summarizes the effects of explosive detonation rate and

TABLE 1. Explosive Properties

	LX-14	PBXW-110	70/30 Octol	Comp B	Pentolite	Amatex 40	TNT
Density (g/cm^3)	1.835	1.75	1.80	1.72	1.67	1.63	1.61
Detonation rate (m/s)	8830	8480	8300	7900	7470	6900	6800
Detonation presure (kbars)	358	315	310	268	233	194	186

From Simon and DiPersio (1971).

detonation pressure. LX-14 is 95% HMX and PBXW-110 is 78% RDX. The Octol is 70/30 (70% HMX, 30% TNT), and Comp B is 60% RDX, 40% TNT. Pentolite is 50% PETN and 50% TNT, and Amatex 40 is 40% RDX, 40% TNT. The densities and detonation velocities are as given earlier in Chapter 4 on Gurney velocity approximations. The detonation pressures are approximated by

$$P\ (\text{kbars}) = 0.25\rho\ (\text{g/cm}^3)\ D^2\ (\text{m/s}) \times 10^{-5}.$$

The penetration and lethality effectiveness increase as the detonation rate and/or the detonation pressure increases. From Table 1, LX-14 would be the most effective, and TNT the least effective, explosive for shaped charge studies. The target hole volume increases with specific explosive energy in an approximately linear fashion. The explosives are ranked according to their penetration and lethality effectiveness. Thus, a high detonation velocity and high detonation pressure explosive is desirable although other factors, such as sensitivity, grain size, and homogeneity, must be considered. Additional data are provided by Simon (1983, 1974).

Charge Diameter

The diameter of the explosive charge, referred to as the charge diameter, or CD, not to be confused with the cone diameter as sometimes happens, is an important design variable. The ratio of the liner diameter to the charge diameter is termed the subcalibration ratio. The subcalibration ratio required depends on the liner and confinement geometry as well as the liner and confinement materials and the explosive used. It is generally agreed that explosive near the base of the liner is necessary to enable the wings or base of the liner to adequately collapse and participate in the penetration process. The control of the liner subcalibration ratio is critical in the formation of forward-folding or backward- (rearward-) folding self-forging fragment (SFF) or EFP liners. Additional subcalibration is used to form implosive hemispherical or

near-hemispherical devices [see, e.g., Kiwan and Arbuckle (1977) and Chou et al. (1981)]. The charge diameter (CD), or outer diameter of the explosive fill, is the reference unit for normalizing shaped charge performance. Thus, to allow comparison between rounds one usually plots penetration versus standoff distance both normalized by the CD.

Charge Length

The length of the explosive charge (L) is necessary to provide a sufficient amount of explosive energy for the liner collapse process. The height of explosive between the apex or pole of the liner and the booster is called the head height. The head height must be large enough to allow, as close as possible, a uniform (planar) detonation wave to reach the liner for a point-initiated charge. Too short a head height causes a highly spherical wave to impact the liner and the collapse may be nonuniform. Rarefaction effects are also more likely to be detrimental. Typically, the tip velocity, jet kinetic energy, and penetration of the jet (recall we are only addressing penetration into monolithic targets) increases as the head height increases, up to a point. A head height of about 1.5 CD provides a value beyond which very little improvement in penetration capability is achieved. Usually a 1 CD head height is ample and a head height of $\frac{5}{8}-\frac{3}{4}$ CD results in a very small penalty in penetration power for point-initiated conical or hemispherical lined charges. Klamer (1964) presents data on the effect of charge length and subcalibration. Some investigators use the charge length (the total height of the charge, L) as the pertinent parameter, that is, the charge length is sometimes confused with the head height in the literature. For point-initiated, conventional charges with a subcalibration ratio less than one, adequate L/CD values range from 1.3 to 1.8.

It is usually desirable to keep the head height or charge length to a minimum to reduce the length of the device and to save weight. Several methods are available to accomplish this. This simplest method is to remove unnecessary explosive by tapering the rear of the charge, that is boattailing. A boattailed charge is shown in Figure 1. Care must be exercised in choosing the break point (or point where the geometric discontinuity commences) to avoid the interference of rarefaction waves on the liner collapse. Usually, the break point occurs just aft of the liner apex or pole. The influence of the explosive fill geometry is further discussed by Kolsky et al. (1949), Evans (1950), Evans and Ubbelohde (1950b), Simon and DiPersio (1971), and Simon (1974, 1983). Typically, only about 10–20% of the total explosive chemical energy is translated into penetrator kinetic energy.

Another technique used to shorten the head height is waveshaping. Waveshaping involves inserting a device in the explosive charge, usually near the detonator or near the apex or pole of the liner, to contour, redirect, or shape the detonation wave to the required geometry in a short distance. Waveshapers are also used to alter the collapse of the liner by changing the angle of

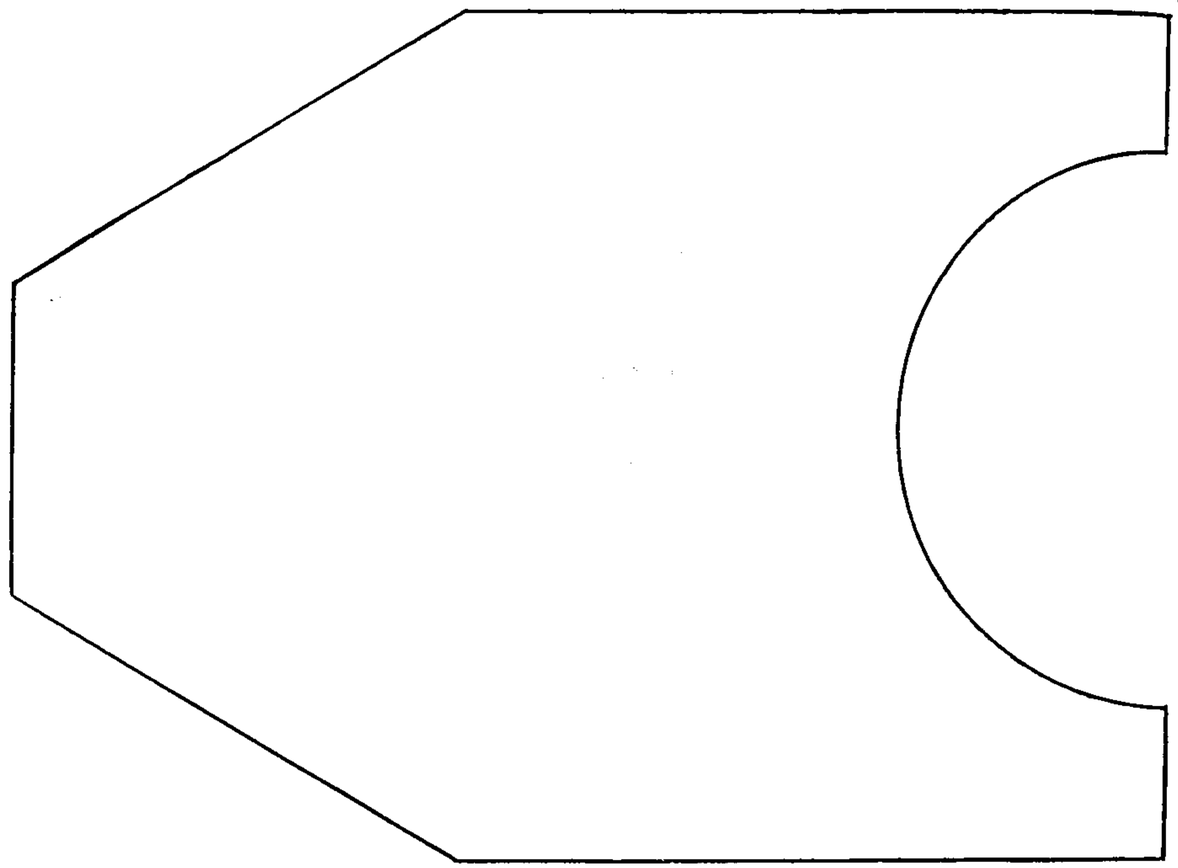

Figure 1. A Boattailed Charge.

incidence of the detonation wave, and thus even enhance performance from a short head height device. Successful waveshapers have been constructed from air, explosives, plastics, ceramics, metals, and even concrete. In addition to the waveshaper material, the other variables involved in waveshaper design are the location of the device in the explosive fill and its geometry and size. Jones (1985) discusses some of the analytical aspects of waveshaping, and Pezzica and Pazienza (1987) and Pezzica et al. (1987) performed computational studies of various waveshaper geometries.

For the explosive fill in general, both cast and pressed explosives are possible, and both are widely used (e.g., Octol and LX-14). In either case, care must be taken to guarantee a uniformity in the density and distribution of the particles (e.g., HMX crystals). Also, it may be necessary to control the grain size of the HMX or RDX particles in the explosive. For example, the median weight average diameter of the HMX grain in 75/25 Octol is about 500 μm and the median weight average diameter of the HMX grain in LX-14 is around 110 μm. A good, tight contact must also be obtained between the explosive and the liner or asymmetries may result.

Also, just as ways of tapering or contouring the metallic liner have been investigated, the explosive can be tapered or contoured, in conjunction with

the confinement body and the liner contour, to control the charge to mass ratio and enhance the collapse of the jet. This is done to optimize the velocity gradient to control jet length, breakup time, and penetration performance.

So far, a point initiation of a shaped charge device has been emphasized. A point initiation consists of a detonator–booster combination attached at a single point, on the centerline of a cylindrical or boattailed explosive charge. Other modes of initation are possible, usually designed to shorten the head height or to enhance the collapse and/or performance of the jet. These alternate methods include peripheral initiation or simultaneous initiation around the circumference of the charge, which is another way to reduce the head height, but can cause detonation wave interactions near the pole or apex of the liner. Peripheral initiation can also be achieved by a single point initiation and a waveshaper.

Various types of lens systems, for example, an air lens (using an air–HE system) or a binary lens (using two different types of HE in contact and of different detonation rates) are also used. These devices reduce the head height, may enhance the performance, and are used in implosion devices, which cause the liner (usually hemispherical) to focus at a given point or region before jetting. See, for example, Kiwan and Arbuckle (1977) and Chou et al. (1981). Also, multipoint initiation devices, which are designed to initiate the secondary explosive at several points simultaneously, and thus form the desired wave contour over a relatively short distance, are sometimes used. Simultaneous initiation over an explosive surface can also be achieved by propagating an explosively generated shock wave through a metal plate. Devices of these types are sometimes termed plane-wave lenses.

In addition, special effects can be achieved by offsetting the detonator–booster combination or by offsetting the liner. Either technique can cause the jet to form at some angle displaced from the centerline of the warhead. Evans and Ubbelohde (1950b) illustrate this case for an offset liner (a spherical cap) where the axis of the jet deviates from the axis of detonation. Other asymmetrical initiation studies were discussed by Trinks (1976), Thomanek (1976), and Walters (1986) for conical liners. Held has also experimented extensively in this field, as reported by Trinks (1976) and Held (1980). Walters (1986) also addressed the asymmetrical initiation of hemispherical shaped charges. Other methods of producing shaped charge jets where the jet particles are intentionally misaligned are discussed by Thomanek (1976), Held (1980), and Segletes (1985). Detonation waves, peripheral initiation, and detonator alignment effects are discussed by Eichelberger and Rostoker (1950). Also, Mayseless et al. (1987) discuss the effects of asymmetries on point initiated and peripherally initiated shaped charges.

The liner and explosive fill combination is also coupled to the confinement or body influence. The confinement, which is a metallic or fiber casing around the explosive charge diameter, is used to assist in loading the charge with a cast explosive; to provide a fragmenting, antipersonnel device based on the

fragmentation of the case; or to keep the detonation pressures high and thus alter or maintain the velocity gradient of the jet. A heavy confinement could allow use of a smaller amount of explosive by preventing the premature release of explosive energy. The outer diameter of the confinement body is called the warhead diameter. It may be thin and of a low-density material such as aluminum (perhaps designed to absorb the launch loads from a gun or missile) or thick and fabricated from a stronger material such as steel. For some applications, such as man-portable rounds, the heavy confinement is usually avoided to save weight. The influence of confinement is discussed, for example, by Klamer (1964), Evans (1950), Chou et al. (1983), and Brown et al. (1987).

The Body Confinement

As coupled with the explosive and liner contour, the material and the geometric shape of the confinement body is critical (e.g., Simon 1983). The body may be tapered to create a localized high-pressure effect, called tamping, or it may be uniform, to uniformly increase the detonation pressure, or tapered to regulate the velocities of the liner and the confinement. The confinement, including its material and geometry is quite influential in determining the method of formation of self-forging-fragments or EFPs, especially forward-folding and rearward-folding devices.

For shaped charge jets the confinement geometry is influential in controlling the jet velocity gradient, and for well-aligned and assembled charges, the performance increases at long standoff distances but is nearly the same as unconfined charges at short and moderate standoff distances. Confinement rings are sometimes required to prevent the detonation products from escaping from the base of the liner. These rings may be as heavy as the confinement thickness. There is an upper limit on the thick confinement of the liner since maintenance of pressure on the liner after collapse is unimportant. Thus, further increase in confinement thickness does not lead to a further increase in jet performance. For steel, a heavy confinement wall thickness of about $\frac{1}{10}$ CD is the maximum reasonable value (Evans 1950). Note that for a fixed warhead (missile) diameter there is a tradeoff between using a light confinement with a larger charge diameter (or liner diameter) and a smaller charge diameter with a heavy confinement. Usually, heavily confined charges are not weight efficient.

Other techniques are available to enhance or inhibit the collapse of shaped charge devices by either varying the explosive–confinement–liner interaction or by introducing additional devices. Localized confinement, that is, a single metallic band around the charge diameter of a warhead can locally enhance the collapse. Extraneous devices such as plastic, or metal, or even liquids positioned inside (on the air side of) the liner can inhibit the collapse process. Other methods of enhancing, disrupting, or inhibiting the collapse to produce specialized jets for specific purposes are possible. See, for example, Kolsky et al. (1949), Kolsky (1949), Merendino et al. (1963), and Held (1980).

13.3. JET CHARACTERISTICS

The liner material, as referred to early in this chapter, is of paramount importance. Favorable jet material properties will be discussed shortly. The material in the liner may even consist of two or more materials. Bimetallic conical and hemispherical liners have been fabricated and successfully tested (Kolsky et al. 1949). Conical liners consisting of a 1 cm LD and 0.37 mm copper and a 0.37 mm steel layer bonded together, with the copper in contact with the HE, were fired into polythene to recover some of the particles. The recovered particles revealed the following: all steel particles (apparently from the inside of the liner and near the tip); particles of steel on the outside and copper on the inside (apparently from midway along the cone slant height); and a slug that was copper on the outside with a steel core. When bimetallic liners of steel outside and copper inside were tested, corresponding results were obtained with the steel and copper roles reversed. See Kolsky et al. (1949) for details. Stratified, that is, layered bimetallic liners were analytically studied by Chou et al. (1985) and experimentally by Walters and Golaski (1987). These latter studies are discussed in the example applications chapter.

The liner material as well as its metallurgy is considered to be important. The characteristics of a good candidate material for a shaped charge liner are listed in Table 2. One requirement is a high melting temperature. Jets from low-boiling-point materials, for example, lead and cadmium, exhibit more marked fluid characteristics than higher-melting-point materials, for example, copper. Von Holle and Trimble (1976, 1977), as discussed earlier, measured the temperature of shaped charge jets. Walsh and Christian (1955) provided a method to determine the shock heating of materials due to explosive loading. Walters et al. (1984a, 1984b) used the EPIC code to calculate the temperature contours of a collapsing lead liner. They concluded that an optimum wall thickness exists for liners of a low melting point. Also, George (1945) performed metallurgical microscopic examinations of recovered slugs from conical liners to deduce the temperatures during deformation or collapse of the liner.

Other desirable characteristics of candidate materials for shaped charge liners include a high density to enhance penetration, a high bulk speed of

TABLE 2. Favorable Characteristics of Shaped Charge Jet Materials

1. High T_M (melt temperature)
2. High ρ (density)
3. High C_B (bulk speed of sound)
4. Fine grain, proper grain orientation, good elongation
5. Availability
6. Cheap
7. Easy to fabricate
8. Nontoxic
9. High dynamic strength

sound to guarantee jet cohesiveness, and a "dynamic" high-strength material. A dynamic high-strength material means a material that exhibits a high degree of strength under severe pressure and high strain rate conditions. Materials of this type do not necessarily correspond to materials of high static strength values. Additional material characteristics are fine-grain materials, with the proper grain orientation, that could result in a high-yield stress material with good elongation characteristics. Note that the yield stress (and strain rate) and material hardness are increased as the grain size decreases according to the Hall–Petch-type response, that is,

$$\sigma = \sigma_0 + KD^{-1/2} \quad \text{or} \quad H = H_0 + K'D^{-1/2},$$

where σ, σ_0 are residual yield stresses, H and H_0 are hardnesses, K, K', σ_0 and H_0 are constants, and D is average grain size or grain diameter. Thus, a fine grain material can produce a high residual stress, or a high hardness, or high strain, or strain rate material according to the Hall–Petch theory (Zerilli and Armstrong 1987).

In addition, the material should be readily available, inexpensive, nontoxic, and easy to fabricate. This requirement precludes elements such as platinum (expensive), osmium (not readily available), and so on.

The characteristics that depict a favorable shaped charge jet are ductility (a smooth, continuous, stretching jet), straightness (not misaligned in reference to the detonation axis), coherency (not overdriven), a favorable velocity gradient, a massive jet (the jet diameter influences the target hole diameter), a fast jet, and a continuous jet or a jet with a long breakup time. Also specialized jets may be required, for example, a spaced jet, or two distinct jets separated in space, a jet with a large tip particle, and so on. Thus, the various design parameters can be used to dramatically alter the properties of the penetrator. For this reason, one liner geometry or warhead configuration is not necessarily superior to any other. The proper design depends on the application and the design constraints.

The factors governing the performance of shaped charges may be summarized as follows: the explosive, the charge length, the charge confinement, the initiation mode, the liner and its shape, the standoff distance (distance between the base of the charge and the target), and any asymmetries present. The effects of air drag were noted earlier; recall DiPersio et al. (1965). The effects of fine grain shaped charge liner material are currently being reported in the open literature (e.g., Dante and Golaski 1985; Zerilli and Armstrong 1987).

Basically, the shaped charge jet performance into RHA targets can be gauged by the jet "factor of merit" (FM) where

$$\text{FM} = \frac{V_j \tau \sqrt{\rho_j}}{\text{CD}}$$

from DiPersio et al. (1967) where V_j is the jet tip velocity, τ is the jet average breakup time, ρ_j is the jet density, and CD is the charge diameter. Thus, for a given charge diameter, penetration is increased by increasing V_j, τ, and ρ_j.

The shaped charge jet parameters that completely describe the jet and hence can be used to model its penetration capability are given in Table 3.

The desired shaped charge jet parameters and the required favorable jet characteristics can be drastically altered by asymmetries. This has been discussed previously in this book; recall Evans (1950), Leidel (1978), Aseltine (1980), and Klamer (1964).

Granted that one is aware of the design variables at his disposal (e.g., liner geometry, explosive fill, etc.) and that one is aware of the jet parameters of importance (e.g., tip velocity, breakup time, jet diameter, etc.), it remains to relate the shaped charge design variables to the jet parameters. Then, the jet parameters can be used as input into one of the penetration models discussed in an earlier chapter to predict the penetration performance of a given shaped charge design. Thus, the problem involves three stages. One first studies the shaped charge liner collapse. Then one uses the results of the liner collapse analysis to study the jet formation. Finally, one uses the free flight or formed jet characteristics to predict penetration, hole growth, and other aspects of terminal ballistics. Hole growth and cratering is a vast field and beyond the basic scope of this book. However, a brief overview of this important area was given in the chapter on penetration.

The jet collapse and jet formation may be estimated by relatively simple analytical models such as those given earlier in the text. These models analyze the jet formation using a PER theory coupled with either a Defourneaux and Taylor angle theory or with a Gurney-type model and a Taylor angle theory.

TABLE 3. Shaped Charge Jet Parameters

1. V_{j_0} — Velocity gradient (jet tip velocity)
2. V_R — Velocity gradient (jet tail velocity)
3. τ or τ distribution (jet breakup time)
4. d_j (jet diameter)
5. l_j (jet length)
6. Lead particle characteristics
7. V.O. (for effective S.O., V.O. is virtual origin)
8. σ_j and constitutive characterization
9. ρ_j and EOS and compressibility effects
10. KE_j (jet kinetic energy)
11. M_j (jet momentum)
12. HE, detonation rate, etc...
13. Spin insensitivity
14. Penetration—three-dimensional effects
    Jet drift
    Sidewall collisions

(See the chapters on Gurney velocity and jet formation). The analytical codes are used for conical and near conical liner geometries and are not universally valid for highly nonconical liners such as hemispheres. Table 4 lists a few of these codes. Dullum and Haugstad (1986) investigated the liner collapse of five different shaped charges using both simple analytical models and more complex computer codes. Considerable discrepancies were found among the computed results. However, this type of comparison, although interesting, is to be expected since most computer codes or analytical models cannot be applied to problems they were not designed to solve or must be modified or adjusted to accommodate the problem at hand.

Other codes exist and are similar to those given in Table 4. These codes calculate the pertinent jet parameters listed earlier. The code output describes the jet geometry, the jet velocity distribution, and jet mass distribution. The jet formation and development may be described when the jet collapse results are used in conjunction with a jet breakup model such as given by Carleone and Chou, Hirsch, Pfeffer, and so on, as discussed in Chapter 8.

Analyses that address the formation mechanisms of shaped charge jets are given by Chou et al. (1985, 1986) and Perez et al. (1977). Chou et al. (1985, 1986) and Walters and Golaski (1987) also analyze the collapse and formation of hemispherical liners.

More sophisticated studies of the liner collapse, including nonconical liners, may be obtained from the hydrocodes. Eulerian,Lagrangian, and hybrid codes are useful for liner collapse studies. Zukas et al. (1982) discuss the hydrocodes in detail. The codes that are most popular in shaped charge studies include HELP, HULL, HEMP, and EPIC. In addition, a relatively new code called HOIL, which represents a marriage between HOIL (from the OIL family of codes) and HEMP, promises to be a valuable tool for the shaped charge

TABLE 4. Shaped Charge Computer Codes

Code Name	Source	Liner Collapse Model
BASC	Harrison (1981a, 1981b)	Modified Defourneaux, Steady Taylor
DESC-1, DESC-2	Carleone et al. (1975)	Modified Defourneaux, Steady Taylor
DESC-3	Flis (1984)	Gurney–Chanteret, Unsteady Taylor
TB/ISL (version TB/81)	Fauquignon (1981) and Pfeffer (1981)	Defourneaux or Hennequin–Pfeffer–Winawer, Steady Taylor
PISCES 2DELK	Behrmann (1973)	Two-D Eulerian Finite-Difference for Explosive, Mass-Points for Liner and Casing
TEMPS	Dyna East (1978)	Two-D Lagrangian Finite-Difference for Explosive, Mass-Points for Liner and Casing

From Chou and Flis (1986).

designer. HOIL was developed by Harrison of the BRL (1984). An earlier chapter discussed numerical calculations in detail.

Other methods of determining the collapse and formation of a shaped charge liner are experimental in nature. Shaped charge measurement techniques have been adequately covered elsewhere. Basically, the experimental methods consist of flash radiography, which provides an X-ray picture of the jet at predetermined times, and thus can be used to observe jet collapse, growth, and formation; camera coverage using framing cameras or streak cameras; and penetration (penetration–time) measurements, which are useful in themselves and can also be used to "back-calculate" the jet parameters. Held (1981a) gives an excellent overview of shaped charge measurement techniques. Other basic references on the pertinent experimental techniques are given by Zukas et al. (1982), Jamet and Thomer (1976), Johannson and Persson (1970), and Charbonnier (1981). Specific experimental references can be found in the *Flash Radiography Symposia* (e.g., Bryant 1976), the *Detonation Symposia*, and the sixteen volumes of the *Proceedings of the International Congress on High Speed Photography* (1954–1984). Experimental techniques pertinent to hypervelocity jets are given by Kronman and Groff (1973) and the studies by Held and associates (1970, 1976a, 1976b, 1981b, 1983, 1984a, 1984b, 1985a, 1985b, 1986a). The experimental techniques employed by Held and associates are summarized in Held (1986b), and Walters et al. (1987).

General references, useful for shaped charge device design, include Baum et al. (1949), the *Rheinmetall Handbook* (1973), the *Army Materiel Command Pamphlet* (1964) (for introductory material), and the *Manual for Shaped Charge Design* (Brimmer 1950). Carleone et al. (1978) explain a design procedure or synthesis method for the design of a fragmentation charge, an EFP, and a shaped charge. Four types of design tools are discussed, namely, simple design formulas, one-dimensional computer codes, two-dimensional computer codes, and experimentation. A design iteration for an EFP and a shaped charge warhead are illustrated. Held (1980), Leidel (1978), and Cox (1964) describe linear cutting charges.

Also, a multitude of shaped charge test parameters and test results were compiled by Arthur D. Little, Inc. (1959). This comprehensive data base includes a great deal of test results involving shaped charge parametric studies and penetration versus standoff distance studies.

REFERENCES

Arbuckle, A. L., Walters, W. P., and Aseltine, C. L. (1980), "Analysis of Uniform Wall and Tapered Hemispherical Liners with Several Explosive Confinement Geometries," ARBRL-TR-02222, March.

Arthur D. Little, Inc. (1959), "Collection and Arrangement of Shaped Charge Data, Third Interim and Final Report, Volume 1. Parameters, Volume II. Tables of Data, Parts 1, 2 and 3, Volume III. Glossary," Report C-59292, December 31.

Aseltine, C. L. (1980), "Analytical Predictions of the Effect of Warhead Asymmetries on Shaped-Charge Jets," Ballistic Research Laboratory Technical Report ARBRL-TR-02214, February.

Aseltine, C. L., Walters, W. P., Arbuckle, A. L., and Lacetera, J. E. (1978), "Hemispherical Shaped Charges Utilizing Tapered Liners," *Proc. 4th Int. Symp. on Ballistics*, Monterey, CA, October 17–19.

Baum, R. A., Stanykovich, R. P., and Skekter, B. I. (1949), *Physics of an Explosion*, New York: Research Information Service, 546. (AD 400151).

Behrmann, L. (1973), "Calculation of Shaped Charge Jets Using Engineering Approximations and Finite-Difference Computer Codes; Volume I, Generalized Analytical Approach to Shaped-Charge Warhead Design," Air Force Armament Laboratory Report AFATL-TR-73-160, August.

Brimmer, R. A. (1950), "Manual for Shaped-Charge Design," Navord Report 1248, NOTS 311, ADB954297, August.

Brown, J., Cullis, I. G., and Griffiths, N. (1987), "The Effects of Confining Studies on Shaped Charges," *Proc. 10th Int. Symp. on Ballistics*, Vol. 2, San Diego, October.

Bryant, L. E. (ed.) (1976), *Proceedings of the Flash Radiography Symposium*, (LC no. 77-5244, 1977) Houston.

Carleone, J. (1987), Section 3, "Mechanics of Shaped Charges," *Basic Principles of Hypervelocity Impact and Related Topics*, Course Notes, Computational Mechanics Associates, April, Baltimore, MD.

Carleone, J., Jameson, R., and Chou, P. C. (1977), "The Tip Origin of a Shaped Charge Jet," *Propell. Explos.*, *2*:126–130.

Carleone, J., Chou, P. C., and Simpson, R. (1978), "A Synthesis Method for Modern Warhead Design," *Proc. 4th International Symp. on Ballistics*, Monterey, October.

Carleone, J., Chou, P. C., and Tanzio, C. A. (1975), "User's Manual for DESC-2, A One-Dimensional Computer code to Model Shaped Charge Liner Collapse, Jet Formation, and Jet Properties," Dyna East Corporation Technical Report No. DE-TR-75-4, December.

Charbonnier, F. (1981), "Flash Radiography," in *Radiography and Radiation Testing*, Vol. 3, *Nondestructive Testing Handbook*, 2nd ed., L. E. Bryant and P. McIntire (eds.), Columbus, OH; ASNT.

Chou, P. C. and Flis, W. J. (1986), "Recent Developments in Shaped Charge Technology," *Propell., Explos. Pyrotech. 11*:99–114.

Chou, P. C., Ciccarelli, R. D., Arbuckle, A. L., and Walters, W. P. (1981), "Jet Formation of an Implosively Loaded Hemispherical Liner," Contract Report, ARBRL-CR-00470, September.

Chou, P. C., Ciccarelli, R. D., and Walters, W. P. (1983), "The Formation of Jets from Hemispherical Liner Warheads," *Proc. 7th Int. Symp. on Ballistics*, The Hague, Netherlands, April 19–21.

Chou, P. C., Flis, W. J., and Forsyth, C. M. (1986), "A Simplified Model of Jet Formation in Hemispherical Shaped Charges," *Proc. 9th Int. Symp. on Ballistics*, Shrivenham, UK, April–May.

Chou, P. C., Walters, W. P., Ciccarelli, R. D., and Weaver, G. W. (1985), "Jet Formation Mechanics of Hemispherical Warheads," BRL Contractor Report, BRL-CR-545, October.

Cox, C. M. (1964), "Memorandum Report on Linear and Conical Shaped Charge Performances," The Firestone Tire and Rubber Company, Defense Research Division, Report No. DRD-4, May.

Dante, J. G. and Golaski, S. K. (1985), "Micrograin and Amorphous Shaped-Charge Liners," *Proceedings of ADPA Bomb and Warhead Section*, White Oak, MD, May.

DiPersio, R., Jones, W., Merendino, A., and Simon, J. (1967), "Characteristics of Jets from Small Caliber Shaped Charges with Copper and Aluminum Liners," BRL Memorandum Report No. 1866, September.

DiPersio, R., Simon, J., and Merendino, A. (1965), "Penetration of Shaped Charge Jets into Metallic Targets," BRL Report No. 1296, September.

Dullum, O. and Haugstad, B. (1986), "A Comparative Investigation of Various Analytical and Numerical Shaped Charge Liner Collapse Models," *Proc. 9th Int. Symp. on Ballistics*, Shrivenham, UK, April–May.

Dyna East Corporation (1978), "A Two-Dimensional Explosive Mass-Point Computer Code (TEMPS)," Dyna East Corporation Technical Report DE-TR-78-3, June.

Eichelberger, R. J., and Rostoker, N. (1950), "Jet and Target Characteristics," with Introduction by E. M. Pugh, First Bimonthly Report, Fundamentals of Shaped Charges, CIT-ORD-28, August 31 (AD 499747).

Evans, W. M. (1950), "The Hollow Charge Effect," *Bulletin of the Institution of Mining and Metallurgy*, No. 520, March.

Evans, W. M., and Ubbelohde, A. R. (1950a), "Some Kinematic Properties of Munroe Jets," *Res. Supp.*, London, 3-8, May.

Evans, W. M., and Ubbelohde, A. R. (1950b), "Formation of Munroe Jets and Their Action on Massive Targets," *Res. Supp.*, London, 3-7.

Fauquignon, C. (1981), "Modelling Techniques for Shaped-Charges in France and French-German Institute of Saint-Louis," *Proc. 7th Annual Technical Meeting on Physics of Explosives*, Livermore, CA, October 21–23.

Flis, W. J. (1984), "User's Manual for DESC-3, A One-Dimensional Computer Code for Shaped Charge Analysis," Dyna East Report DE-TR-84-01, November.

George, H. P. (1945), "Mechanism of Collapse of Conical Hollow Charge Liners," Frankford Arsenal Report R-667, October.

Harrison, J. T. (1981a), "Improved Analytical Shaped-Charge Code: BASC," Ballistic Research Laboratory Technical Report No. ARBRL-TR-02300, March.

Harrison, J. T. (1981b), "BASC, an Analytical Code for Calculating Shaped Charge Properties," *Proc. 6th Int. Symp. on Ballistics*, Orlando, FL, October 27–29.

Harrison, J. T. (1984), "A Two Stage, Hydrodynamic, Numerical Technique, 'HOIL' and an Analysis of the Results of a Hemispherical, Shaped Charge Liner Collapse," *Proc. of 8th Int. Symp. on Ballistics*, Orlando, FL, October.

Held, M. (1970), "Orthogonal Multistreak Recording Technique," *Ninth Int. Congress on High Speed Photography*, Denver, pp. 126–129.

Held, M. (1976a), "The Performance of the Different Types of Conventional High Explosive Charges," *Second Int. Symposium on Ballistics*, Daytona, FL, March.

Held, M., Ludwig, D., and Nikowitsch, P. (1976b), "SST-Synchro-Streak-Technique," *Twelfth Int. Congress on High Speed Photography*, Toronto, pp. 234–237.

Held, M. (1980), "Cutting Charges," *5th Int. Symp. on Ballistics*, Toulouse, France, April.

Held, M. (1981a), "Shaped Charge Measurement Techniques—Overview," *Proc. 7th Annual Meeting on Physics of Explosives*, Livermore, CA, October.

Held, M. (1981b), "Evaluation of Shaped Charge Penetration Efficiency by Advanced Diagnostic Techniques," *Sixth Int. Sym. on Ballistics*, Orlando, FL, October.

Held, M. (1983), "Characterizing Shaped Charge Performance by Stand-Off Behavior," *Seventh Int. Sym. on Ballistics*, The Hague, 19–21 April.

Held, M. (1984a), "High-Speed Photography in Detonics," *Proc. of the 16th International Congress on High Speed Photography and Photonics*, SPIE, Strasbourg, France.

Held, M. and Nikowitsch, P. (1984b), "Comparative Investigation of Flash X-Ray Pictures and SST-Records for Diagnostic Evaluation of Shaped Charge Jets," *Sixteenth Int. Congress on High Speed Photography and Photonics*, Strasbourg, France, pp. 614–618.

Held, M. (1985a), "Flash X-Radiography in Ballistics," *Mat. Eval.*, *43*:1104–1123.

Held, M. (1985b), "Determination of the Material Quality of Copper Shaped Charge Liners," *Propell., Explos. Pyrotech. 10*:125–128.

Held, M. (1986a), "The Orthogonal Synchro-Streak-Technique as a Diagnostic Tool, Particularly for Shaped Charge Jets," *Propell., Explos., Pyrotech., 11*:170–175.

Held, M. (1986b), *Fundamental Aspects of Hypervelocity Impact and Shaped Charge Phenomena*, Vol. 3, Course Notes, Computational Mechanics Associates, Baltimore, MD, April.

Jamet, F., and Thomer, G. (1976), *Flash Radiography*, New York: Elsevier Scientific.

Johannson, C. H., and Persson, P. A. (1970), *Detonics of High Explosives*, London: Academic.

Jones, D. A. (1985), "Wave Shaping in the MRL 38 mm Shaped Charge," Department of Defense, Materials Research Laboratories, Melbourne, Victoria, Australia, Report MRL-R-980, December.

Kiwan, A. R., and Arbuckle, A. L. (1977), "Study of Liner Collapse, Jet Formation and Characteristics from Implosive Shaped Charge Systems," BRL-R-2028, November.

Klamer, O. A. (1964), "Shaped Charge Scaling," Ammunition Engineering Directorate, Picatinny Arsenal Technical Memorandum 1383, Dover, NJ, March.

Kolsky, H. (1949), "A Study of the Mechanism of Munroe Charges, Part II—Charges with Hemispherical Liners," *Res. Supp.*, London, 2-2:96–98.

Kolsky, H., Snow, C. I., and Shearman, A. C. (1949), "A Study of the Mechanism of Munroe Charges, Part I—Charges with Conical Liners," *Res. Supp.*, London, 2-2:89–95.

Kronman, S., and Groff, R. W. (1973), "A Stereo Segmental Flash Radiographic Technique," BRL-MR-2343, December.

Leidel, D. J. (1978), "A Design Study of An Annular-Jet Charge for Explosive Cutting," Ph.D. Dissertation, Drexel University, Philadelphia, PA, June.

Mayseless, M., Miller, S., Niv, E., and Peretz, D. (1987), "Experimental and Computational Analysis of the Effect of Asymmetries on Peripherally Initiated Shaped Charges," *Proc. 10th Int. Symp. on Ballistics*, Vol. 2, San Diego, October.

Merendino, A., Regan, J. M., and Kronman, S. (1963), "A Method of Obtaining a Massive Hypervelocity Pellet from a Shaped Charge Jet," BRL Memorandum Report No. 1508, August.

Perez, E., Fauquignon, C., and Chanteret, P. (1977), "Fundamental Studies of Shaped Charge Mechanisms," *Proc. 3rd Int. Symp. on Ballistics*, Karlsruhe, Germany, March.

Pezzica, G., and Pazienza, G. (1987), "Calculation of the Wave-Shaper Effects on Detonation Wave in Shaped Charges," *Propell., Explos., Pyrotech., 12*:125–129.

Pezzica, G., Pazienza, G., and Vignolo, G. M. (1987), "Numerical Modeling of Shaped Charges With Wave Shapers," *10th Int. Symp. on Ballistics*, San Diego, October.

Pfeffer, M. (1981), "Thompson-Brandt/Institute Saint Louis Computer Code Modelling of Shaped Charge Performance," *Proc. 7th Annual Technical Meeting on Physics of Explosives*, Livermore, CA, October 21–23.

Proceedings of the Int. Symposium on Detonation (*Vols. 1–8*), available from Naval Surface Weapons Center, Silver Spring, MD.

Proceedings of the Int. Congress on High Speed Photography: Vol. 1, Washington, 1952, published HSP, 5, SMPTE, NY, 1954; Vol. 2, Paris, 1954, published Dunod, Paris, 1956; Vol. 3, London, 1956, published Butterworth, London, 1957; Vol. 4, Koln, Germany 1958, published Verlag Helwich, Darmstadt, 1959; Vol. 5, Washington, 1960, published SMPTE, NY, 1962; Vol. 6, The Hague, Netherlands, 1962, published Tjeenk Willink & Zoon, Haarlan, 1963; Vol. 7, Zurich, 1965, published Verlag Helwich, Darmstadt, 1967; Vol. 8, Stockholm, published Almqvist & Wiksell, Stockholm, 1968; Vol. 9, Denver, 1970, published SMPTE, NY, 1971; Vol. 10, Nice, 1972, published ANRT, Paris, 1973; Vol 11, London, 1974, published Chapman & Hall, London, 1975; Vol. 12, Toronto, 1976, published SPIE, Washington, 1977; Vol. 13, Tokyo, 1978, published *J. Soc. Prec. Eng.*, Tokyo, Distribution, SPIE, US, 1979; Vol. 14, Moscow, 1980; Vol. 15, San Diego, 1982, published SPIE, Washington, 1983; Vol. 16, Strasbourg, France, 1984, published SPIE, 1984.

Pugh, E. M. et al. (1946), "Protection Against Shaped Charges," Final Report, Carnegie Institute of Technology, National Defense Research Committee, NRDC Report No. A-384 and Office of Scientific Research and Development, OSRD Report No. 6384, February.

Rheinmetall, (1973), *Rheinmetall Weapons Engineering Handbook*, Dusseldorf, FSTC-HT-23-0500-75.

Segletes, S. B. (1985), "Confinement Fabrication Technique for Asymmetrically Confined Shaped Charge Warheads," United States Patent 4,153,666, April.

Simon, J. (1983), "Shaped Charge Research Circa 1960–1980," presented at MBB, Schrobenhausen, W. Germany, September.

Simon, J. (1974), "The Effect of Explosive Detonation Characteristics on Shaped Charge Performance," *Proceedings of the Army Science Conference*, Vol. 3, pp. 99–112, West Point, NY, June.

Simon, J., and DiPersio, R. (1971), "The Evaluation of the Effect of Explosive Filler on Shaped Charge Performance and Lethality Effectiveness," BRL Report 1552, October.

Thomas, L. H. (1951), "A Zero Order Theory of the Initial Motion of Fluted Hollow Charge Liners," in "Transactions of Symposium on Shaped Charges," held at the Ballistic Research Laboratory, Aberdeen Proving Ground, MD, BRL Report No. 837, November (AD 1531).

Thomanek, F. R. (1976), "Unsymmetrically Affected Rotational Shaped Charges," *Proc. of the 2nd Int. Symp. on Ballistics*, Daytona Beach, FL, March.

Trinks, W. (1976), "Shaped Charges and Armor Protection: Their Alternate, Continuous Development," *Jahrbuch der Wehrtechnik*, 8, (translation FSTC 1375-75, AD B015556), May.

Tuck, J. L. (1943), "Note on the Theory of the Munroe Effect," UK Report, A.C. 3596 (Phys. Ex. 393-WA-638-32), March 27.

U.S. Army Materiel Command (1964), "Engineering Design Handbook, Ammunitions Series, Section 2, Design for Terminal Effects," Pamphlet No. ACMP 706-245, July (AD 389304).

von Holle, W. G., and Trimble, J. J. (1976), "Temperature Measurement of Shocked Copper Plates and Shaped Charge Jets by Two-Color IR Radiometry," *J. Appl. Phys.*, *47*(6).

von Holle, W. G., and Trimble, J. J. (1977), "Temperature Measurements of Copper and Eutectic Metal Shaped Charge Jets," BRL Report R 2004, August.

Walsh, J. M., and Christian, R. H. (1955), "Equation of State of Metals from Shock Wave Measurements," *Phys. Rev.*, *97*(6), March 15.

Walters, W. P. (1986), "Asymmetric Initiation of Shaped-Charges," *SECTAM XIII Proceedings, Southeastern Conference on Theoretical and Applied Mechanics*, Columbia, SC, April.

Walters, W. (1987), *Fundamental Aspects of Hypervelocity Impact and Shaped Charge Phenomena*, Course Notes, Computational Mechanics Associates, April, Baltimore, MD.

Walters, W. P., and Golaski, S. K. (1987), "Hemispherical and Conical Shaped Charge Liner Collapse and Jet Formation," BRL Technical Report, BRL-TR-2781, February.

Walters, W. P., Jonas, G. H., and Zukas, J. A. (1984a) "Explosive Loading of Lead," *Proc. of SECTAM XII, The Southeastern Conference on Theoretical and Applied Mechanics*, Pine Mountain, GA, May, Auburn, AL: Auburn University Press.

Walters, W. P., Jonas, G. H., and Zukas, J. A. (1984b), "Explosive Loading of Lead Hemispherical Liners," in *Advances and Trends in Structures and Dynamics*, A. K. Noor and R. J. Hayduk (eds.), New York: Pergamon Press.

Weickert, C. A. (1986), "Spinning Self-Forging Fragments and Shaped Charges," Ph.D. Dissertation, Drexel University, Philadelphia, PA, June.

Zerilli, F. J., and Armstrong, R. W. (1987), "Dislocation-Mechanics-Based Constitutive Relations for Material Dynamics Calculations," *J. Appl. Phys.*, *61*(5):1816–1825.

Zukas, J. A., Nicholas, T., Swift, H. F., Greszczuk, L. B., and Curran, D. R. (1982), *Impact Dynamics*, New York: Wiley.

CHAPTER 14

EXAMPLE APPLICATIONS

Shaped charges, as discussed in the earlier chapters, come in all shapes and sizes. That is, a multitude of charges have been designed for various applications over the years. A few of these are depicted in the following figures.

The reader is urged not to draw direct comparison between the flash radiographs of the various jets, except for those intended (and specified as such) for direct comparison. A direct comparison is prohibited by the different magnification factors resulting from diverse experimental setups as well as the various reductions in the photographic/printing process. The flash radiographs contained herein are intended only to illustrate various shaped charge jet characteristics and not detailed measurement of jet properties.

Note also that the reported flash times provide only a relative time measure between the various experiments since the start, or X-ray reference time, may vary from study to study. This time difference is usually of the order of a few microseconds.

The following pages present the "picture book" of shaped charge examples and applications.

14.1. CONICAL SHAPED CHARGE LINERS

Figure 1 depicts the most conventional shaped charge liner geometries, namely, the conical liner, the hemispherical liner, and the trumpet liner. In Figure 1*b* the simulated collapse of the hemispherical liner from the EPIC-2 hydrocode is also shown for times of 46 and 76 μs after detonation.

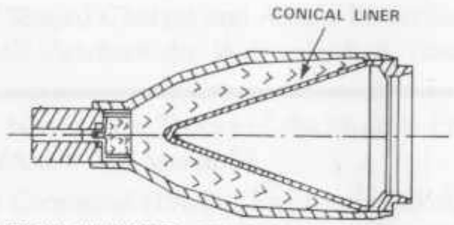

a) UNIFORM-THICKNESS, CONSTANT-ANGLE CONICAL LINER DESIGN

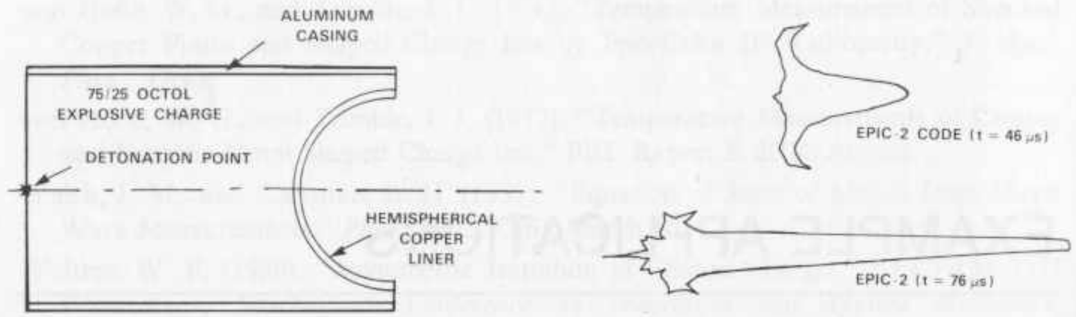

b) UNIFORM-THICKNESS, HEMISPHERICAL LINER DESIGN

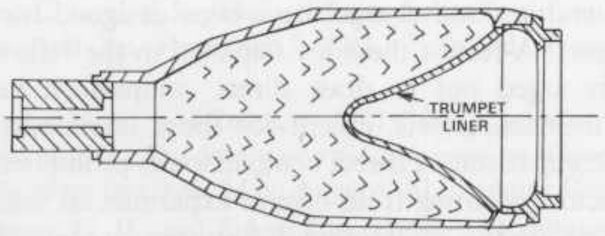

c) UNIFORM-THICKNESS, TRUMPET LINER DESIGN

Figure 1. Basic liner designs (a—Arvidsson and Ohlsson 1984, b—Chou et al. 1983, c—Davison and Arvidsson 1985).

Certain specialized liner designs are shown in Figure 2, and the references cited in this figure provide detail regarding the application of these specialized designs. Figure 3 shows another specialized application due to Geiger and Honcia (1977). In this design, the high explosive and liner are both planar symmetric.

Figure 4 illustrates the effect of flutes on a spinning shaped charge liner. A fluted liner spun at optimum frequency gives a jet with characteristics similar to the jet from a smooth (unfluted) liner fired in a static mode (Figure 4*b*). Figure 4*a* shows a distorted jet fired from a smooth liner when the charge was spinning. Fluted liners were discussed earlier, and Weickert (1986) provides additional details.

Figure 5 illustrates the collapse sequence of a conical shaped charge. Figures 6*a* and 6*b* further illustrate the collapse sequence of a conical liner.

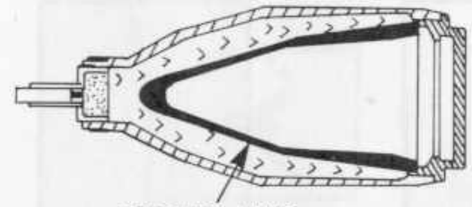

a) OPTIMIZED LINER DESIGN

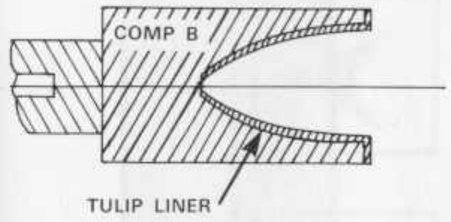

b) TULIP LINER DESIGN

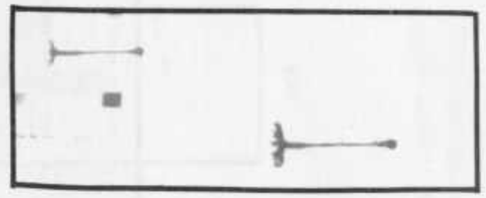

FLASH X-RAY OF TULIP LINER JET AT 40 AND 60 μs AFTER INITIATION

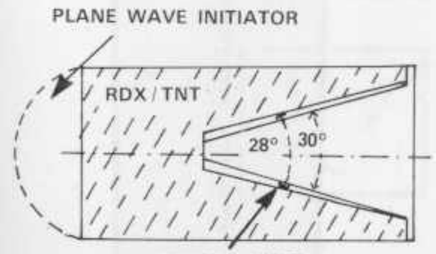

TAPERED CONICAL LINER

c) TAPERED CONICAL LINER DESIGN

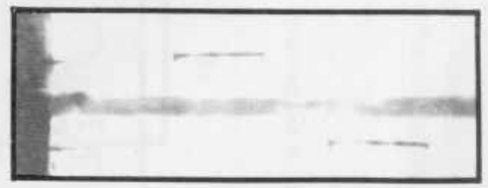

FLASH X-RAY OF TAPERED CONICAL LINER JET WITH RDX 40/TNT 60 AT 33 AND 43 μs AFTER INITIATION

Figure 2. Specialized liner designs (a—Davison and Arvidsson 1985, b and c—Chanteret and Jamet 1984).

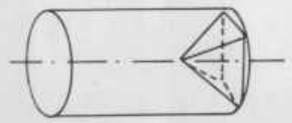

PYRAMIDAL LINER

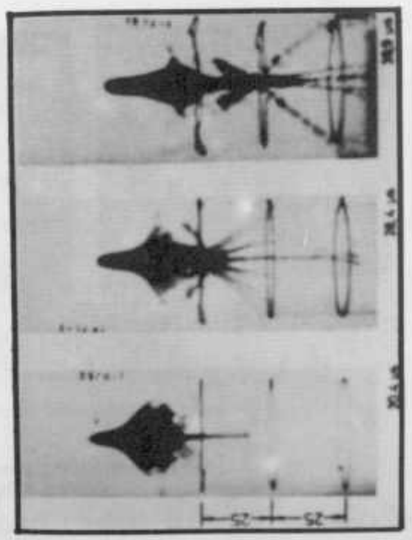

Figure 3. Planar symmetric liner design (Geiger and Honcia 1977).

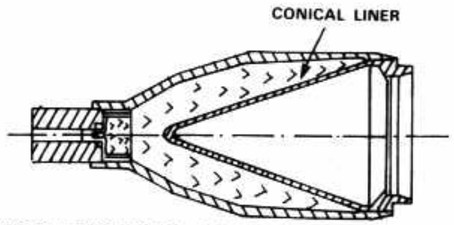

a) UNIFORM-THICKNESS, CONSTANT-ANGLE CONICAL LINER DESIGN

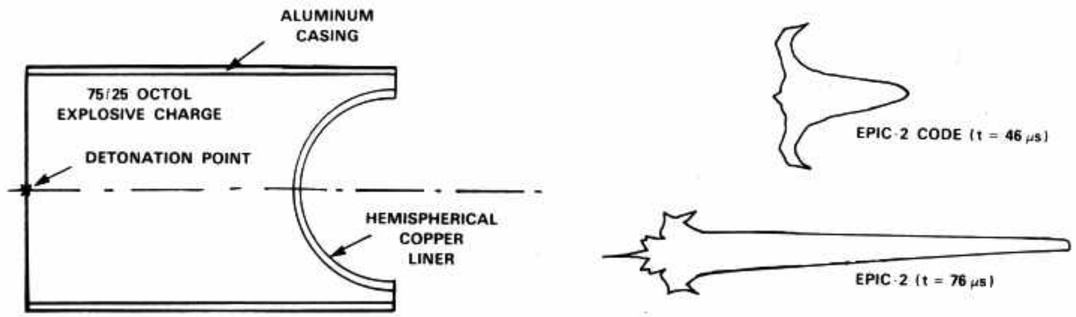

b) UNIFORM-THICKNESS, HEMISPHERICAL LINER DESIGN

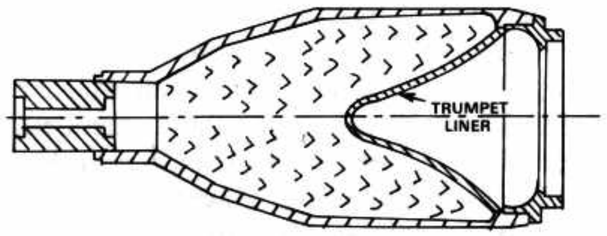

c) UNIFORM-THICKNESS, TRUMPET LINER DESIGN

Figure 1. Basic liner designs (a—Arvidsson and Ohlsson 1984, b—Chou et al. 1983, c—Davison and Arvidsson 1985).

Certain specialized liner designs are shown in Figure 2, and the references cited in this figure provide detail regarding the application of these specialized designs. Figure 3 shows another specialized application due to Geiger and Honcia (1977). In this design, the high explosive and liner are both planar symmetric.

Figure 4 illustrates the effect of flutes on a spinning shaped charge liner. A fluted liner spun at optimum frequency gives a jet with characteristics similar to the jet from a smooth (unfluted) liner fired in a static mode (Figure 4*b*).

a) OPTIMIZED LINER DESIGN

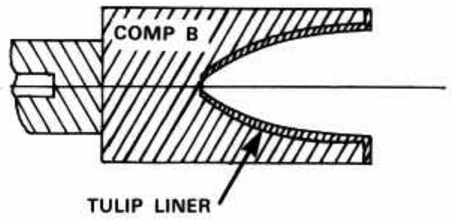

b) TULIP LINER DESIGN

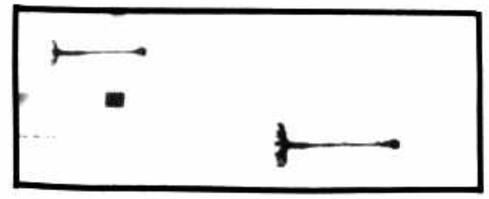

FLASH X-RAY OF TULIP LINER JET AT 40 AND 60 μs AFTER INITIATION

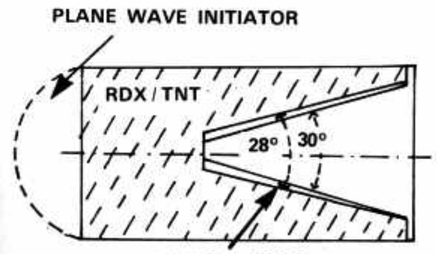

TAPERED CONICAL LINER

c) TAPERED CONICAL LINER DESIGN

FLASH X-RAY OF TAPERED CONICAL LINER JET WITH RDX 40/TNT 60 AT 33 AND 43 μs AFTER INITIATION

Figure 2. Specialized liner designs (a—Davison and Arvidsson 1985, b and c—Chanteret and Jamet 1984).

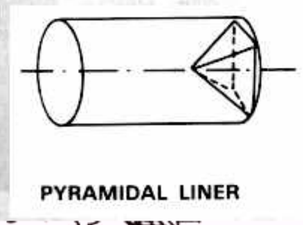

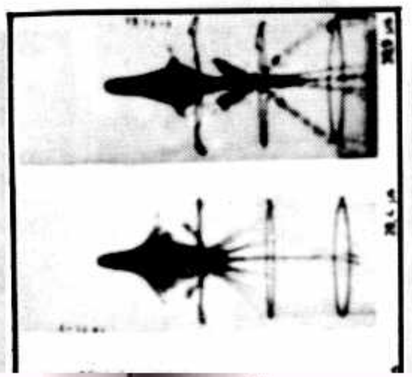

designs (a—Davison and Arvidsson 1985, b and
).

c) UNIFORM-THICKNESS, TRUMPET LINER DESIGN

Figure 1. Basic liner designs (a—Arvidsson and Ohlsson 1984, b—Chou et al. 1983,

Figure 2. Specialized liner
c—Chanteret and Jamet 1984

Figure 3. Planar symmetric liner design (Geiger and Honcia 1977).

Figure 5 illustrates the collapse sequence of a conical shaped charge. Figures 6*a* and 6*b* further illustrate the collapse sequence of a conical liner.

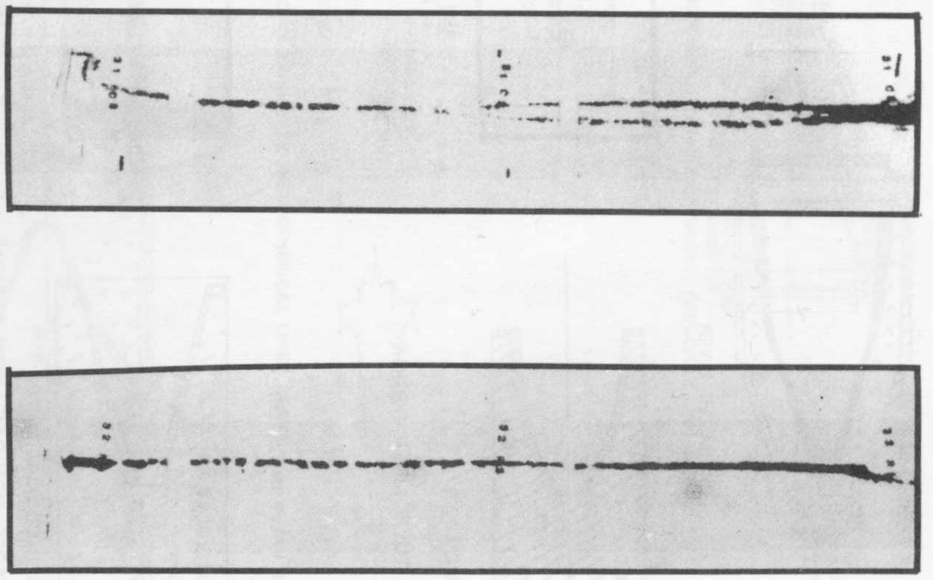

Figure 4. Jet radiographs showing the effect of flutes (AMCP 1964; Weickert 1986).

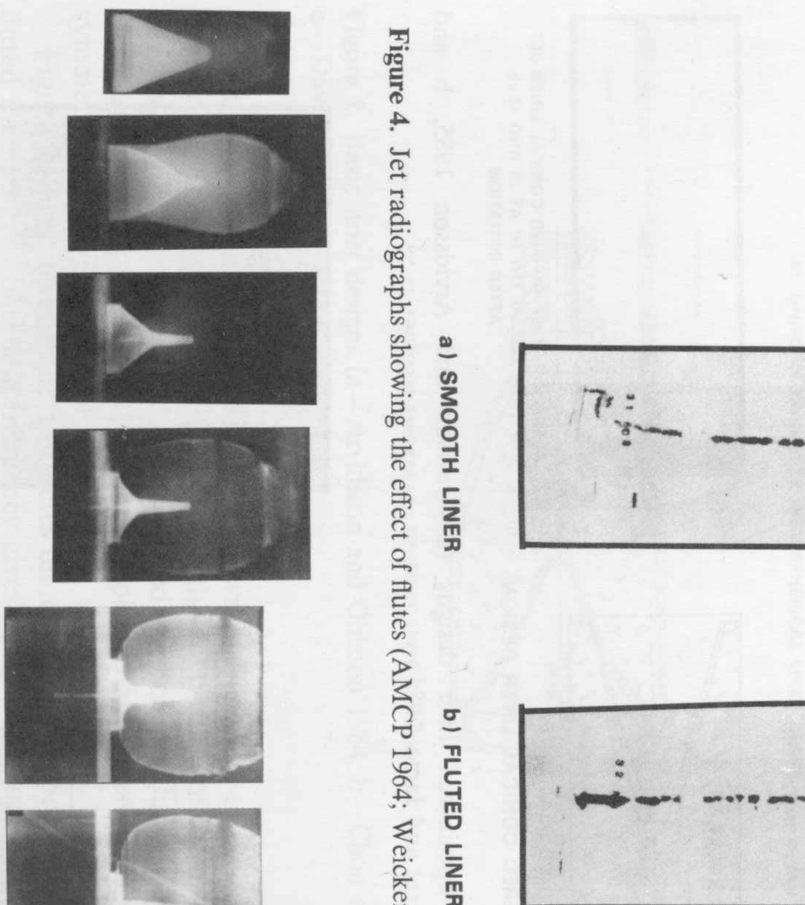

Figure 5. Collapse sequence (from left to right) of a conical shaped charge (courtesy BRL).

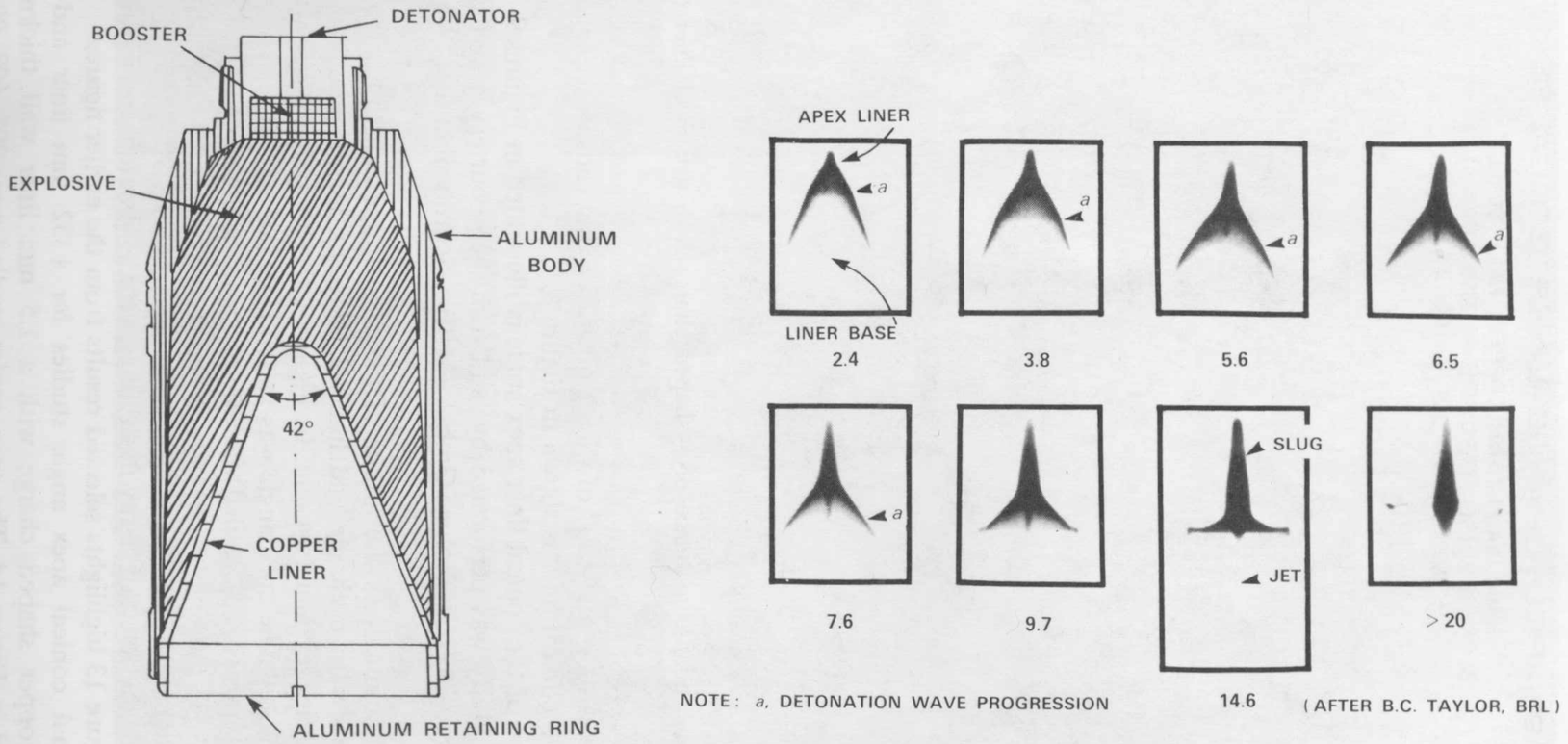

Figure 6. (a) Cross section of a conical shaped charge. **(b)** The sequential copper cone collapse at times indicated in microseconds. Time zero is when detonation wave reaches liner apex (Simon and DiPersio 1972).

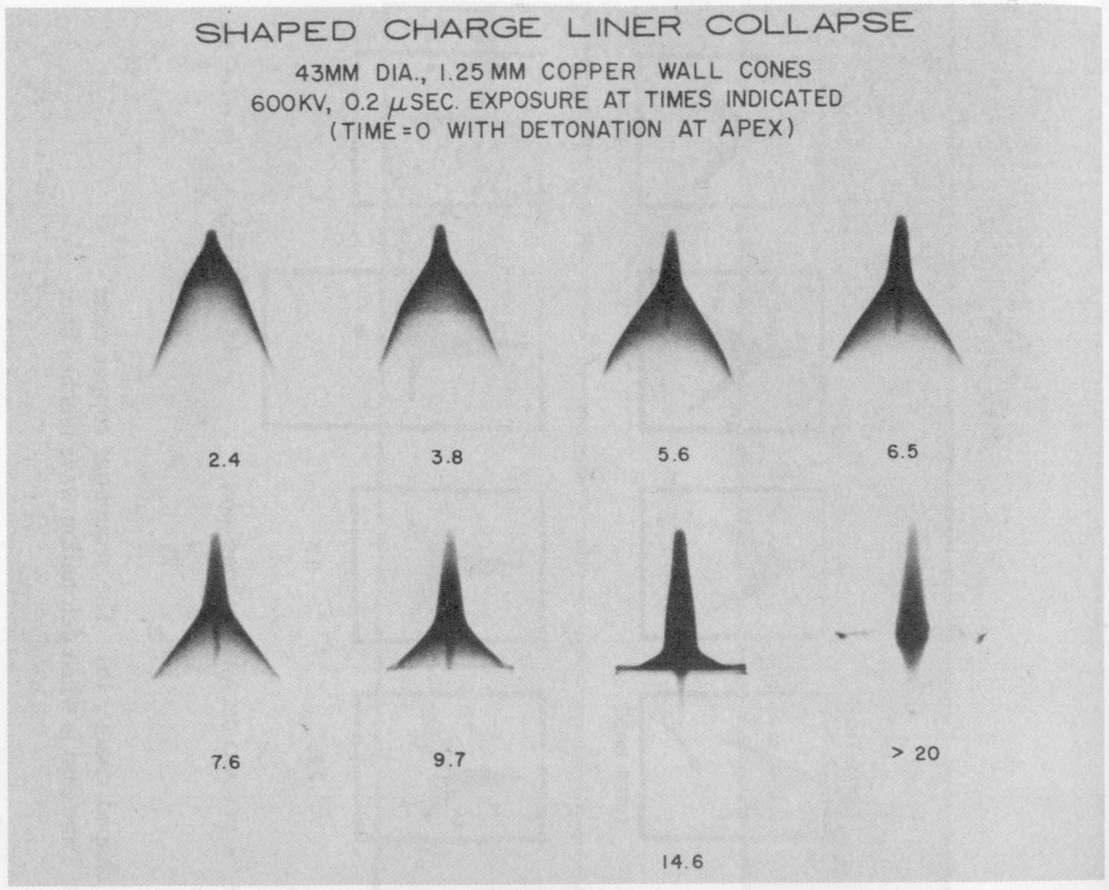

Figure 7. The collapse sequence of a shaped charge with a conical liner (courtesy BRL).

Figure 7 presents a "closeup" of Figure 6*b*. A framing camera sequence of the collapse of a conical liner is shown in Figure 8.

The effect of the conical liner apex angle is illustrated in Figures 9–16. The apex angle study was performed by, and furnished courtesy of, M. Held of Messerschmitt-Bolkow-Blohm Gmbh, (MBB), Schrobenhausen, West Germany.

Figure 9 summarizes the results of the conical apex angle (2α) study for copper liners with a charge and liner diameter of 58 mm and a liner wall thickness of approximately 4 mm. In Figure 9, the X-ray flash time was 35 μs after detonation. The apex angle was varied from 80° to 180°.

Figure 10 presents a detailed view of conical apex angles of 160°, 170°, and 180°. Figure 11 continues the series for apex angles of 130°, 140°, and 150°. Figure 12 completes the series for apex angles of 80°, 90°, 100°, 110°, and 120°. Again, the relevant X-ray flash times were 35 μs after detonation of the charge. Figure 13 highlights selected results from the earlier figures.

Additional conical apex angle studies for a 32 mm liner and charge diameter copper shaped charge with a 1.5 mm liner wall thickness are summarized in Figure 14. The apex angles studied were 30°, 60°, 90°, 120°,

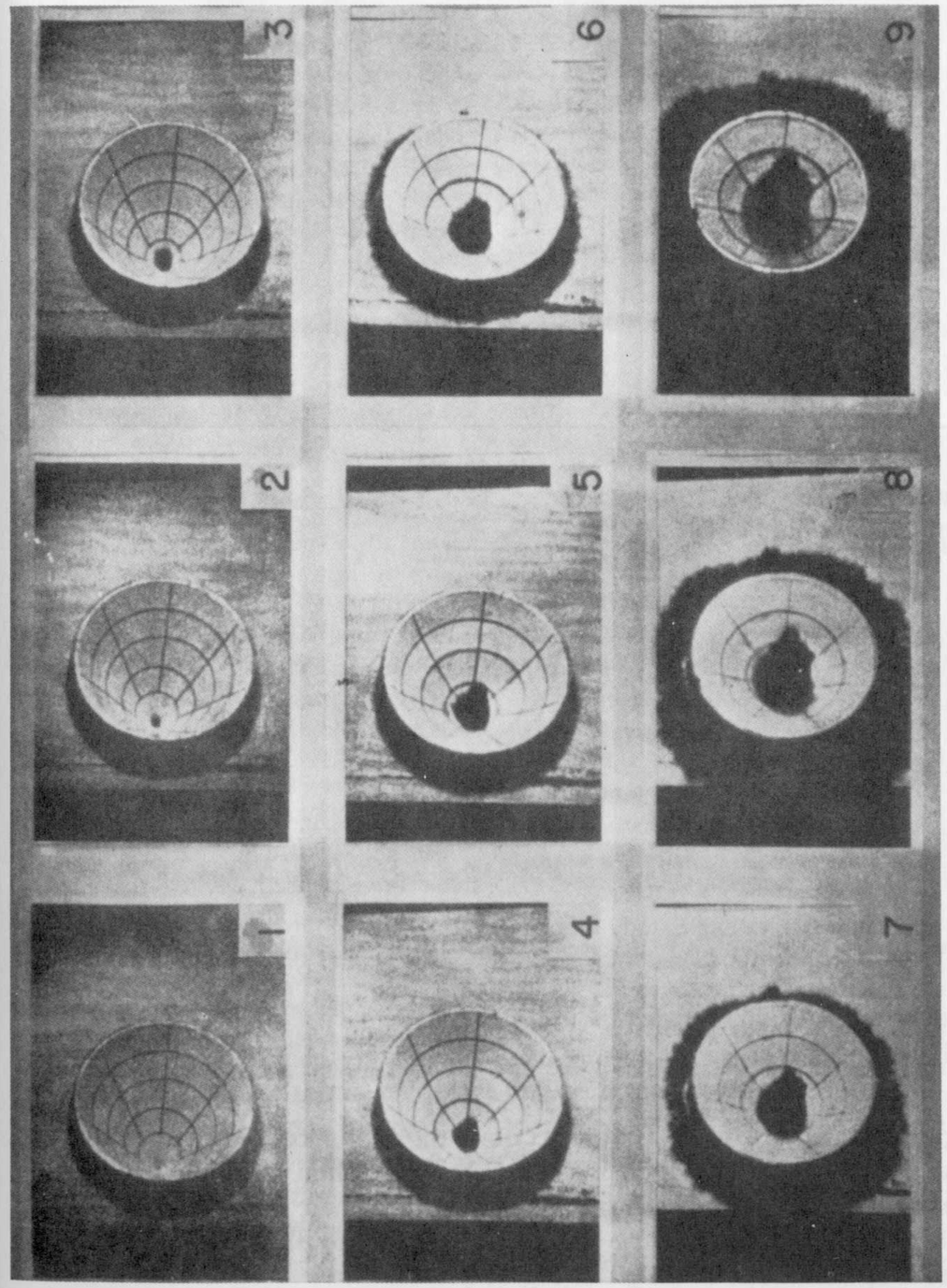

Figure 8. Selected frames of framing camera sequence of cone collapse in 60°, 10 cm aluminum cone (Cook 1958).

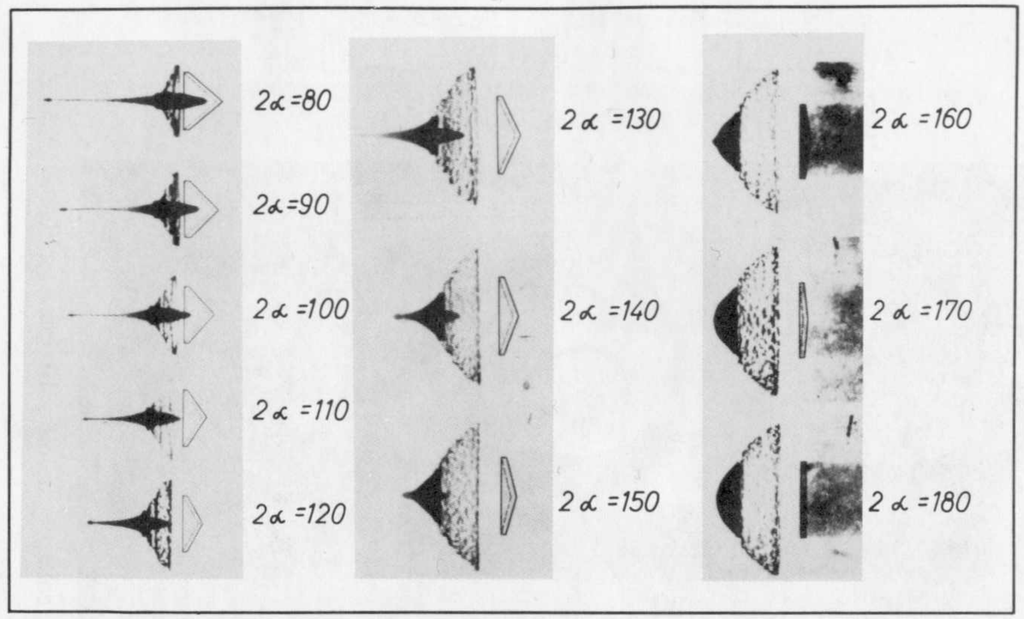

Figure 9. Conical apex angle study 35 μs after detonation (courtesy of M. Held, MBB, Schrobenhausen).

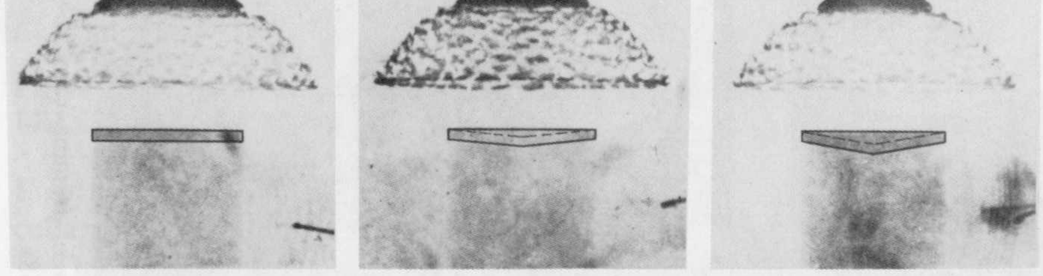

Figure 10. Conical apex angle study for apex angles of 180°, 170°, and 160° (courtesy of M. Held, MBB, Schrobenhausen).

150°, and 180°. The flash times were 15, 30, 45, and 60 μs, as noted in the figure. The jet tip velocity is denoted by V_s.

Figures 15 and 16 illustrate the jet formation of a copper conical lined shaped charge with a 32 mm charge diameter and 1.5 mm wall thickness. The conical apex angle was 60°. The indicated flash times are measured from the arrival of the detonation wave at the tip (apex) of the cone. Note the particulation (breakup) of the jet in Figure 16.

Figure 17 shows the jet from a conical shaped charge just prior to breakup. The necking of the jet is clearly visible.

Figure 18 is a special radiograph designed to show the tip region of the jet from a conical shaped charge. Figure 19 shows the jet formation from a

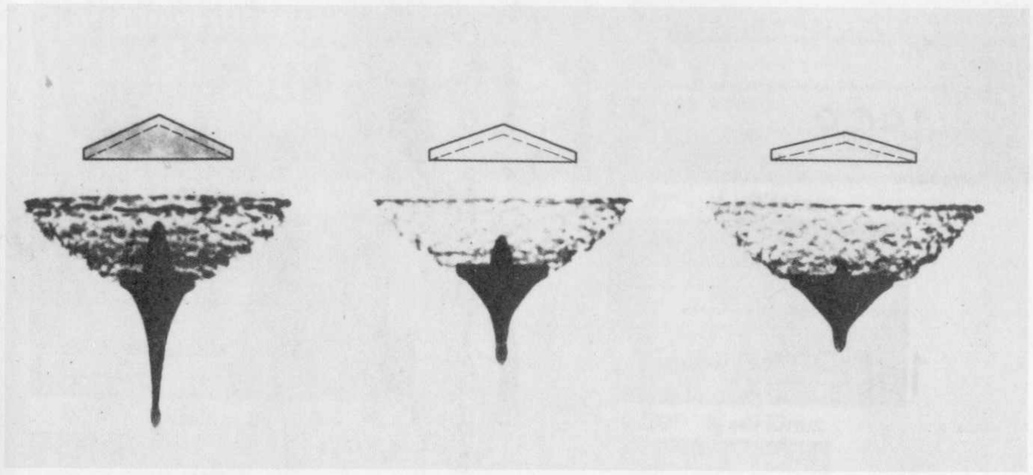

Figure 11. Conical apex angle study for apex angles of 130°, 140°, and 150° (courtesy of M. Held, MBB, Schrobenhausen).

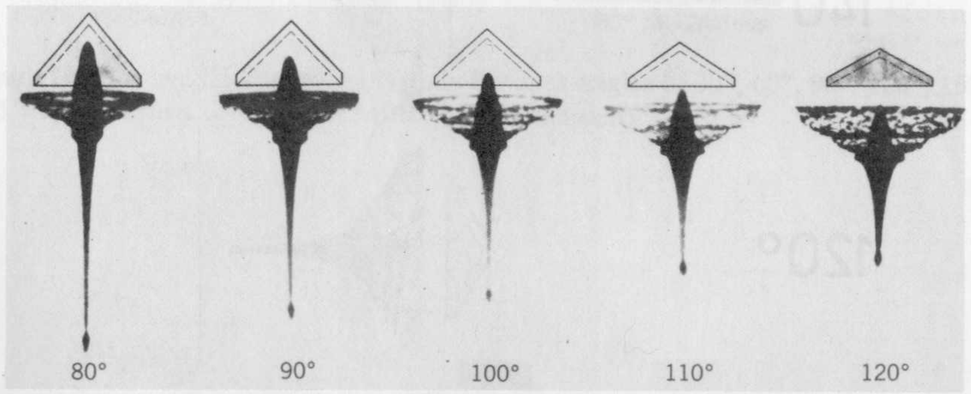

Figure 12. Conical apex angle study for apex angles of 80°, 90°, 100°, 110°, and 120° (courtesy of M. Held, MBB, Schrobenhausen).

heavily confined shaped charge. This radiograph shows the slug or the rear of the jet.

Figure 20 shows a copper jet from a 100 mm diameter shaped charge obtained by the Orthogonal-Synchro-Streak Technique (OSST) (Held 1986). The records on the top of the figure are the direct observations and the lower records were obtained by angle mirrors. The first upper strip shows a dark region in the upper left-hand corner that is artifically introduced by a small electric detonator fired at the edge of the field of view at a predetermined time after the detonation of the shaped charge. This yields an exact correlation between the shaped charge detonation time and the start of the recording. This is one way to allow accurate calculation of the jet tip and jet particle velocities. Held (1986) provides further details.

Note that in these optical records, the tip of the jet is engulfed in a cloud of vapor. This is probably due to ablation of the jet that travels about 9 km/s

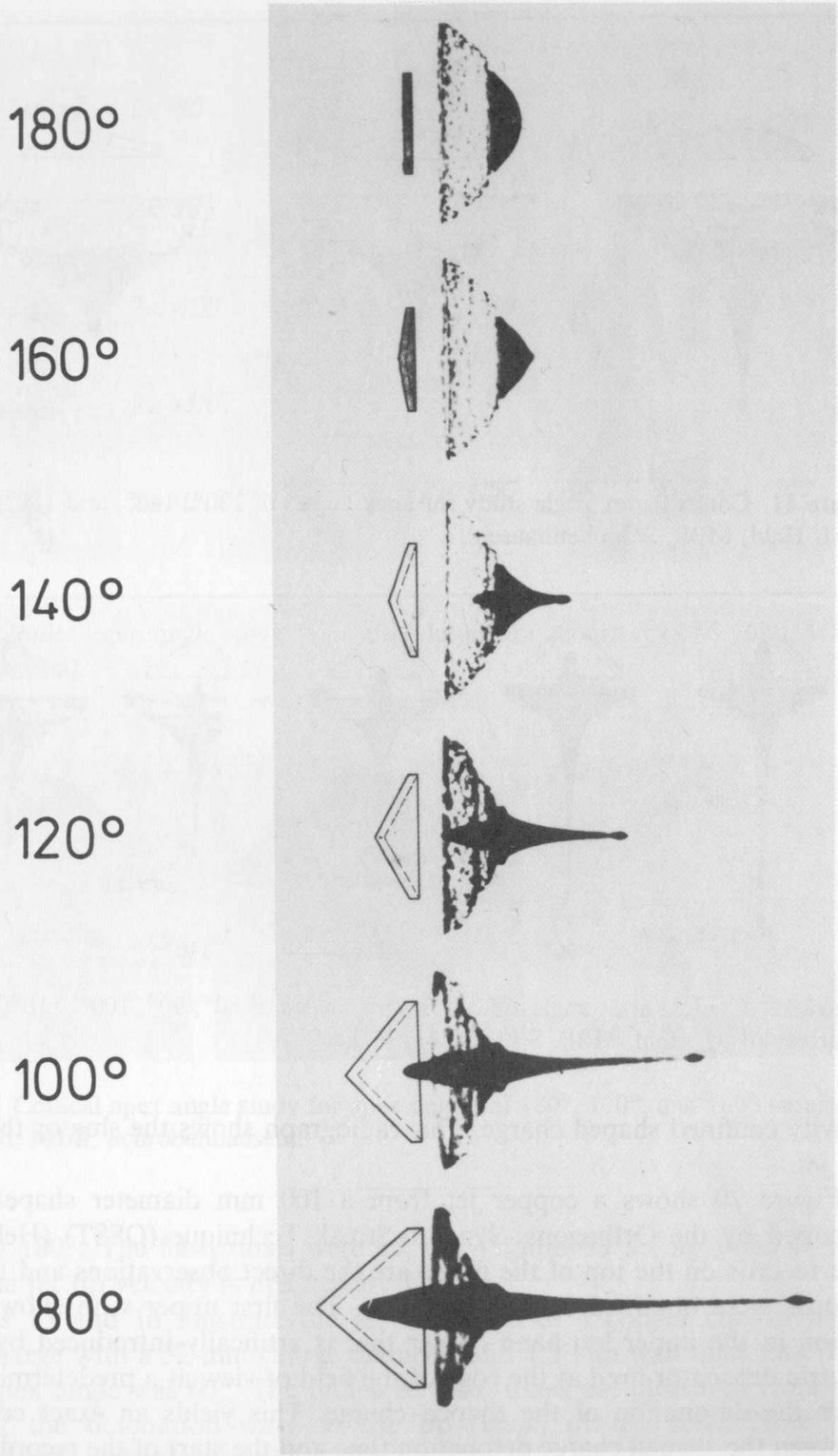

Figure 13. Conical apex angle series, selected results (courtesy of M. Held, MBB, Schrobenhausen).

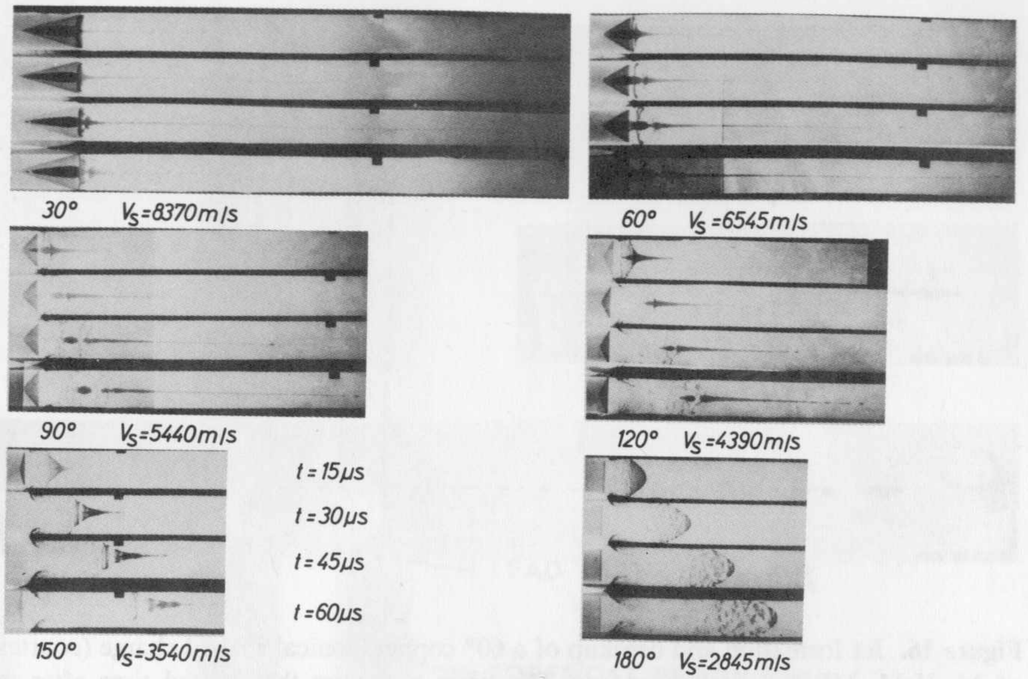

Figure 14. Conical liner apex angle study for apex angles of 30°, 60°, 90°, 120°, 150°, and 180° (courtesy of M. Held, MBB, Schrobenhausen).

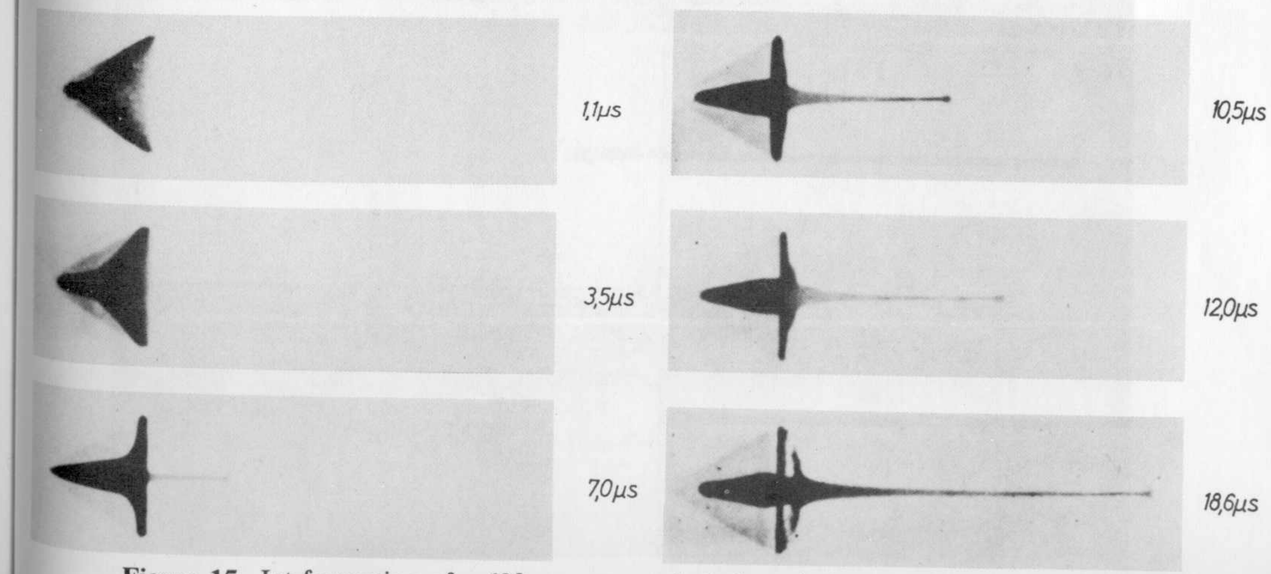

Figure 15. Jet formation of a 60° copper, conical shaped charge (courtesy of M. Held, MBB, Schrobenhausen). The times given are the elapsed time after the detonation wave reached the apex of the liner.

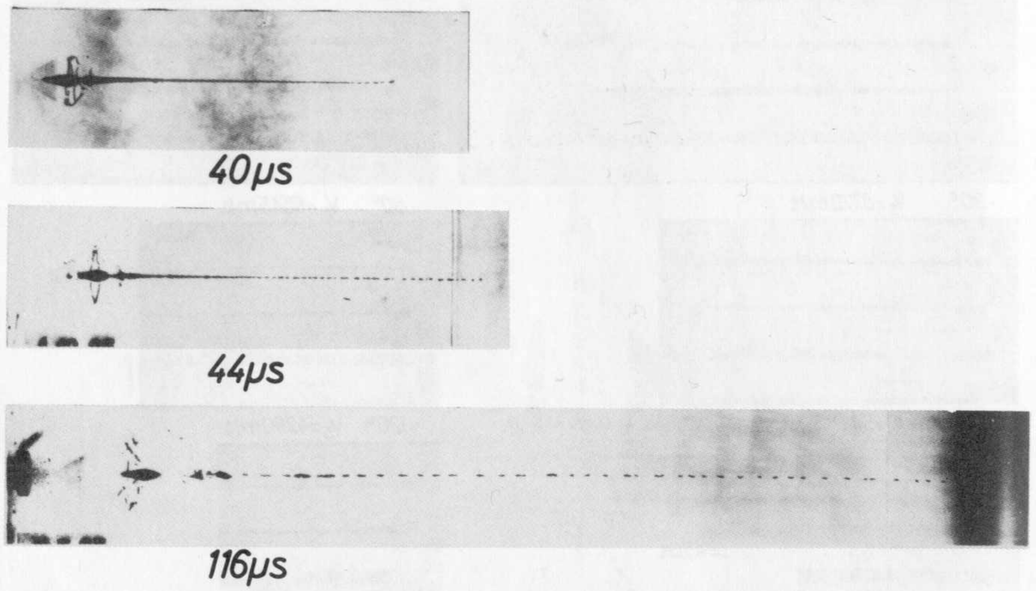

Figure 16. Jet formation and breakup of a 60° copper, conical shaped charge (courtesy of M. Held, MBB, Schrobenhausen). The times given are the elapsed time after the detonation wave reached the apex of the liner.

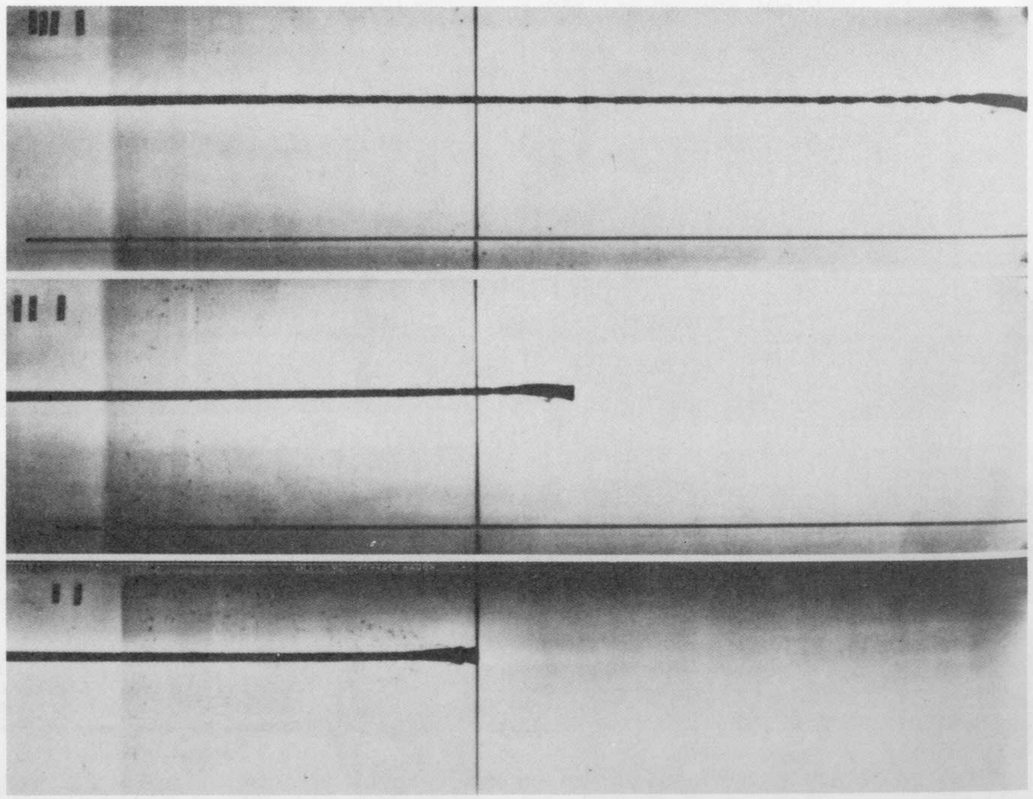

Figure 17. Jet from a conical shaped charge showing early necking just prior to the onset of jet breakup.

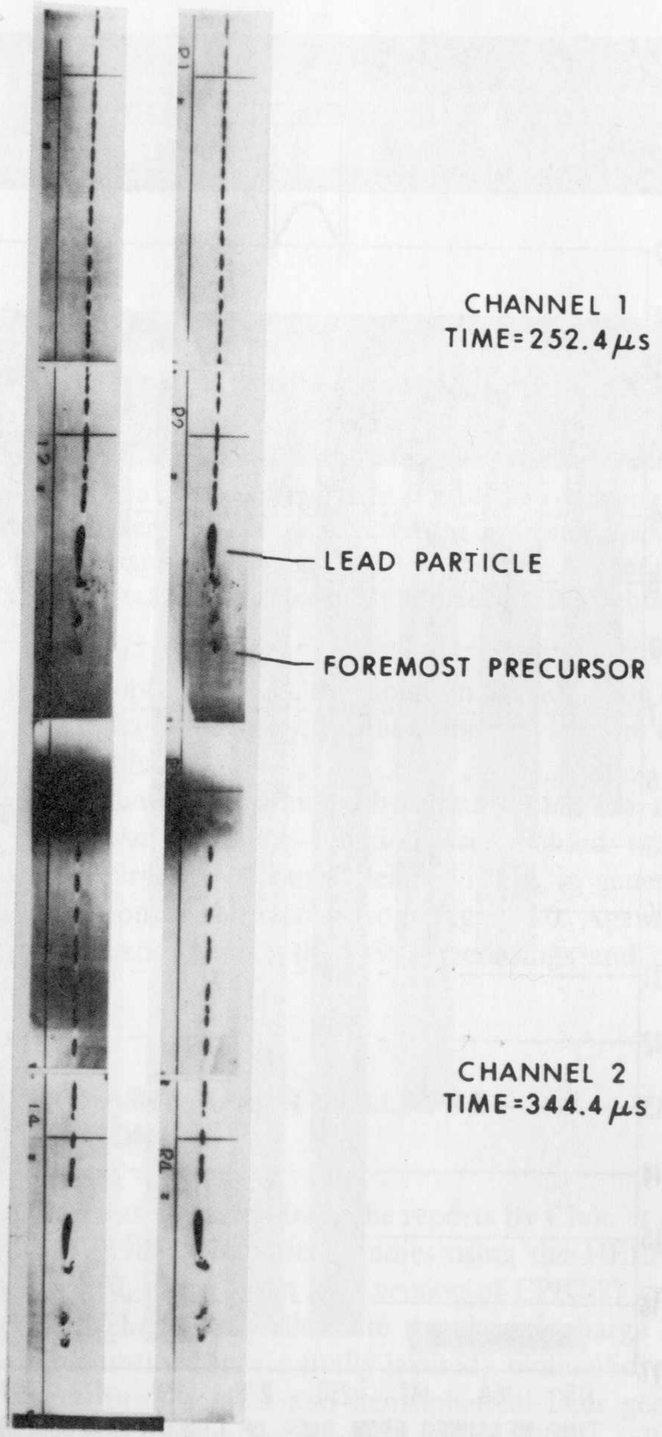

Figure 18. The tip region of a shaped charge jet.

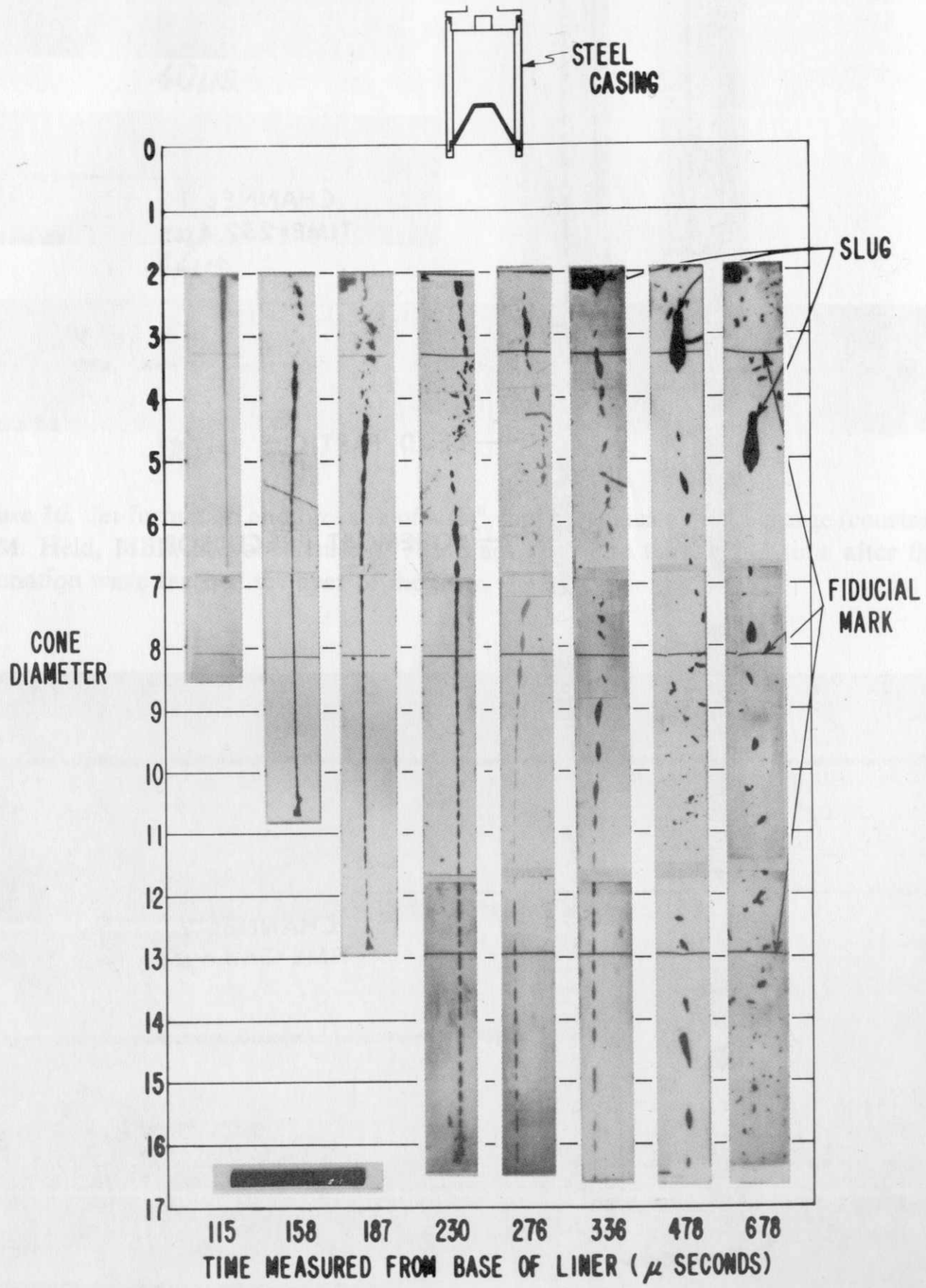

Figure 19. The jet from a heavy confined shaped charge at various distances. Note that the front of the jet was allowed to leave the film in order to radiograph the slug (Simon and DiPersio 1972).

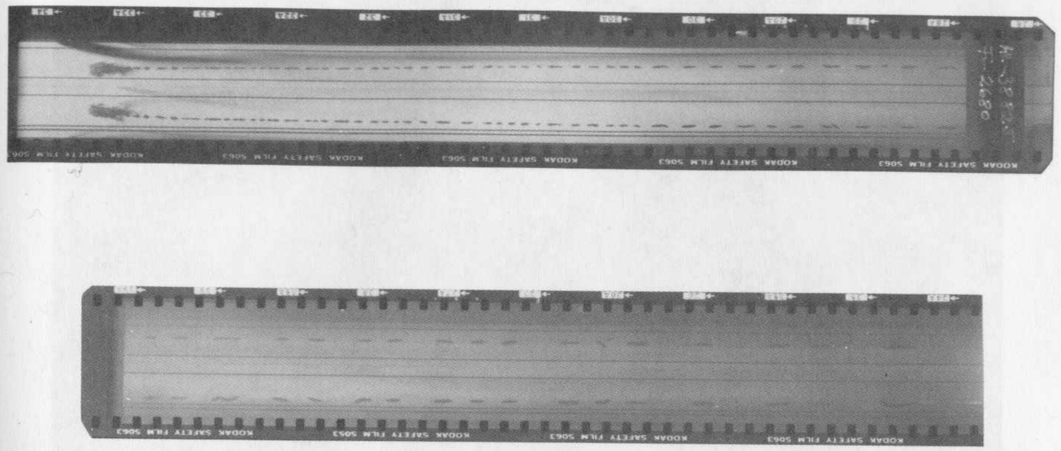

Figure 20. OSST record of a shaped charge jet from a 100 mm diameter, copper shaped charge. The record was taken at 0.5 km/s. The straight horizontal lines are the fiducial lines and are 40 mm apart (1st to 2nd and 3rd to 4th). A continuously writing CORDIN Model 330 camera was used (courtesy M. Held, MBB, Schrobenhausen).

through the air. On an optical record, this ablation phenomenon can be clearly seen. However, due to its low density, this ablation veil is more difficult to see in flash X-ray radiographs.

The tip of the jet is usually surrounded by a multitude of small particles all of which in turn create a trailing ablation veil. Behind the jet tip, the particulated shaped charge jet becomes clearly visible, in general, as can be seen in the lower portion of the record from Figure 20. Again, Held (1986) provides a complete description of the OSST recordings and presents additional examples.

14.2. SHAPED CHARGE LINER COLLAPSE AND JET FORMATION

The following section was extracted from the reports by Chou et al. (1985) and Walters and Golaski (1987). Numerical studies using the HELP and EPIC-2 computer codes (DEFEL is the Dyna East version of EPIC-2) were performed by Chou et al. (1985) that clearly illustrate the shaped charge liner collapse and jet formation for stratified (horizontally layered), bimetallic, copper–nickel shaped charge liners. Both conical and hemispherical liner geometries were considered. Partial experimental verification of the liner collapse and jet formation process was obtained by Walters and Golaski (1987) using a diffusion bonding technique to fabricate the liners and recovering some of the jet particles in water.

Figure 21 shows the stratified, copper–nickel, bimetallic, conical liner. The HELP code numerical simulation, using massless tracer particles to track the flow of the material, is shown in Figure 22. Figure 23 illustrates the cross

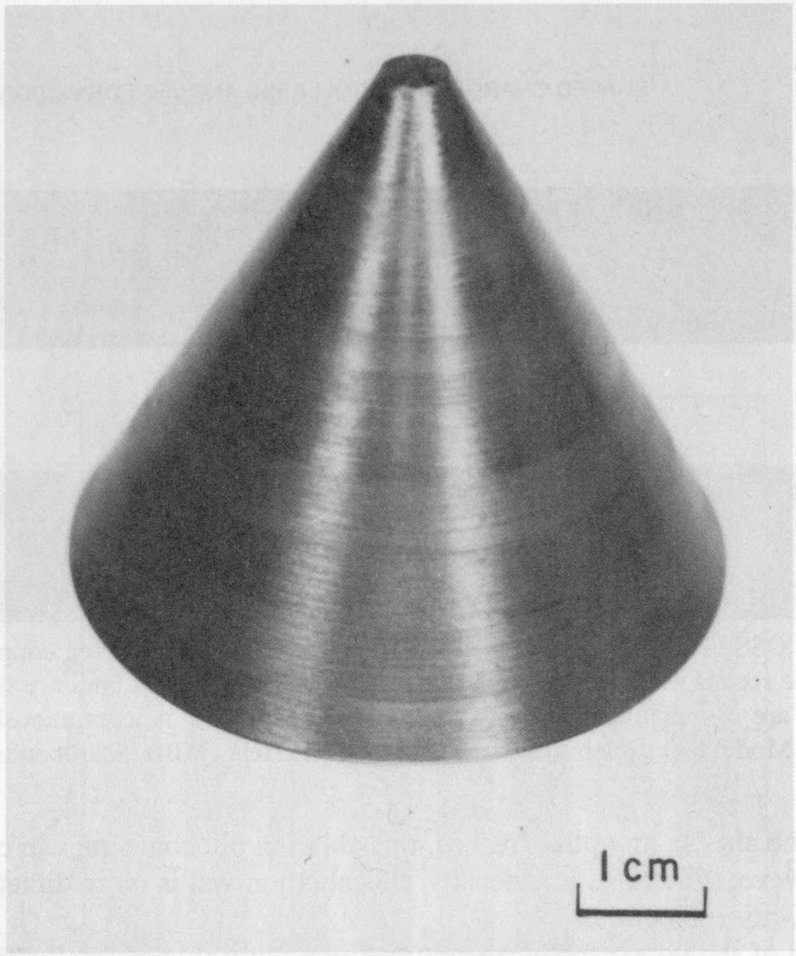

Figure 21. Finish machined, stratified, copper–nickel, conical shaped charge liner (Walters and Golaski 1987).

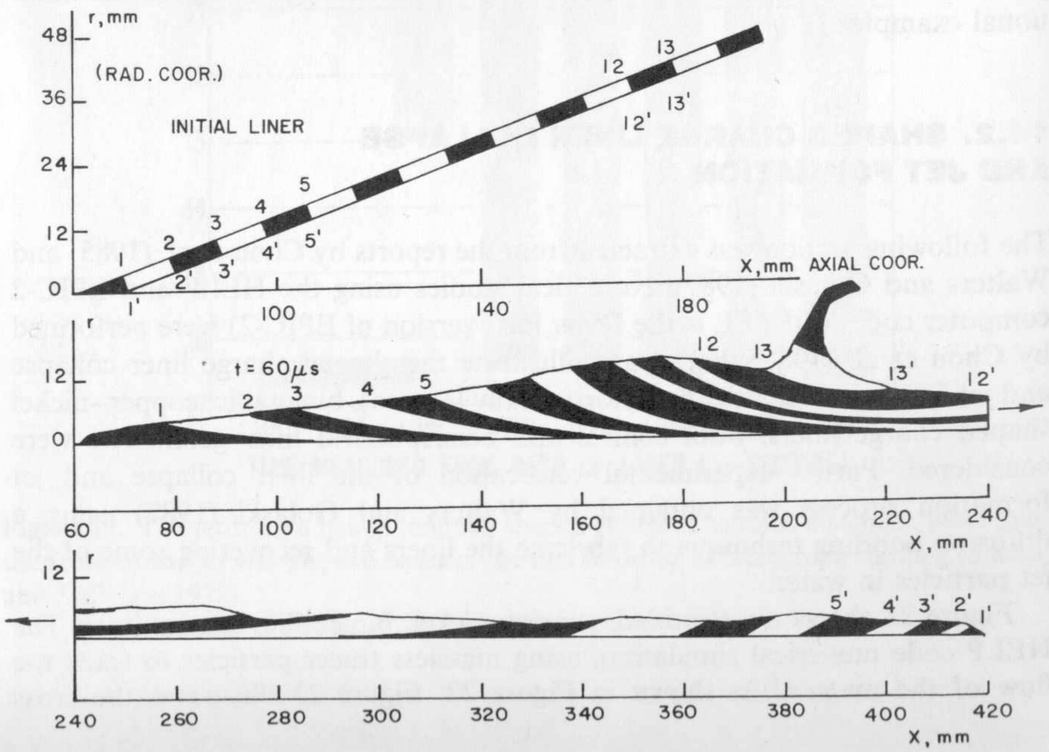

Figure 22. HELP code simulation of a 42° conical liner charge, initial liner geometry

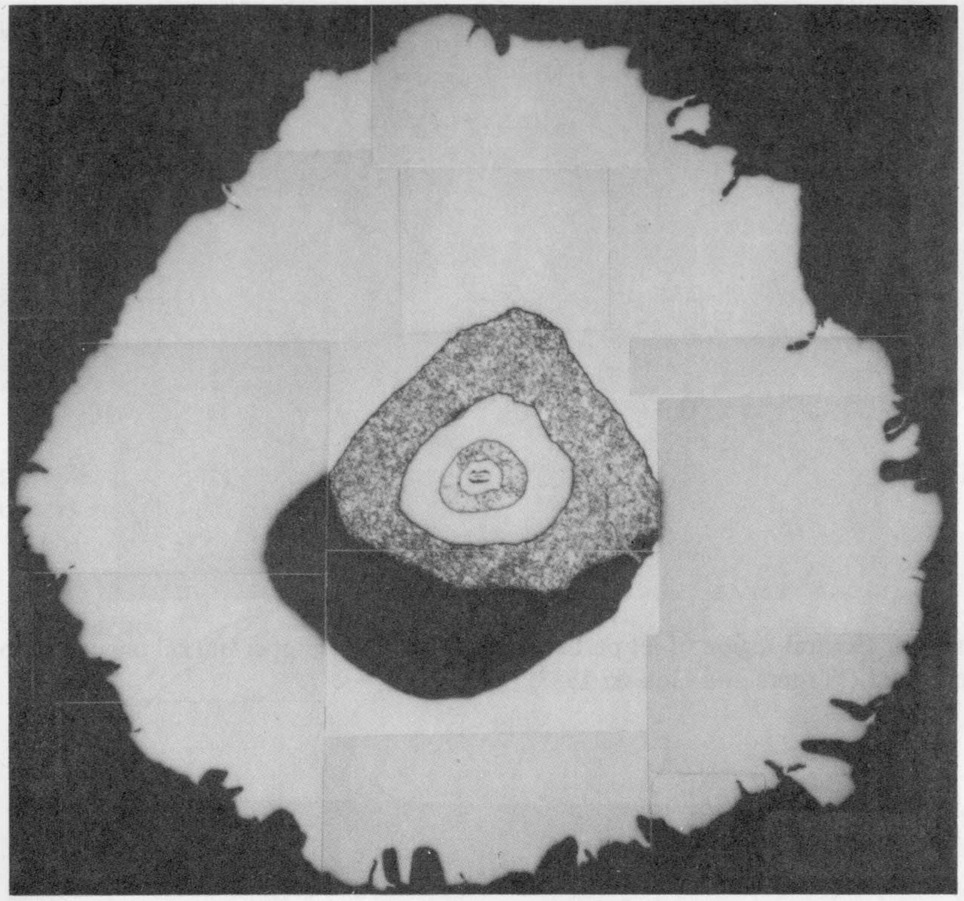

Figure 23. Cross section of jet particle from a stratified copper–nickel conical shaped charge liner (Walters and Golaski 1987).

section of a recovered jet particle revealing the flow of jet material. This particle is probably from the latter half of the jet (since the front-most particles probably eroded during impact with the water). Figure 24 shows a magnified view of the central region of the jet particle in Figure 23. Figure 25 presents a free-flight (in air) flash radiograph from the bimetallic, conical liner. Note that the jet collapses and forms as expected, probably due to the similar behavior of copper and nickel under shock loading conditions as well as the identical densities of copper and nickel. Finally, Figure 26 shows the slug recovered from the stratified, bimetallic liner.

A similar theoretical-experimental study was performed for stratified, bimetallic shape charge liners with the same materials. Figure 27 reveals the unique collapse pattern of point-initiated hemispherical liners, namely, a tubular, layered collapse. Figures 28 and 29 show the agreement between the hydrocodes and show the application of the massless tracer particles to follow the material flow. The late time (76 μs) jet formation is revealed in Figure 30.

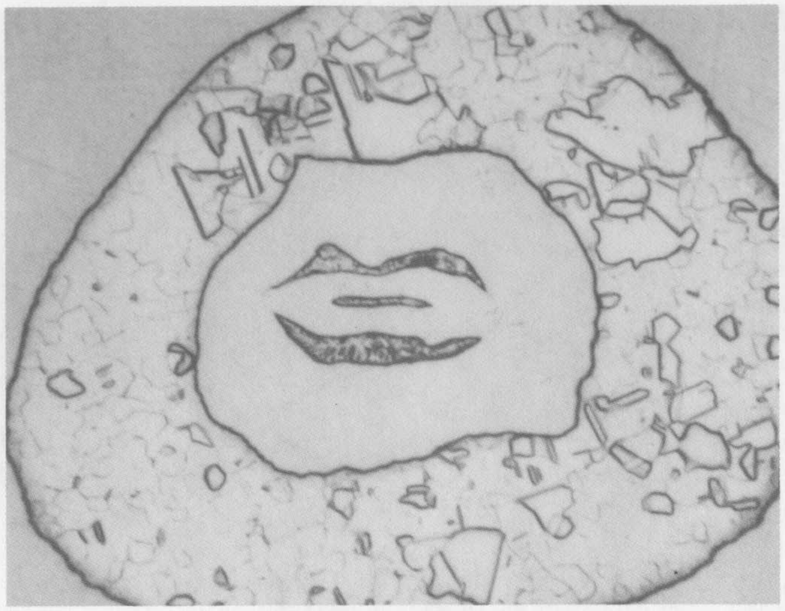

Figure 24. Central region of jet particle from a stratified copper–nickel conical shaped charge liner (Walters and Golaski 1987).

Figure 25. Free-flight flash radiographs of the jet from a stratified copper–nickel conical shaped charge liner (Walters and Golaski 1987).

As illustrated in Figure 31, a surface-initiated charge and a point-initiated charge do not collapse in the same manner.

The stratified, bimetallic, copper–nickel, hemispherical liner is shown in Figure 32. Figure 33 shows the free-flight flash radiograph from the point-initiated, hemispherical liner shaped charge. Again, the copper–nickel liner collapses, and the jet forms, as expected.

Figure 34 shows a cross section of a recovered jet particle (again, probably from the latter half of the jet) that reveals the tubular, layered collapse of the point-initiated, hemispherical liner. Figure 35 shows a cross section of one-half of the recovered jet particle that clearly shows the tubular, layered collapse of the liner.

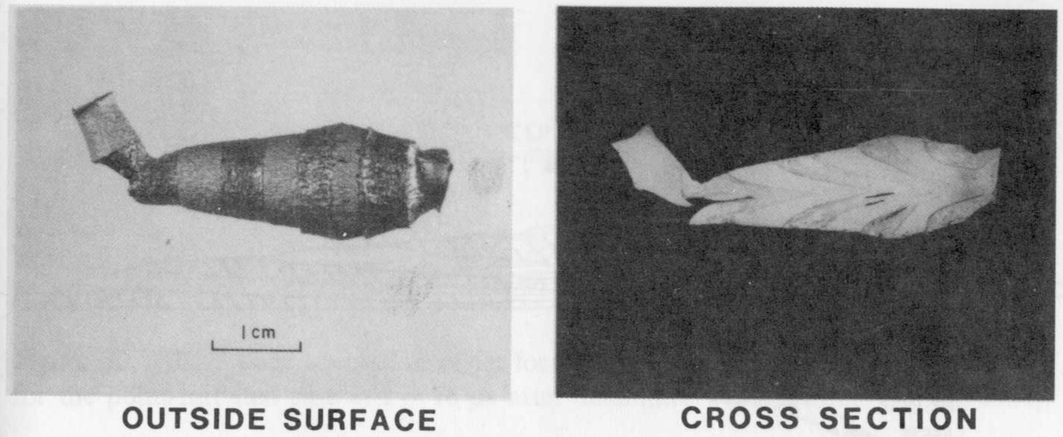

Figure 26. Recovered slug from a stratified copper–nickel conical shaped charge liner (Walters and Golaski 1987).

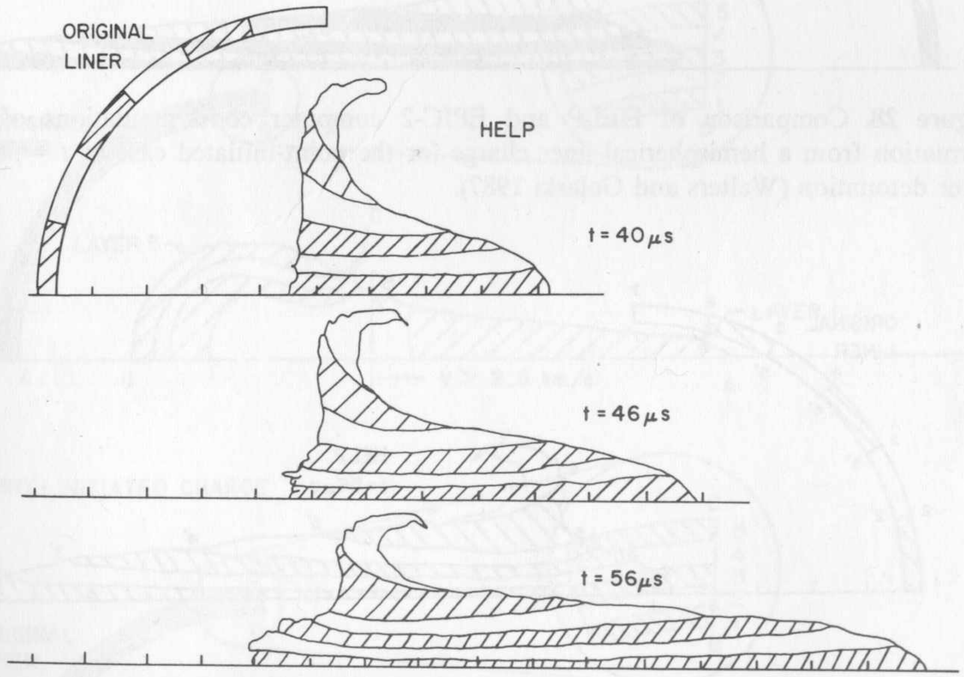

Figure 27. HELP code simulation of jet formation from a hemispherical liner charge for the point-initiated case at three times after detonation (Walters and Golaski 1987).

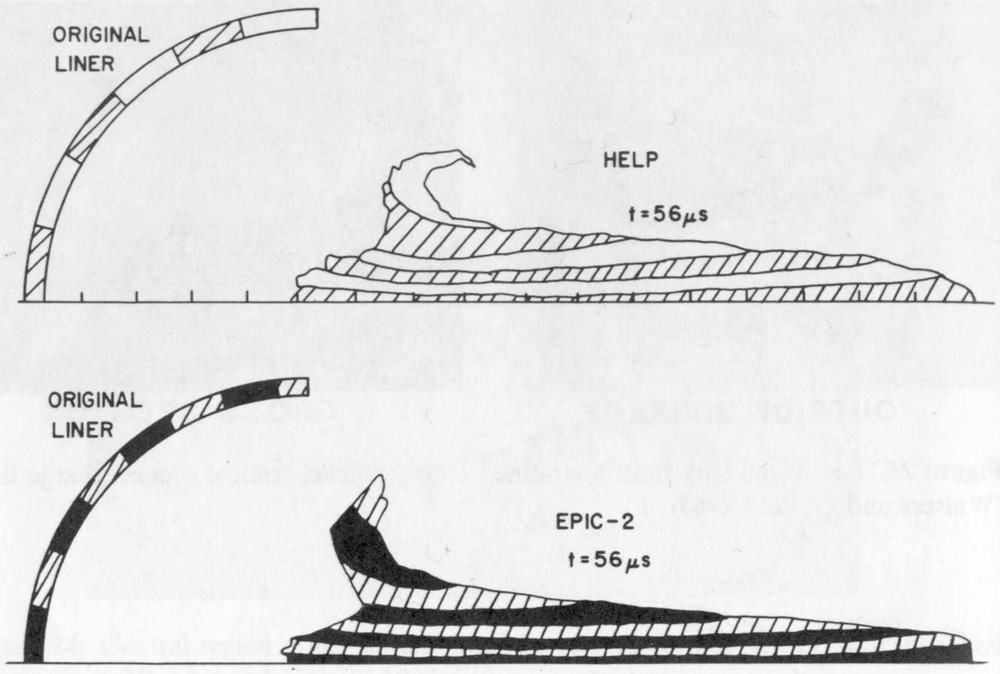

Figure 28. Comparison of HELP and EPIC-2 computer code simulations of jet formation from a hemispherical liner charge for the point-initiated case at $t = 56$ μs after detonation (Walters and Golaski 1987).

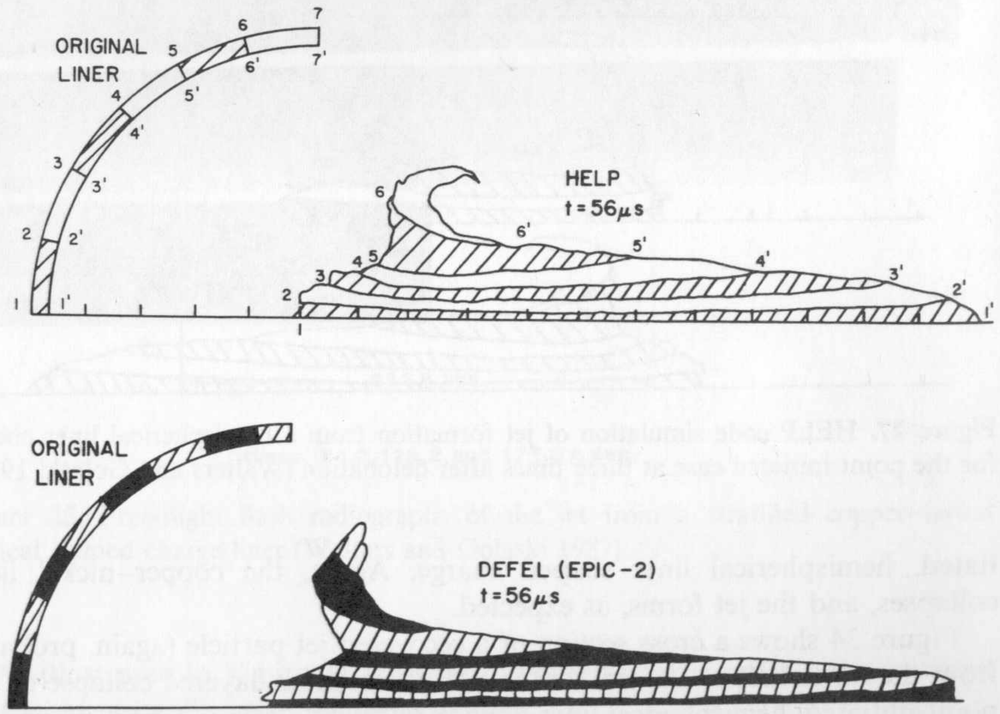

Figure 29. Computer code (HELP and DEFEL) simulation of jet formation of a hemispherical liner charge (Walters and Golaski 1987).

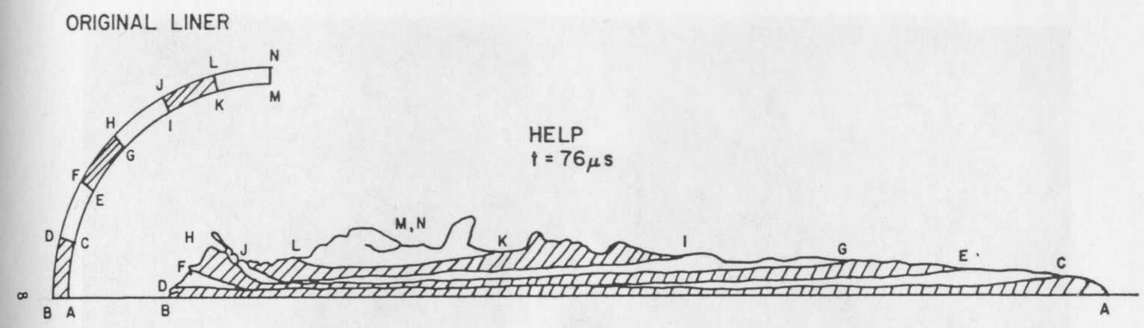

Figure 30. HELP code simulation of jet formation from a hemispherical liner charge for the point-initiated case at $t = 76$ μs after detonation (Walters and Golaski 1987).

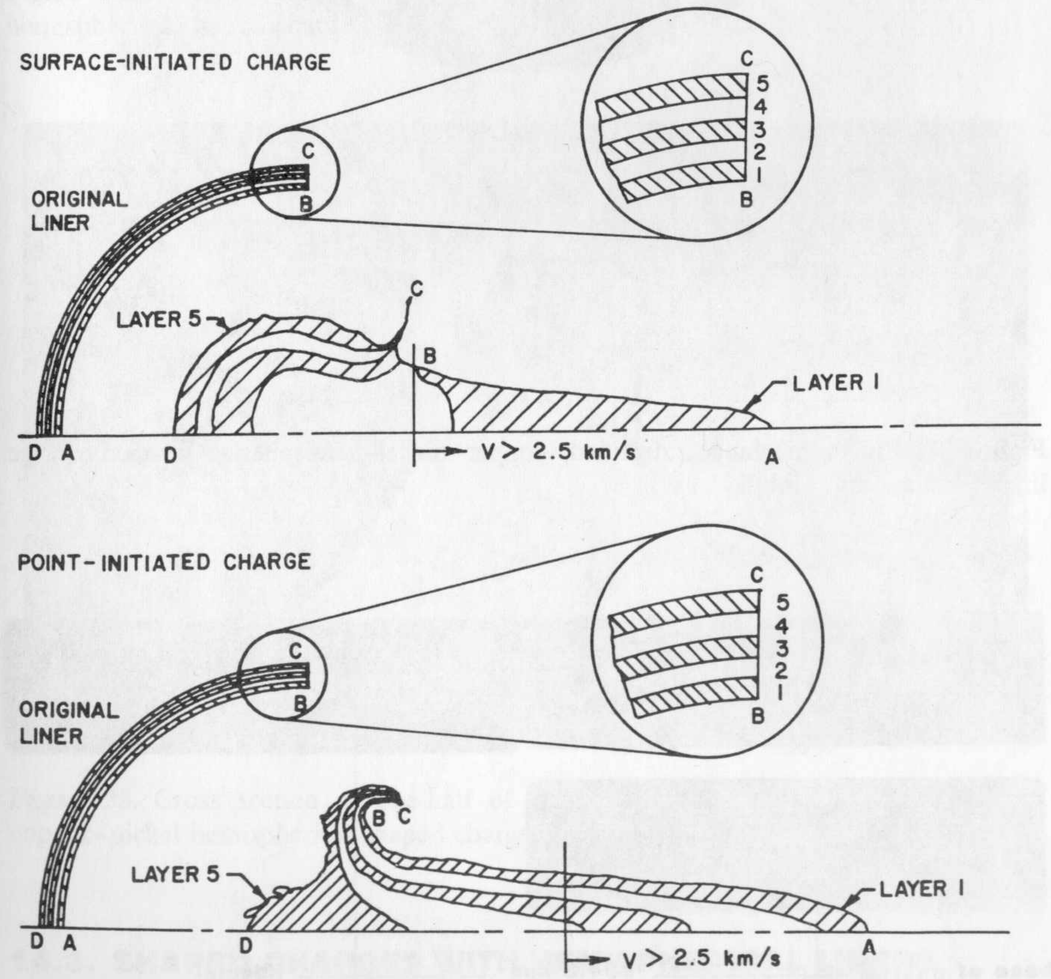

Figure 31. HELP code jet geometries showing layers of tracer particles at comparable times after detonation (Walters and Golaski 1987).

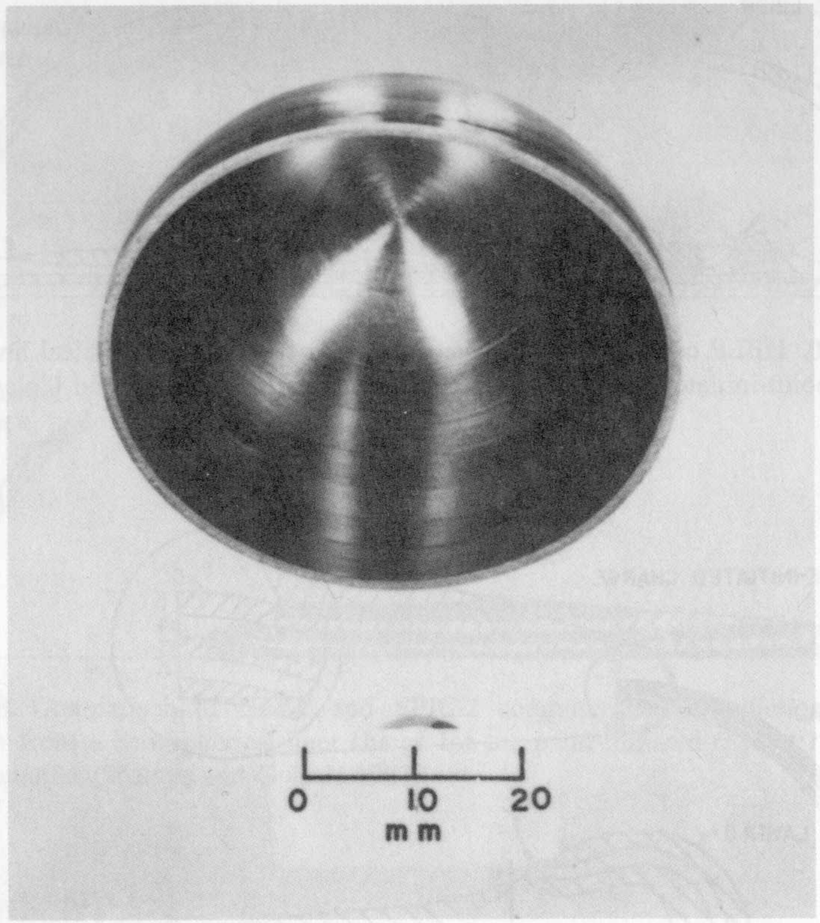

Figure 32. Finish machined, stratified, copper–nickel hemispherical shaped charge liner (Walters and Golaski 1987).

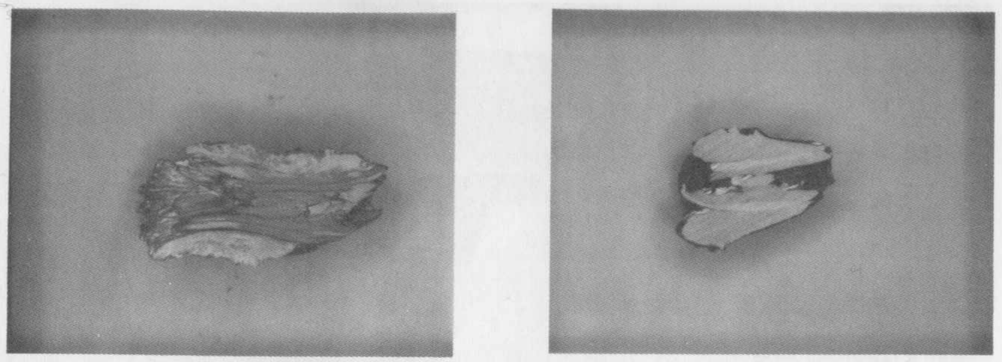

Figure 34. Cross section of recovered jet particles from a stratified copper–nickel hemispherical shaped charge liner (Walters and Golaski 1987).

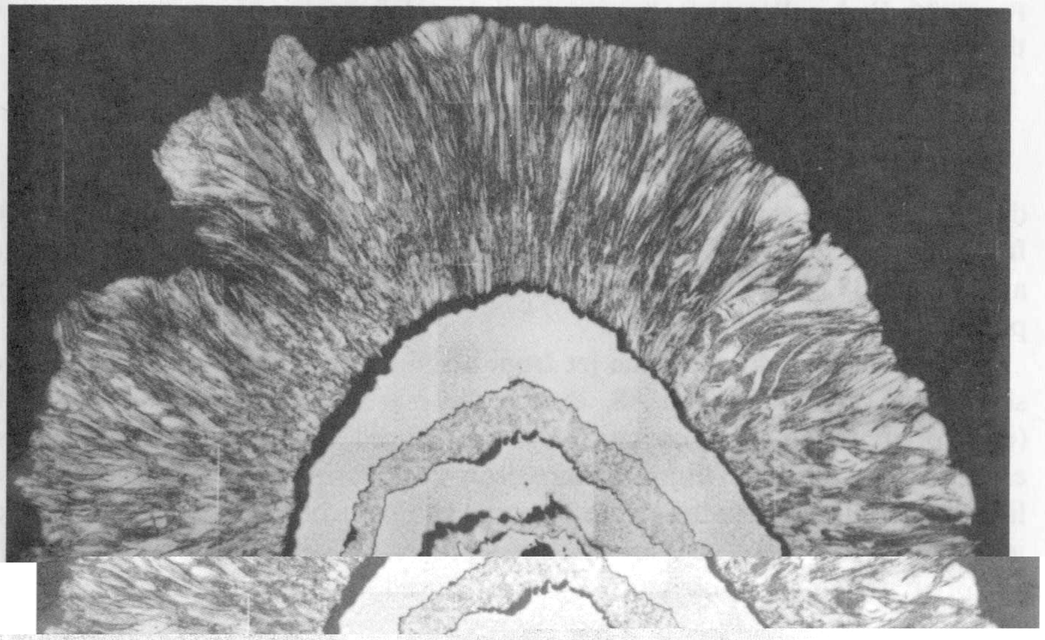

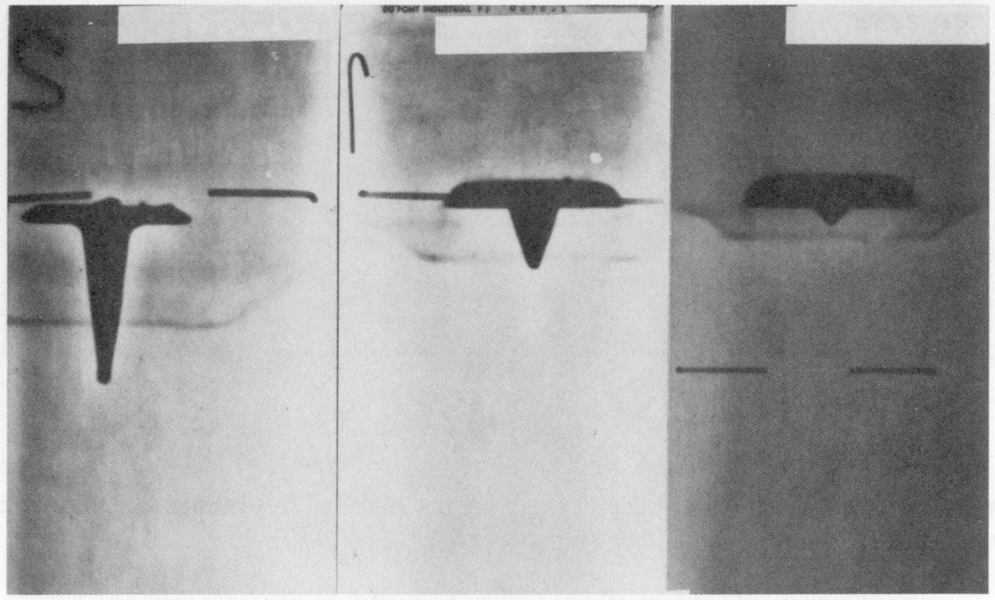

Figure 36. Early collapse of a hemispherical shaped charge liner. Note the inversion of the pole region.

Figures 37 and 38 show the formation and particulation of 127 mm diameter shaped charges with hemispherical liners made from OFHC (oxygen free high conductivity) copper. Figure 37 covers the 300–400 μs time range and Figure 38 covers the 500–600 μs time range. Note the tumbling of the jet particles at the long flash times.

Figures 39 and 40 show the jet from a shaped charge identical to the one shown in Figures 37 and 38, except the liner was fabricated from ETP (electrolytic tough pitch) copper. Note the "jagged" nature of the jet particles, especially at the later times. Comparison of Figures 37–40 reveals that the liner material and metallurgy are important in controlling the shaped charged jet ductility.

Figure 41 shows the jet from a shaped charge with an OFHC copper hemispherical liner, as in Figures 37 and 38, but this liner was simply hydroformed and not finish machined as the others were. Note that the "jagged" particle behavior returns for this nonprecision liner.

Figure 42 shows a framing camera record of the collapse of a hemispherical shaped charge liner. Figures 43*a*–43*d* show a collapse sequence, obtained by a high-speed framing camera, for an ETP copper, hemispherical shaped charge liner. Figure 43*a* shows the initial setup, where a mirror was used to obtain two views of the collapsing jet. The grid and numbers on the liner surface were used to obtain the liner collapse velocities. Note that the pole region forms first. The detonation products were not screened and begin to appear in Figure 43*c*. The jet eventually is obscured by the detonation products and only the

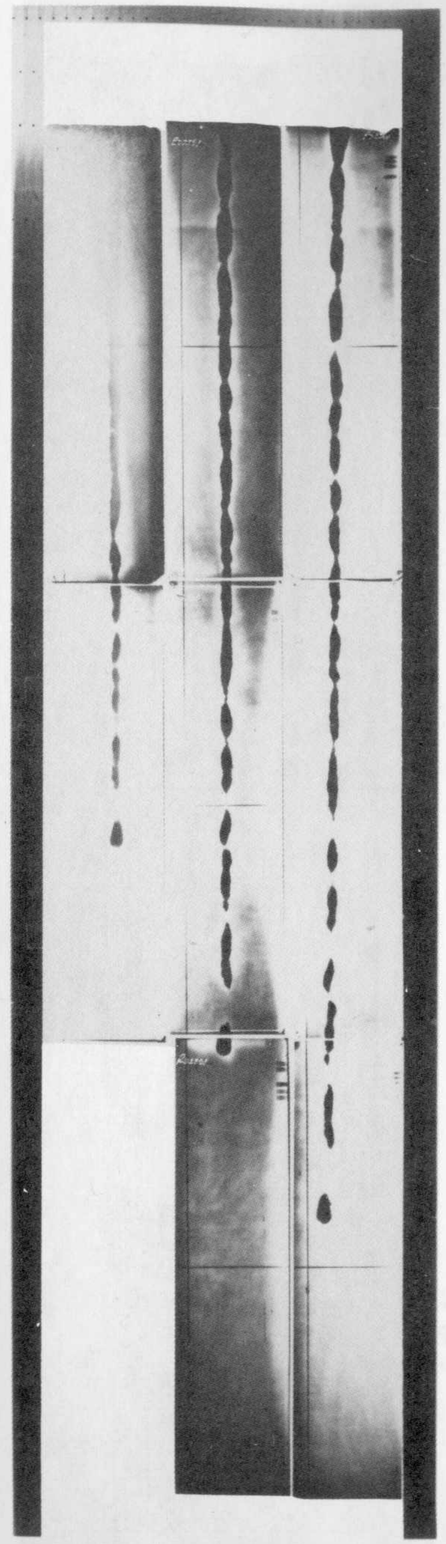

Figure 37. Jet from a shaped charge with an OFHC copper, hemispherical liner. Flash times are 303, 344, and 378 μs.

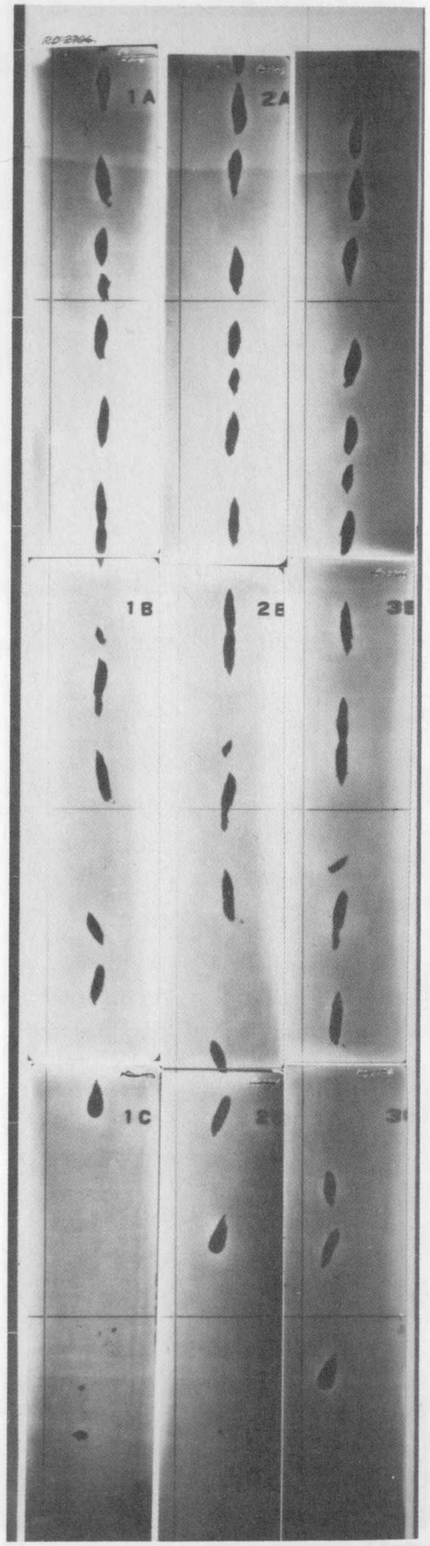

Figure 38. Jet from a shaped charge with an OFHC copper, hemispherical liner. Flash times are 543, 568, and 593 μs.

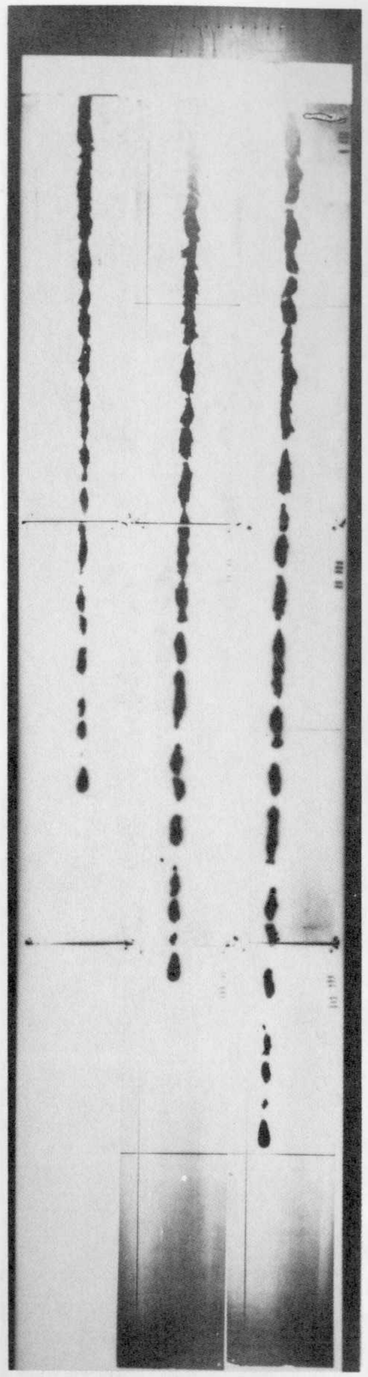

Figure 39. Jet from a shaped charge with an OFHC copper, hemispherical liner. Flash times are 303, 344, and 380 μs.

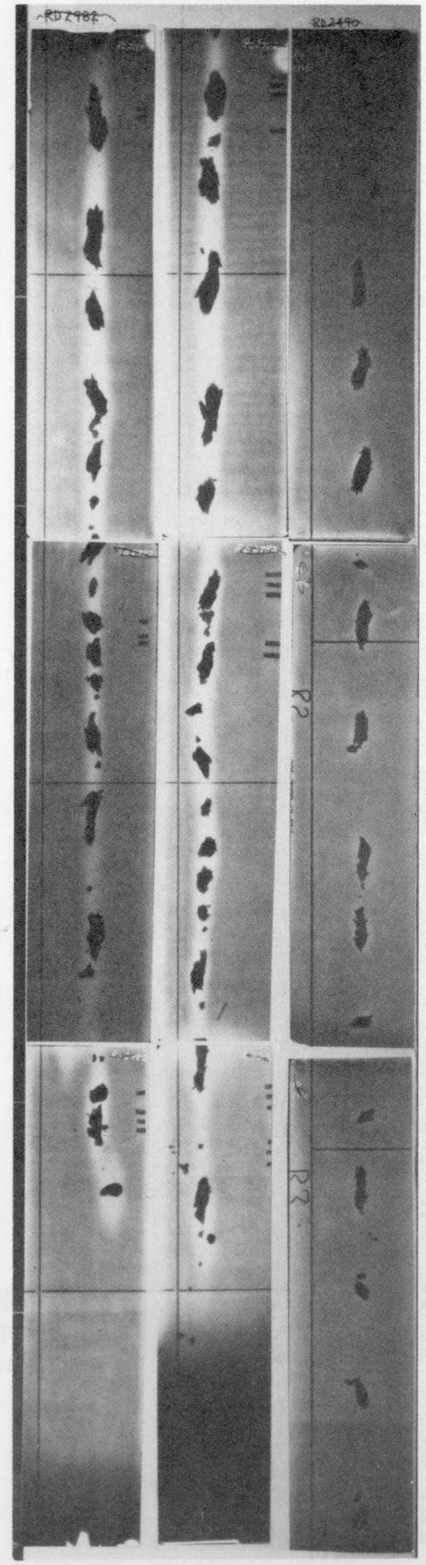

Figure 40. Jet from a shaped charge with an ETP copper, hemispherical liner. Flash times are 450, 476, and 500 μs.

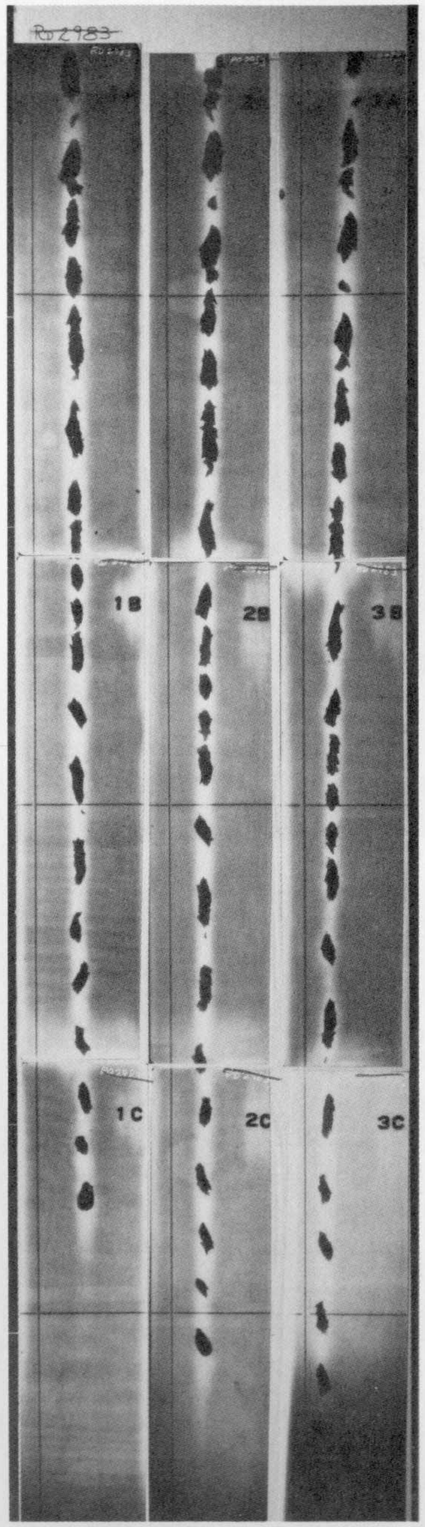

Figure 41. Jet from a shaped charge with an OFHC copper, hemispherical liner. Flash times are 450, 475, and 500 μs. The liner was not finish machined.

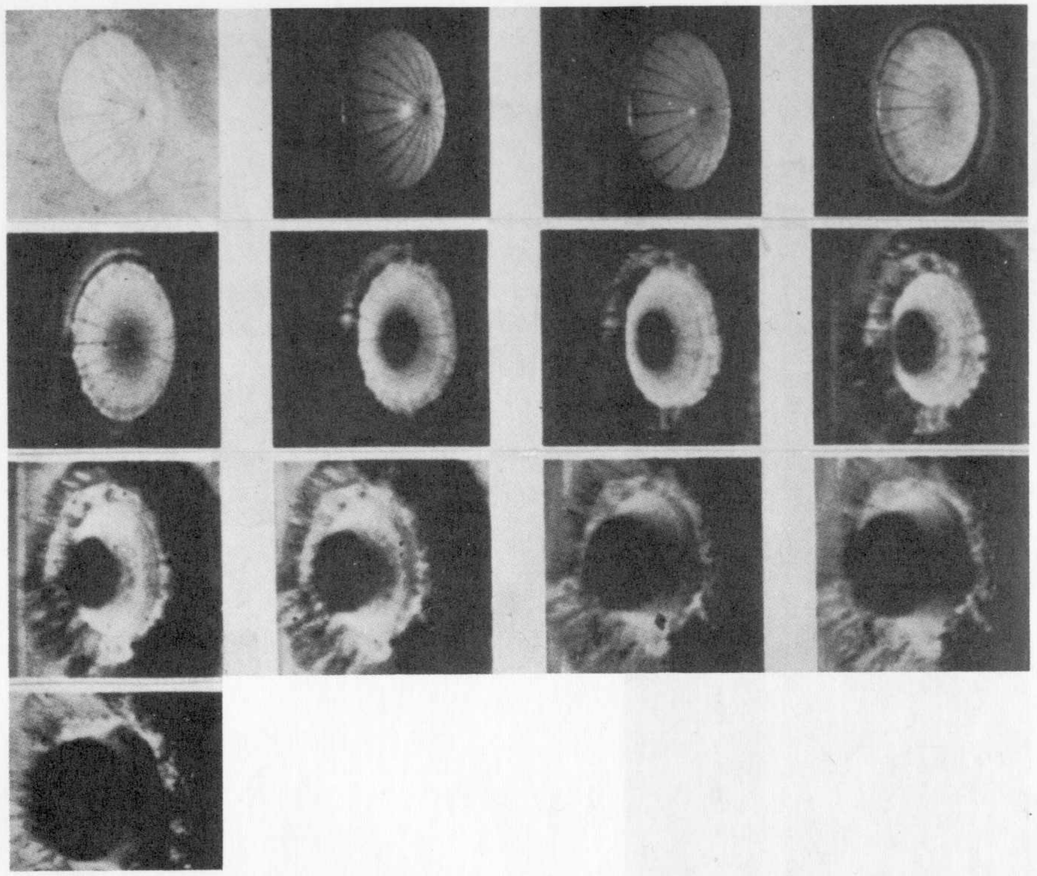

Figure 42. Microsecond, framing camera flash bomb illuminated, sequence of collapse

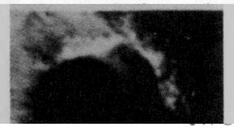

record of
ge with a

Figure 43*d* (due to the mirror arrangement). Figure 43*b* represents an elapsed time of about 6.4 μs since Figure 43*a*. Figure 43*c* is about 12.8 μs after the frame shown in Figure 43*a*. Finally, Figure 43*d* occurs at about 32 μs.

Figure 44 depicts a flash radiograph (X-ray) study of the collapse of a shaped charge with a hemispherical liner. Note again the inversion of the pole and the appearance of the "Mexican sombrero" at 15 μs. These flash radiographs were taken by S. Kronman of the BRL several years ago.

14.4. EXPLOSIVELY FORMED PENETRATORS

Numerical simulations of the various self-forging fragments (SFFs) or explosively formed penetrators (EFPs) are shown in this section. Details are given by Weickert (1986).

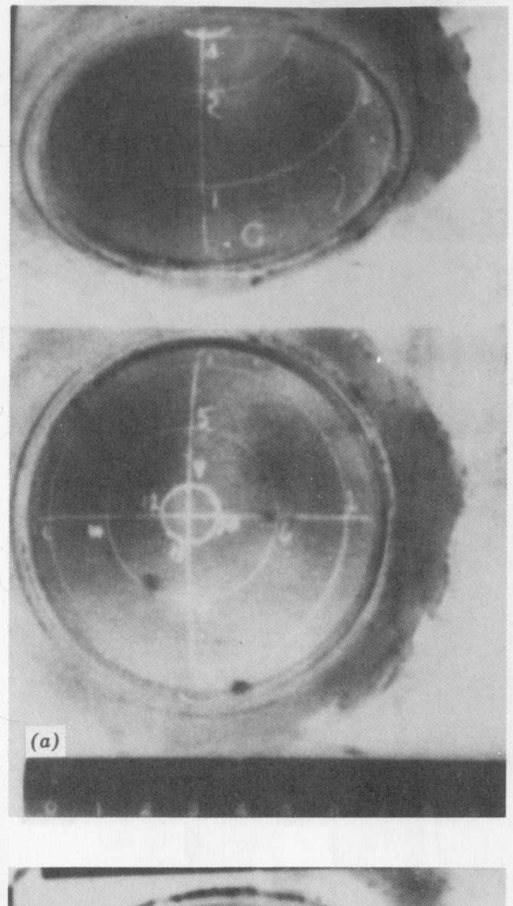

Figure 43a. A framing camera record of the collapse of a shaped charge with a hemispherical liner.

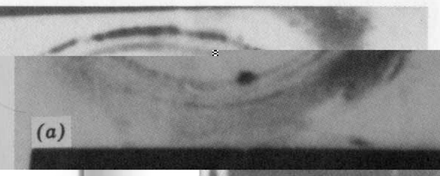

Figure 43a. A framing camera record of the collapse of a shaped charge with a

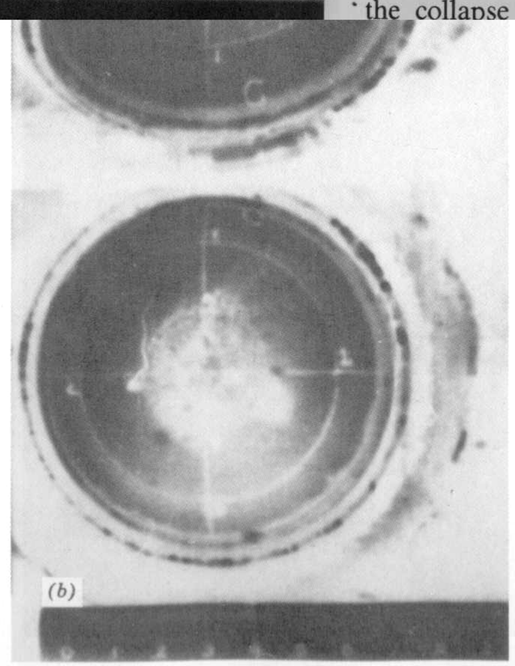

Figure 43b. A framing camera
the collapse of a shaped char
hemispherical liner.

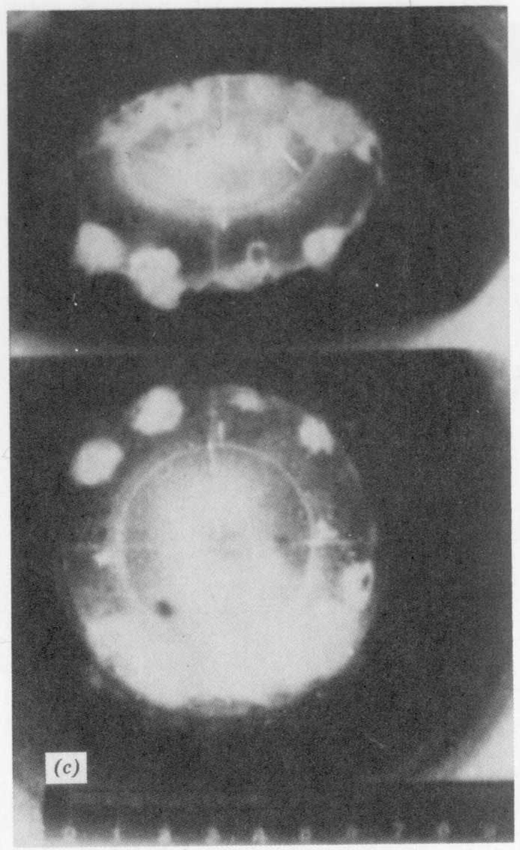

Figure 43c. A framing camera record of the collapse of a shaped charge with a hemispherical liner.

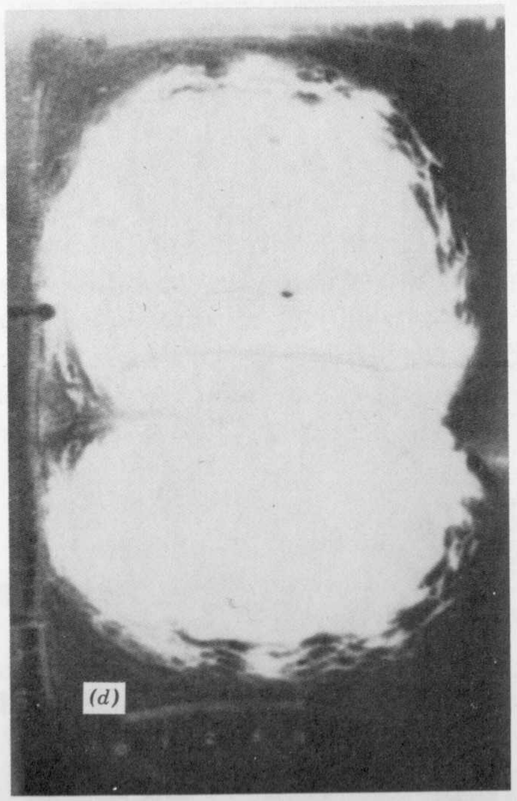

Figure 43d. A framing camera record of the collapse of a shaped charge with a hemispherical liner.

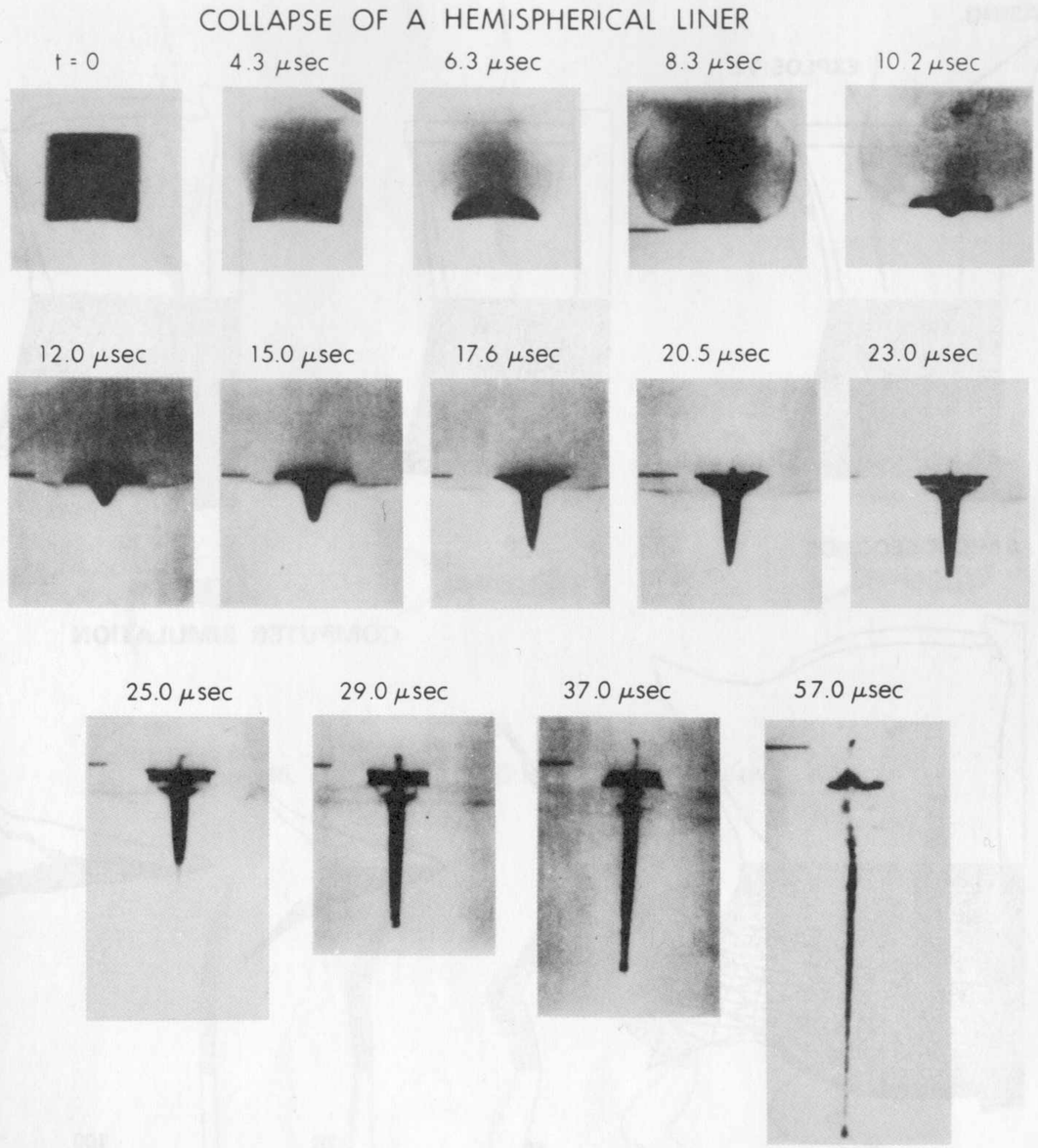

Figure 44. Flash radiograph study of the collapse and formation of a shaped charge with a hemispherical liner (obtained by S. Kronman, BRL).

Figures 45–47 illustrate a forward-folding, a backward-folding, and a W-fold penetrator, respectively.

Figure 48 illustrates various EFP designs, and Figures 49 and 50 show EFPs resulting from confined or cased charges. Figures 51 and 52 further illustrate penetrator shapes resulting from various liner geometries, that is, parabolic and hyperbolic.

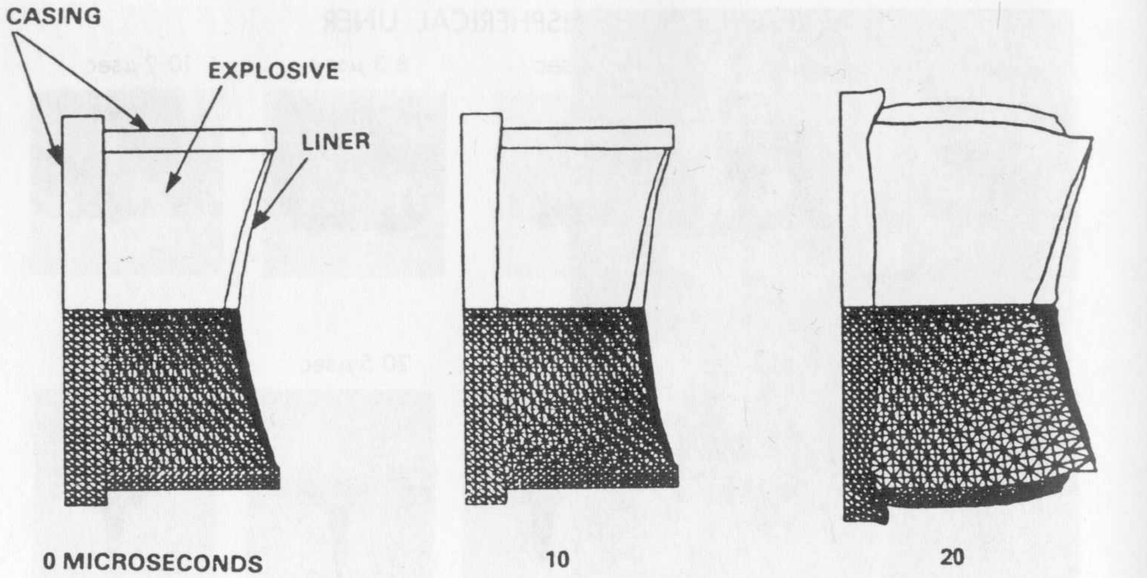

Figure 45. Forward-fold SFF formation (Weickert 1986).

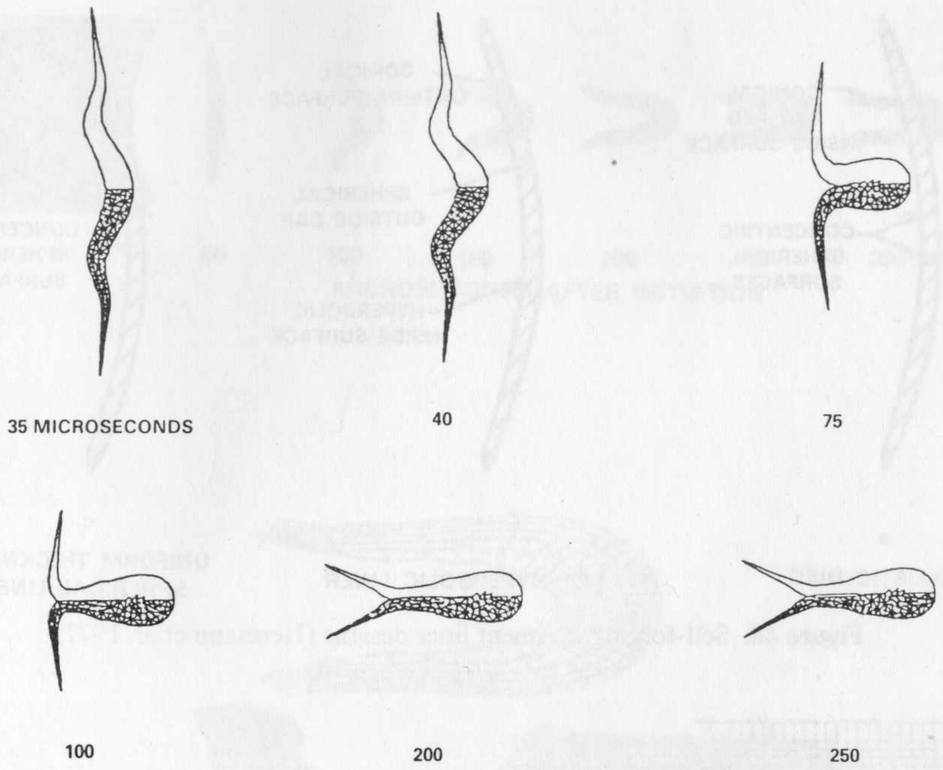

Figure 46. Backward-fold SFF formation (Weickert 1986).

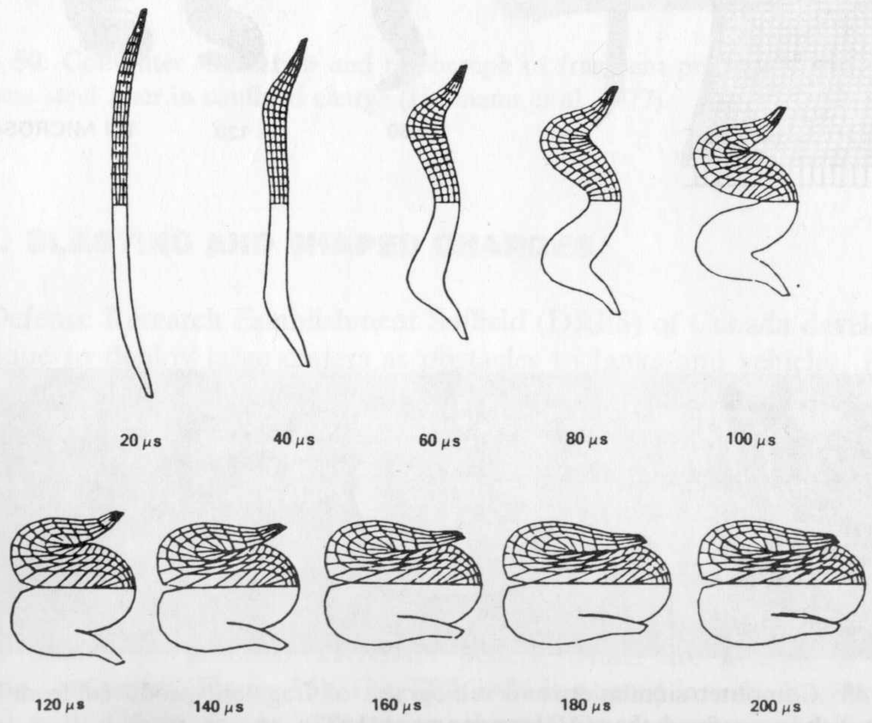

Figure 47. W-fold SFF formation (Hallquist 1980).

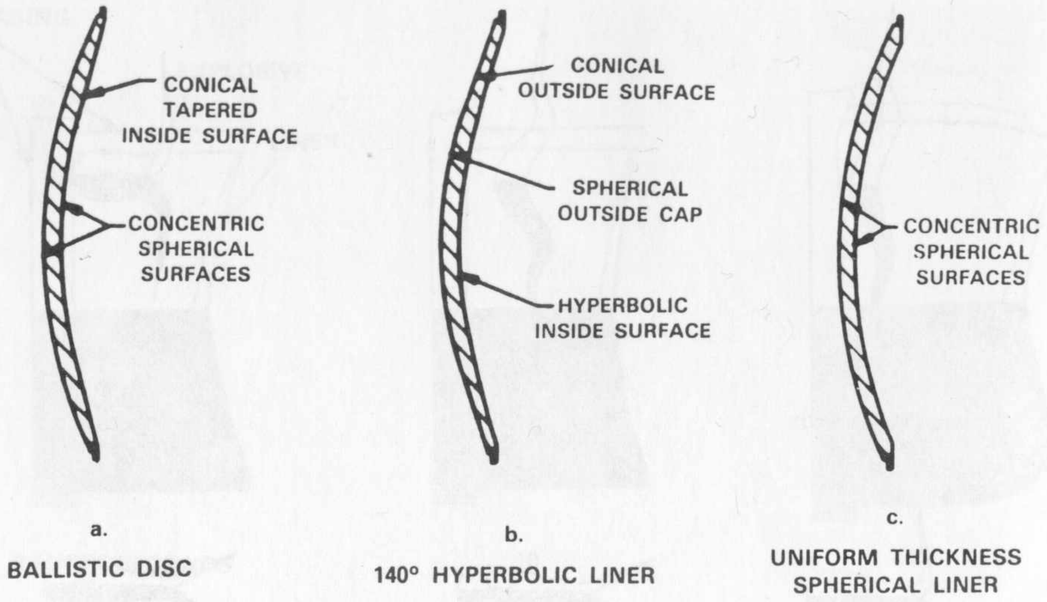

Figure 48. Self-forging fragment liner designs (Hermann et al. 1977).

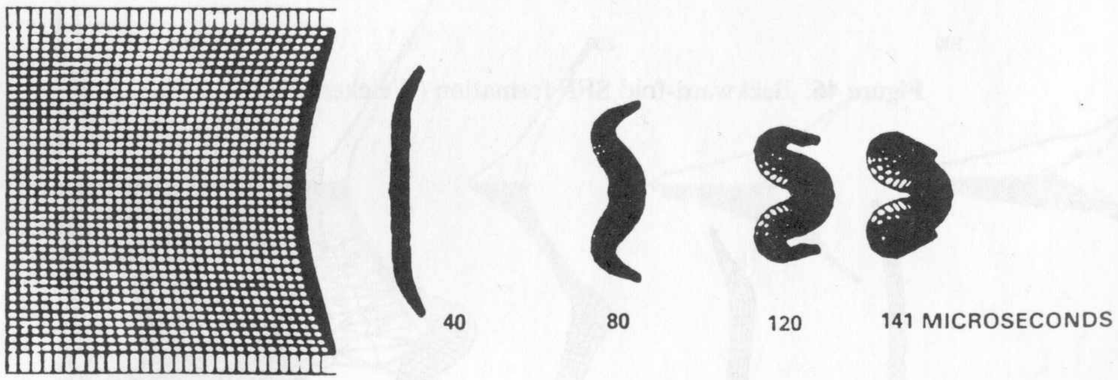

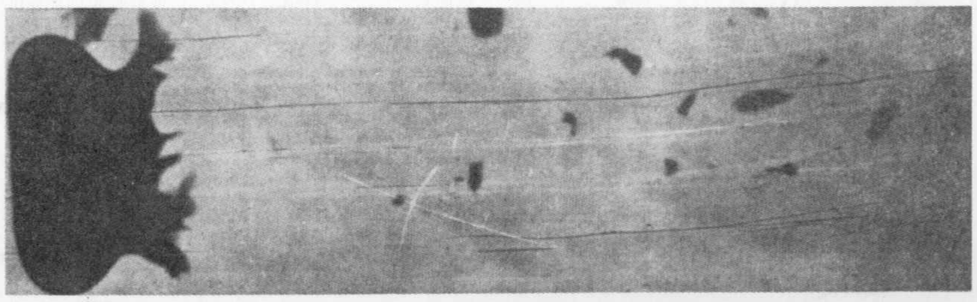

Figure 49. Computer simulation and radiograph of fragment produced from a steel ballistic disk in confined charge (Hermann et al. 1977).

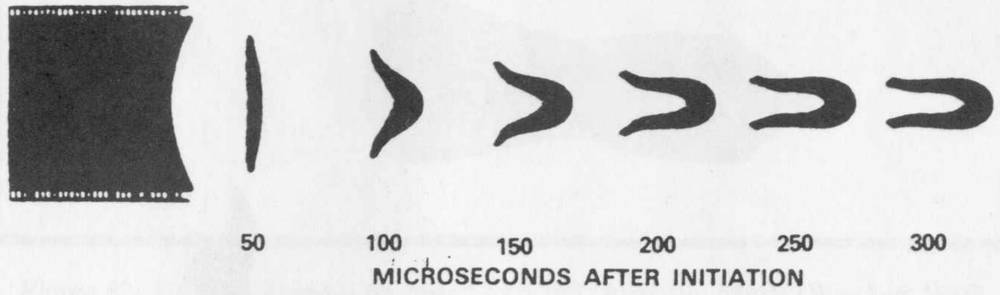

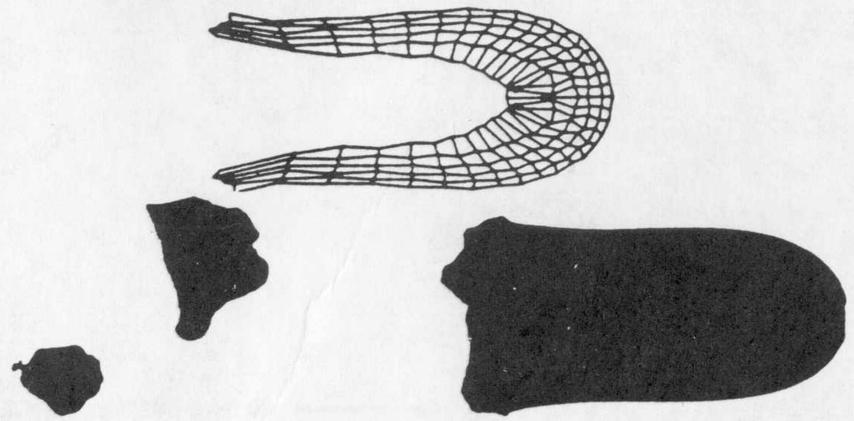

Figure 50. Computer simulation and radiograph of fragment produced from uniform thickness steel liner in confined charge (Hermann et al. 1977).

14.5. BLASTING AND SHAPED CHARGES

The Defense Research Establishment Suffield (DRES) of Canada developed a technique to deploy large craters as obstacles to tanks and vehicles. First, a shaped charge is employed to create a borehole. A typical demolition charge used by the Canadian Armed Forces is shown in Figure 53. Figure 54 shows the demolition charge positioned to create the borehole. The three-prong stand under the shaped charge is designed to provide the appropriate standoff distance.

After the borehole is formed, it is filled with a granular explosive called TRIGAN, developed by the Canadian Defense Research Establishment. Figure 55 shows the granular TRIGAN pellets, which are housed in plastic carrying containers (Figure 56). The TRIGAN is poured into the borehole and primed with C4 to act as a cratering charge. On-site preparation includes adding water to the TRIGAN, which significantly increases its detonation

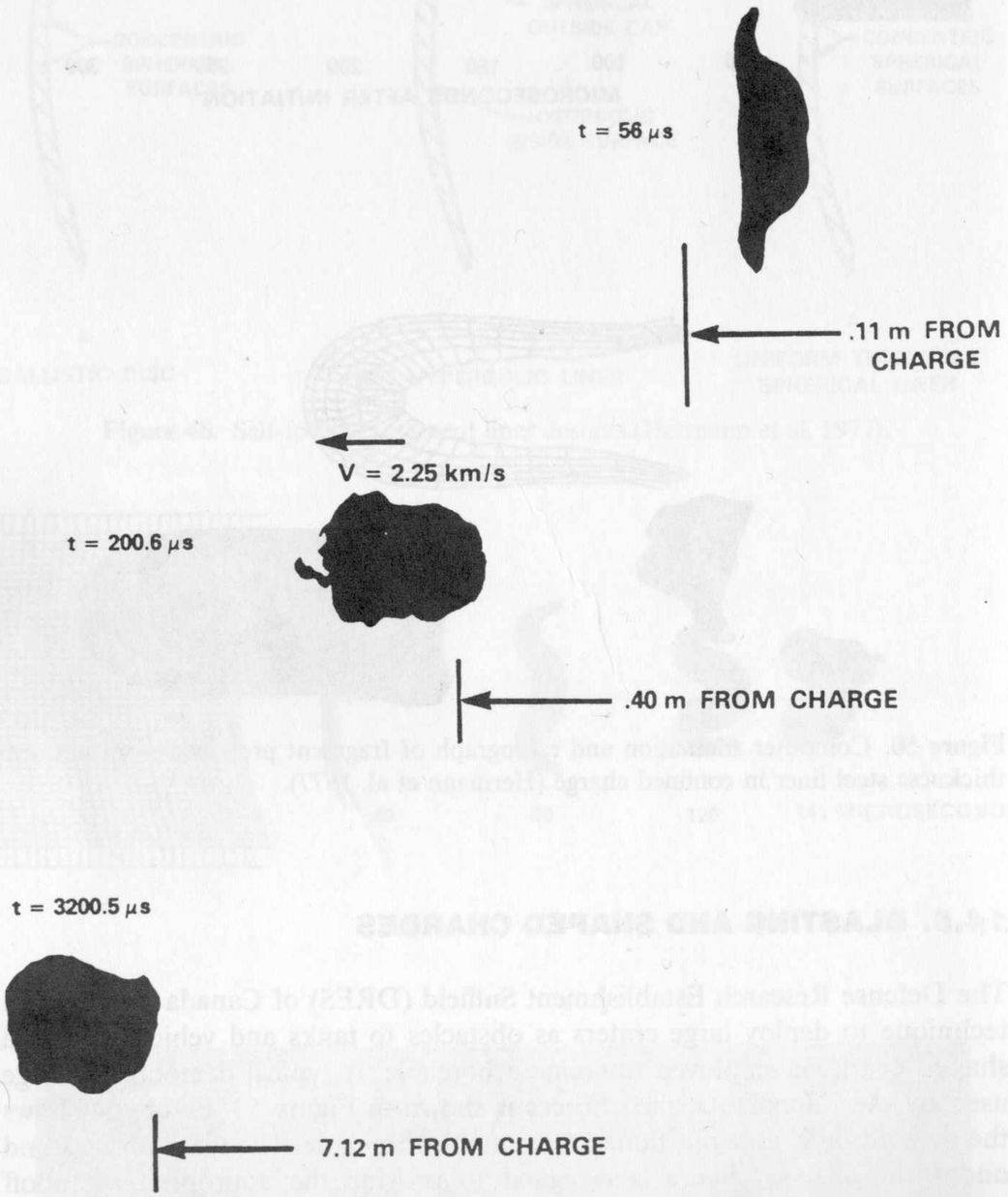

Figure 51. X-radiographic sequences of a parabolic lined SFF charge that generates a ball fragment (PI 1979).

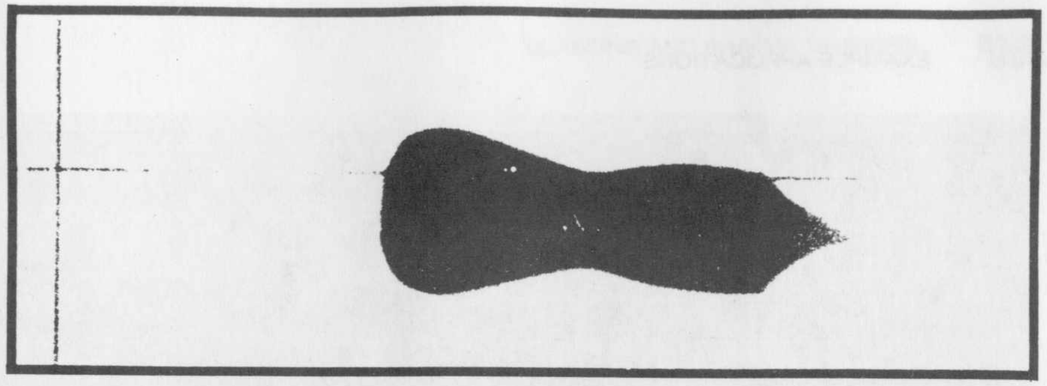

Figure 52. Copper fragment produced by a 140° hyperbolic liner (Weickert 1986).

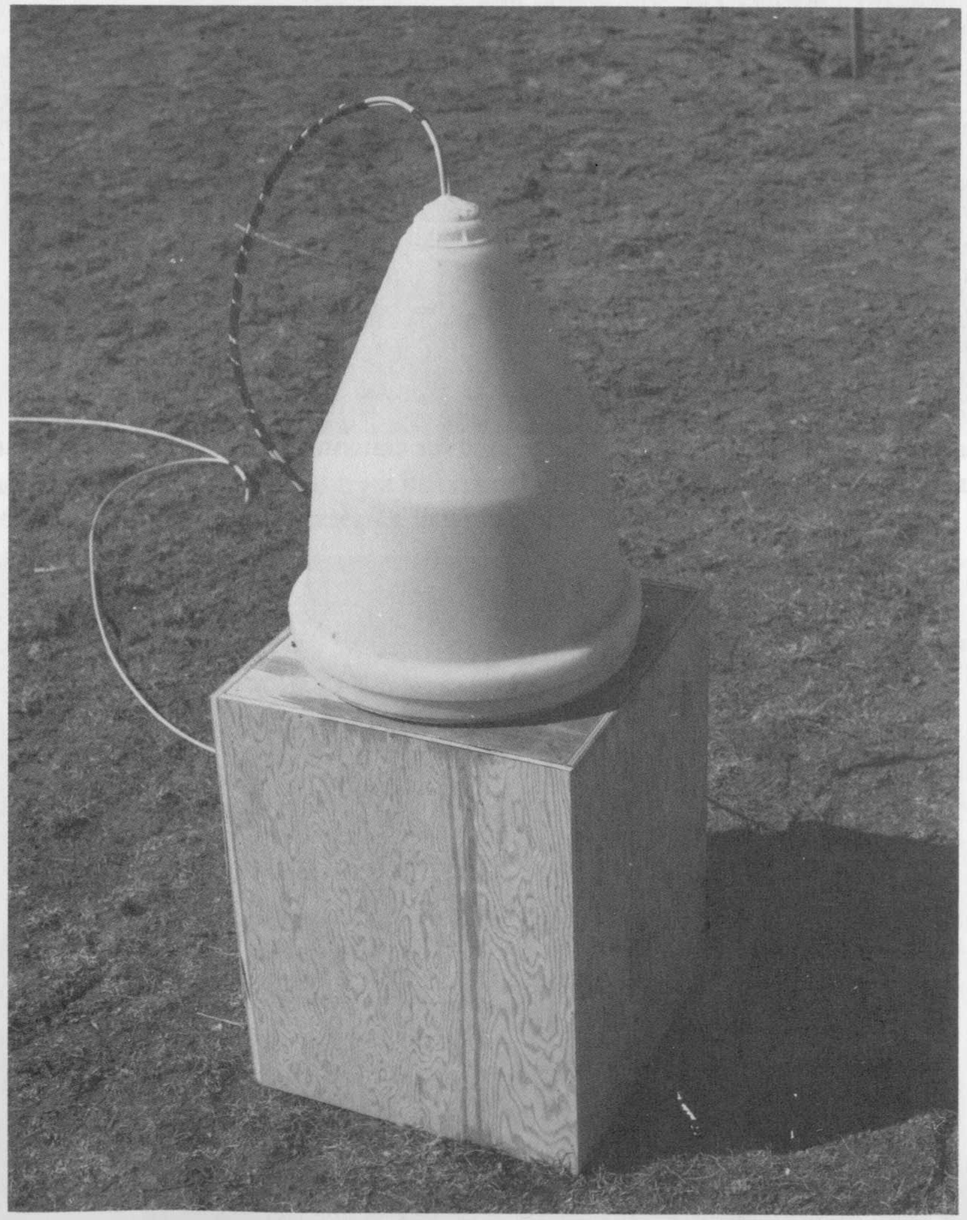

Figure 53. A demolition charge used by the Canadian Armed Forces (courtesy Defense Research Establishment Suffield).

Figure 54. The setup of a shaped charge used for cratering (courtesy Defense Research Establishment Suffield).

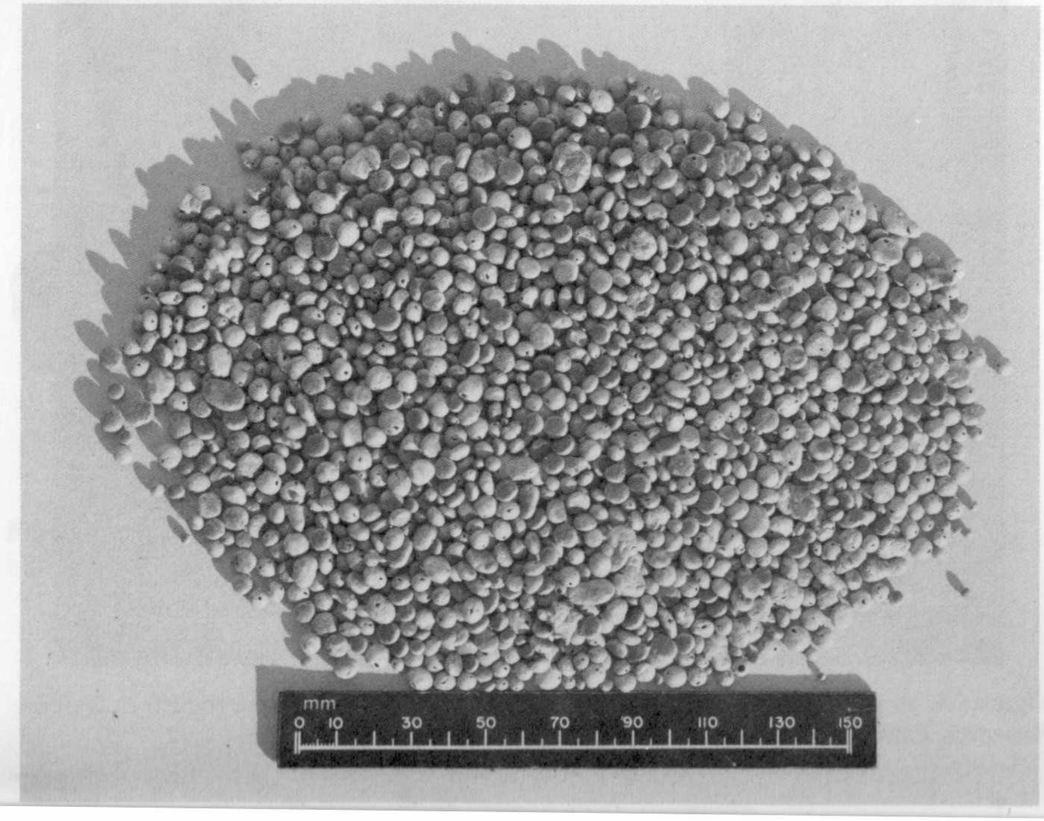

Figure 56. TRIGAN is poured from its original plastic containers into a shaped charge borehole (courtesy Defense Research Establishment Suffield)).

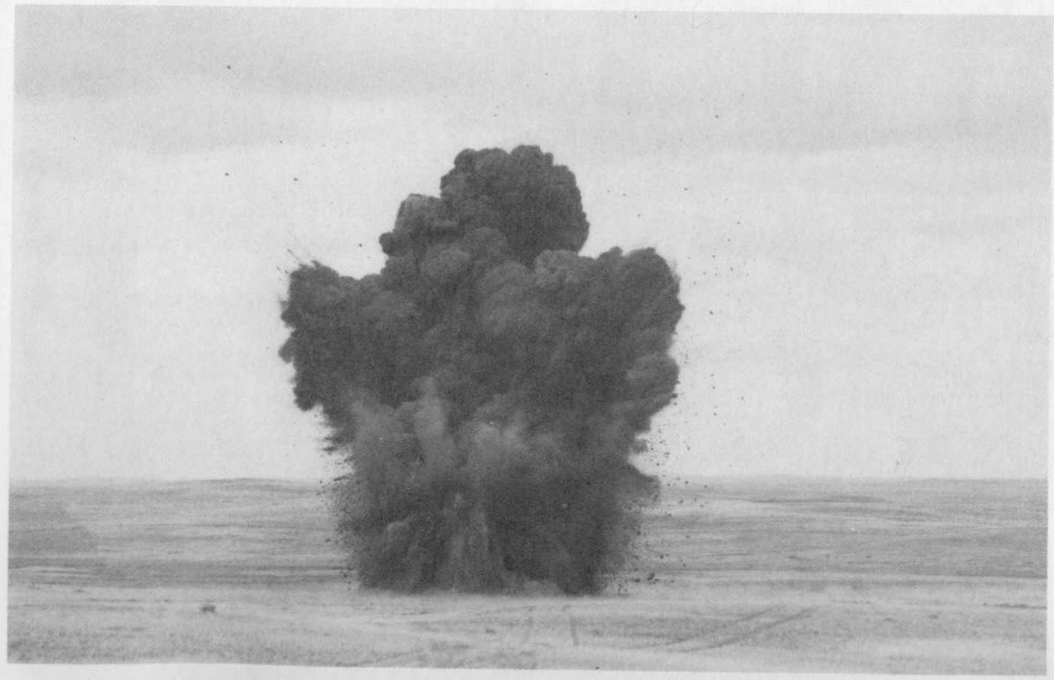

Figure 57. Detonation of TRIGAN cratering charges (courtesy Defense Research Establishment Suffield).

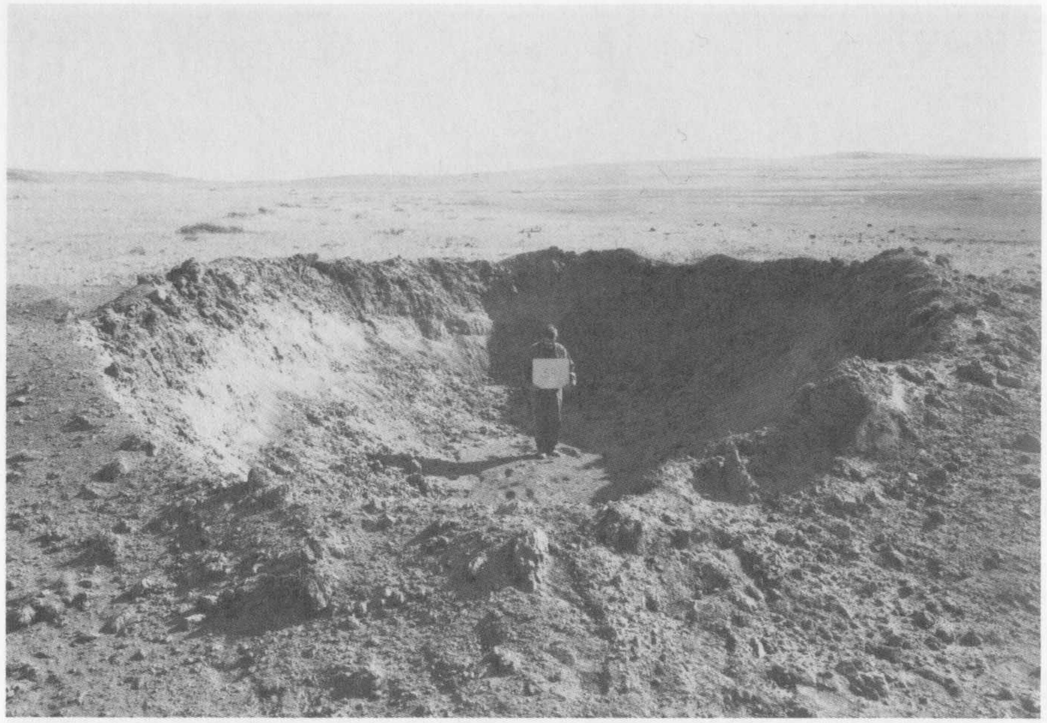

Figure 58. A typical countermobility obstacle produced by the detonation of TRIGAN charges (courtesy Defense Research Establishment Suffield.

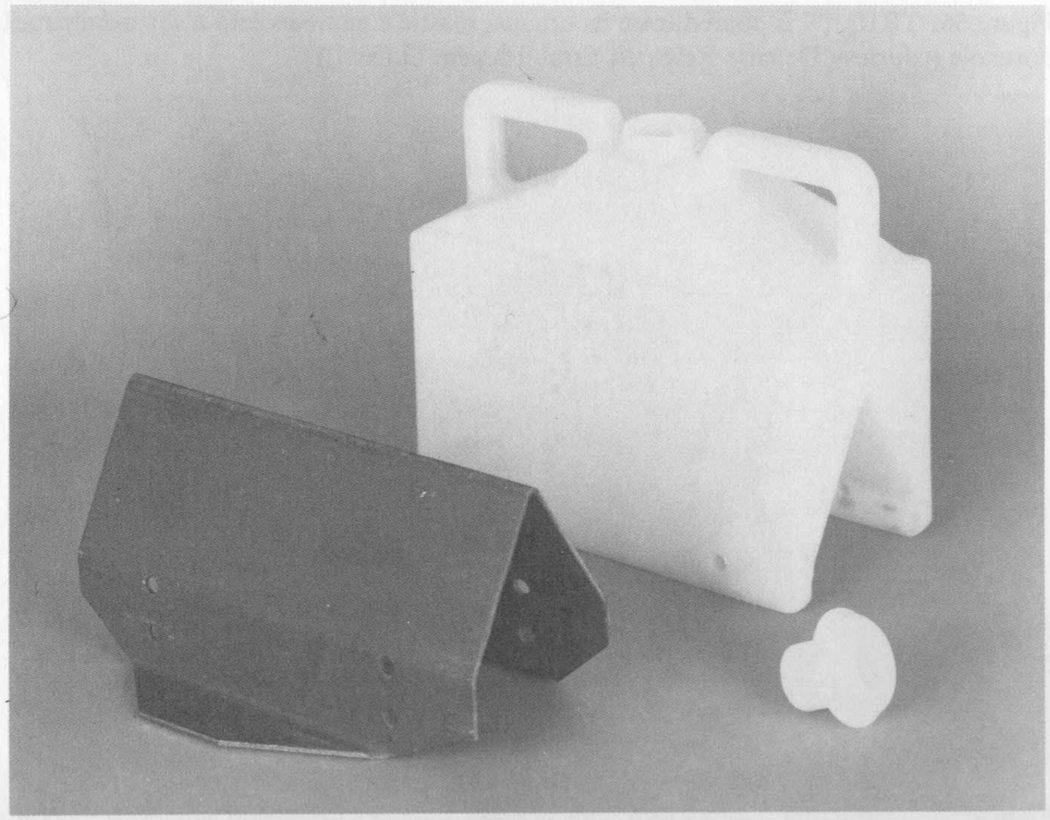

Figure 59. A linear shaped charge container and liner (courtesy Defense Research Establishment Suffield).

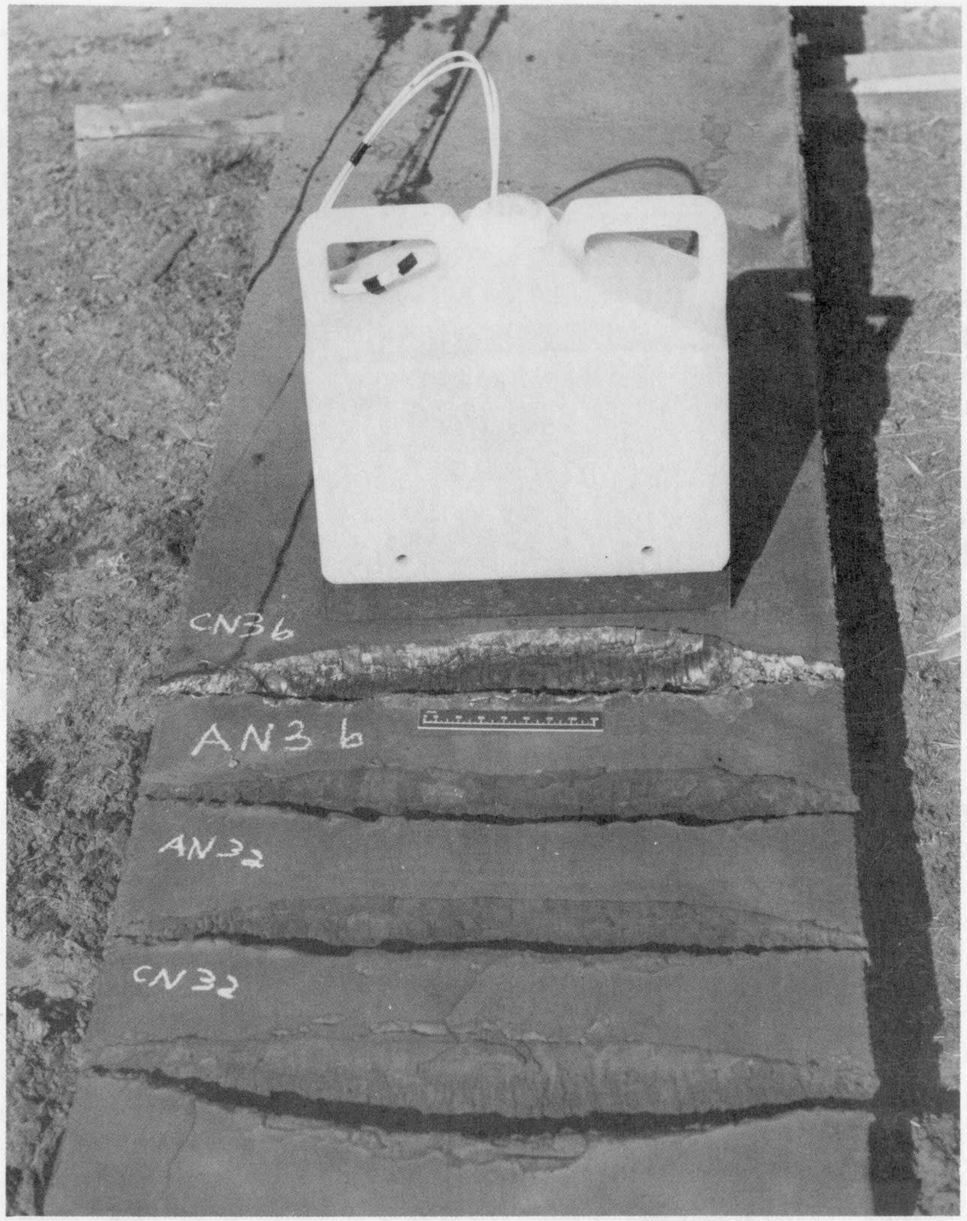

Figure 60. The linear shaped charge mounted on a 20 cm thick steel plate, showing also cuts produced with various thicknesses of the steel liner (courtesy Defense Research Establishment Suffield).

velocity and pressure. Figure 57 shows the resultant blast, and Figure 58 shows the countermobility obstacle (crater) produced.

In addition to the cylindrical shaped charge used for creating boreholes, a linear shape is available for use as a cutting charge. The linear shaped charge can be assembled on site (see Figure 59) and contains 10 kg of TRIGAN and a liner made of mild steel. The liner is also shown in Figure 59. This demolition charge is shown in Figure 60, mounted on a 20 cm thick steel plate and

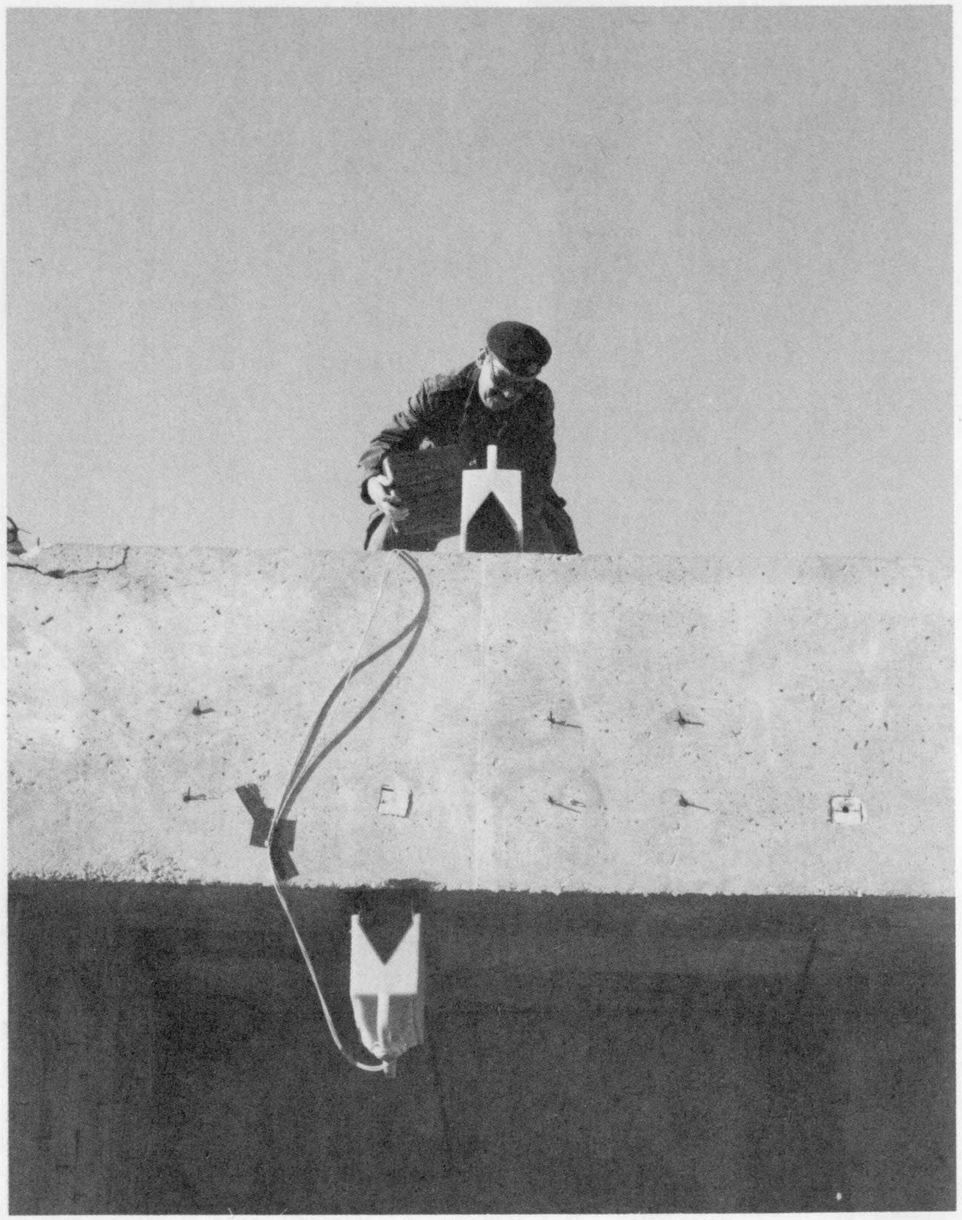

Figure 61. The linear cutting charge attached to a heavily reinforced bridge like structure (courtesy Defense Research Establishment Suffield).

showing cuts in the plate produced by various thicknesses of the mild steel liner.

Figure 61 shows this linear cutting charge used as a demolition charge and attached to a heavily reinforced bridge like structure. Figure 62 shows the structure after demolition. The indentation in the screw cap (Figure 59) is filled with plastic explosive that acts as a primer for the TRIGAN.

The preceding discussion and Figures 53–62 were furnished courtesy of Defense Research Establishment Suffield.

14.6. SPECIAL APPLICATIONS AND EFFECTS

Earlier chapters discussed special applications of shaped charges including linear cutting charges and the like. Figures 63 and 64 illustrate some of these charges. Figure 64 shows typical perforation or cutting performances and representative hole profiles for cutting charges, conventional shaped charges, and self-forging fragment charges.

The effects of charge imperfections on jet formation of conical liners are shown in Figure 65. Charge inhomogeneity (the upper half of the charge loaded with Comp B and the bottom half of the charge loaded with TNT), crossing axes effects (the liner and explosive charge axis of symmetries are not parallel), and offset initiation effects are illustrated.

Figures 66 and 67 illustrate the effect of off-center initiation on a conical liner. The initiation assembly was offset to the maximum possible angle from the charge axis of symmetry, 11.4° in this case. Walters (1986) provides details.

Figures 68–73 present the offset angle study for a shaped charge with a hemispherical liner. Figures 68 and 69 show the reference case, that is, the collapse and formation of the hemispherical shaped charge for a zero offset angle, or the detonator aligned on the charge axis of symmetry. Figures 70 and

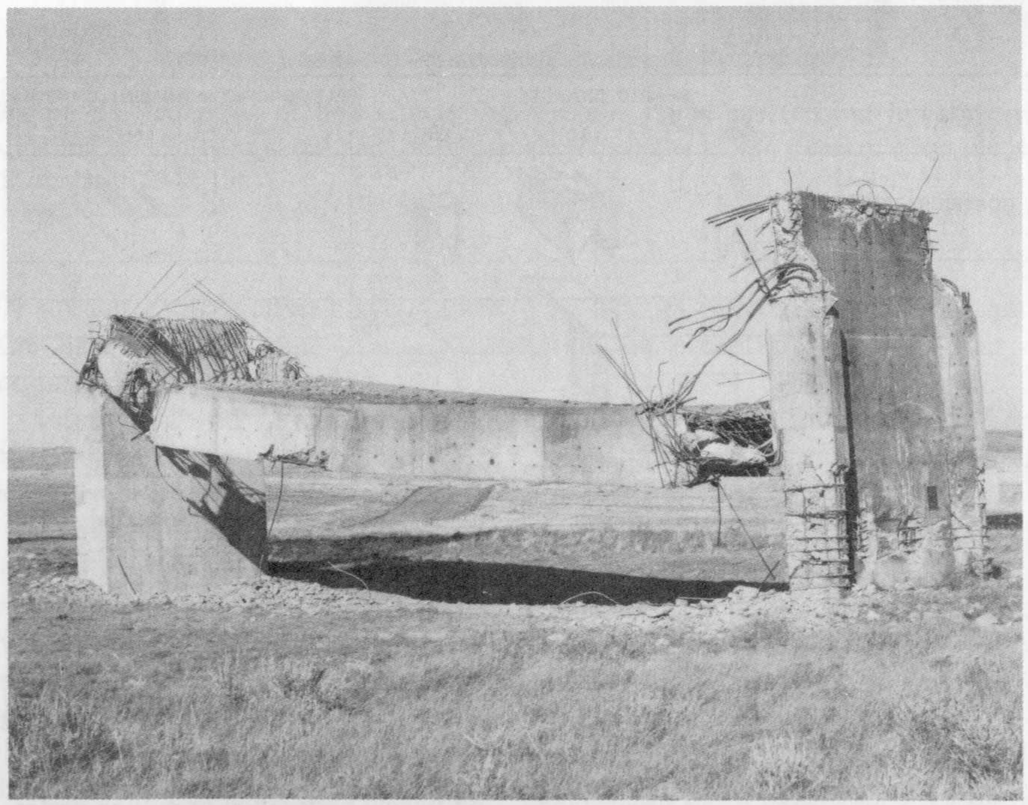

Figure 62. The bridge like structure after demolition (courtesy Defense Research Establishment Suffield).

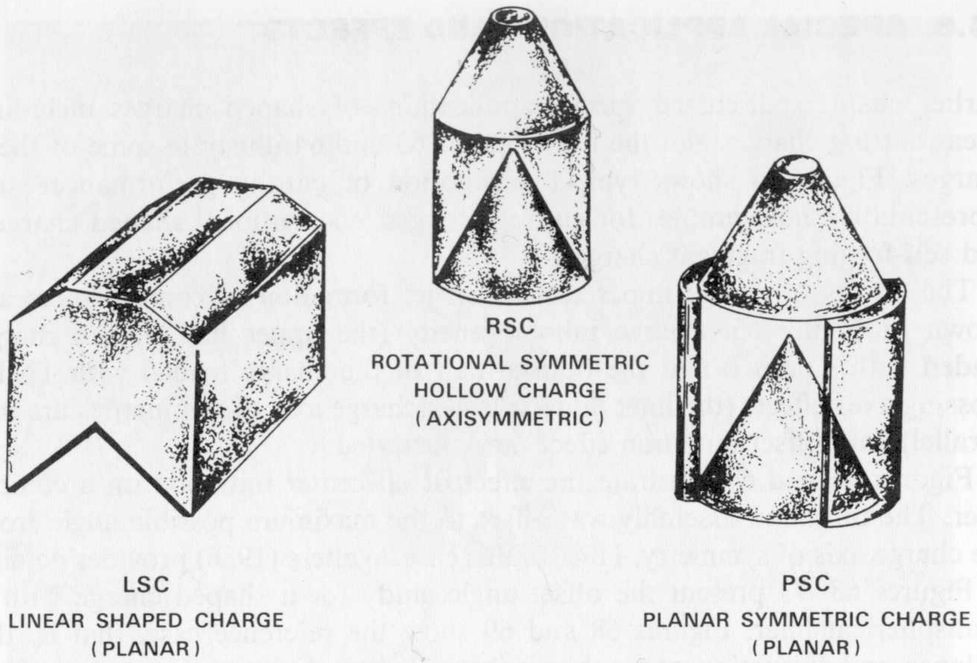

Figure 63. Typical shaped charges for penetration and cutting functions (Held 1980).

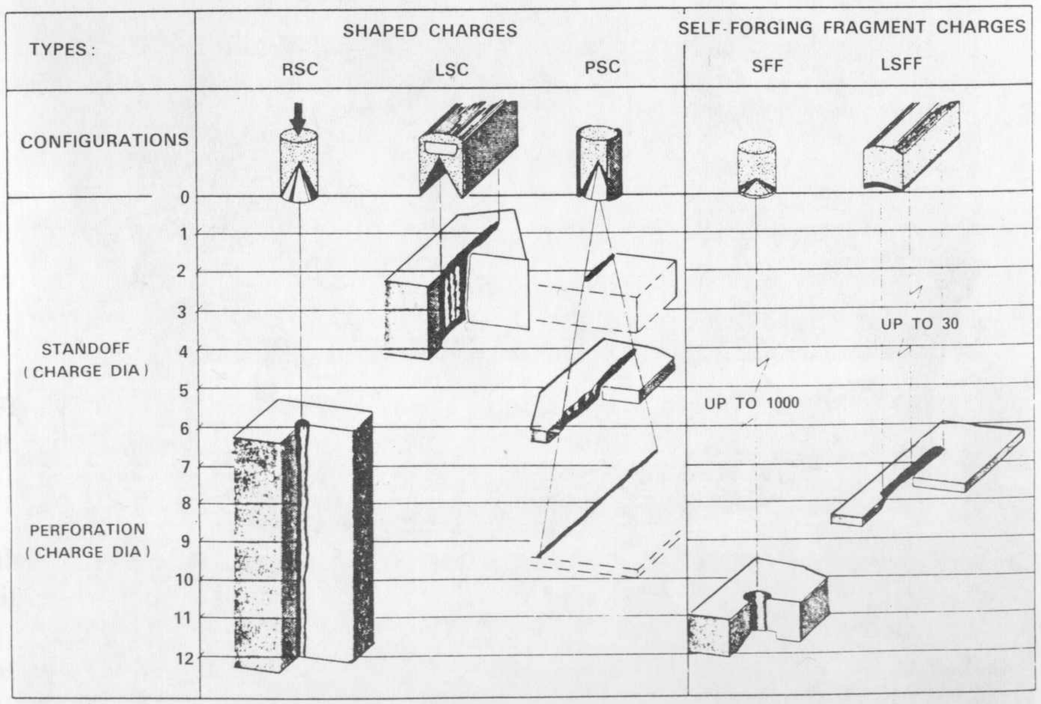

Figure 64. Comparison of the usual standoff and typical perforation or cutting performances and of hole profiles into mild steel for shaped charges and self-forging fragment charges (Held 1980).

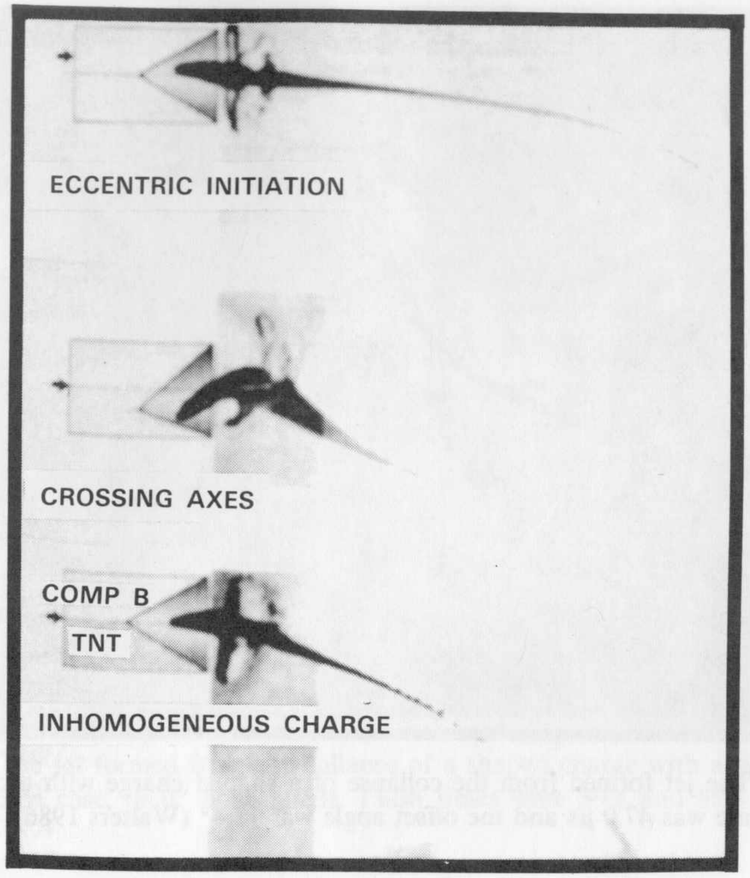

Figure 65. Examples of how charge imperfections, such as eccentric initiation or crossing axes of charge and liner or inhomogeneous high explosive charge effect the jet formation (Held 1983).

71 are for a small offset angle, namely 0.5°. The jet deflects only slightly, and the hemispherical liner is more tolerant of an eccentric initiation than a conical liner.

Figures 72 and 73 show the shaped charge with a hemispherical liner and the maximum possible offset angle, 17.35° in this case. Of course, the jet is severely bowed, as is the jet from a conical liner.

Figures 74 and 75 show the jet from a hemispherical shaped charge liner initiated using a dual-point initiation, that is, two initiation assemblies located at the maximum offset angle and 180° apart. Note how the jet "opens up" as witnessed by the hollow region in Figure 74. At later times (Figure 75) the jet splits and becomes an effective long standoff cutting charge. Again, details are given by Walters (1986).

The quality of the jet obtained from shaped charges with hemispherical, lead liners was studied by Walters et al. (1985). In particular, lead hemispheres of different wall thicknesses were examined under explosive loading conditions. The three wall thicknesses used in the study are given in Table 1,

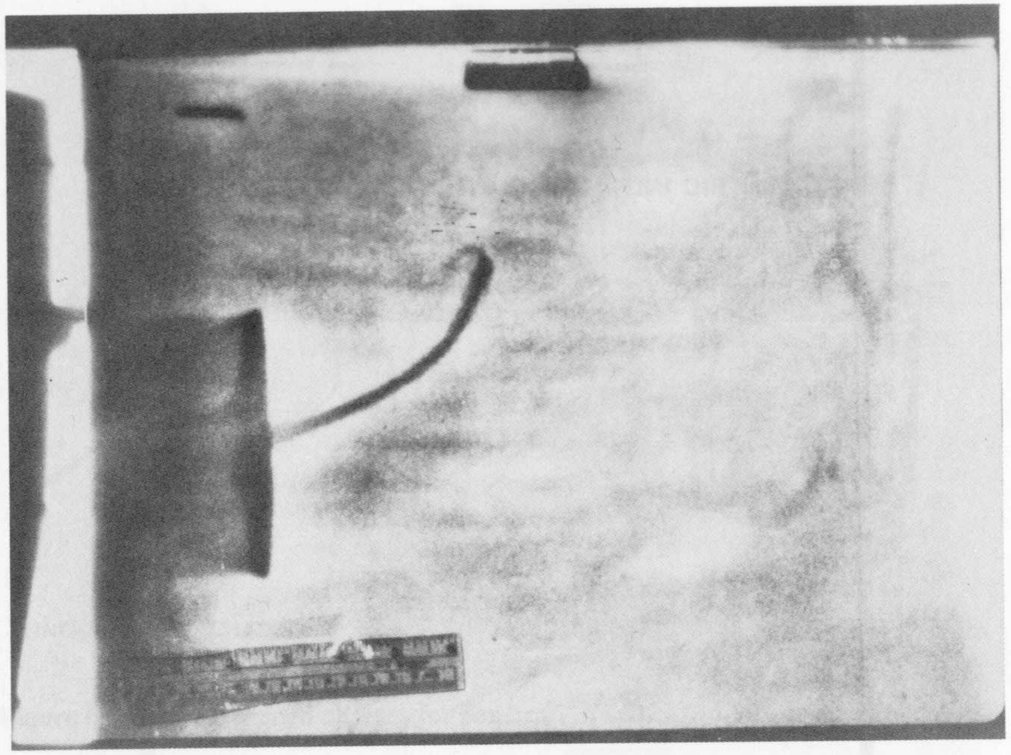

Figure 66. The jet formed from the collapse of a shaped charge with a conical liner. The flash time was 47.0 μs and the offset angle was 11.4° (Walters 1986).

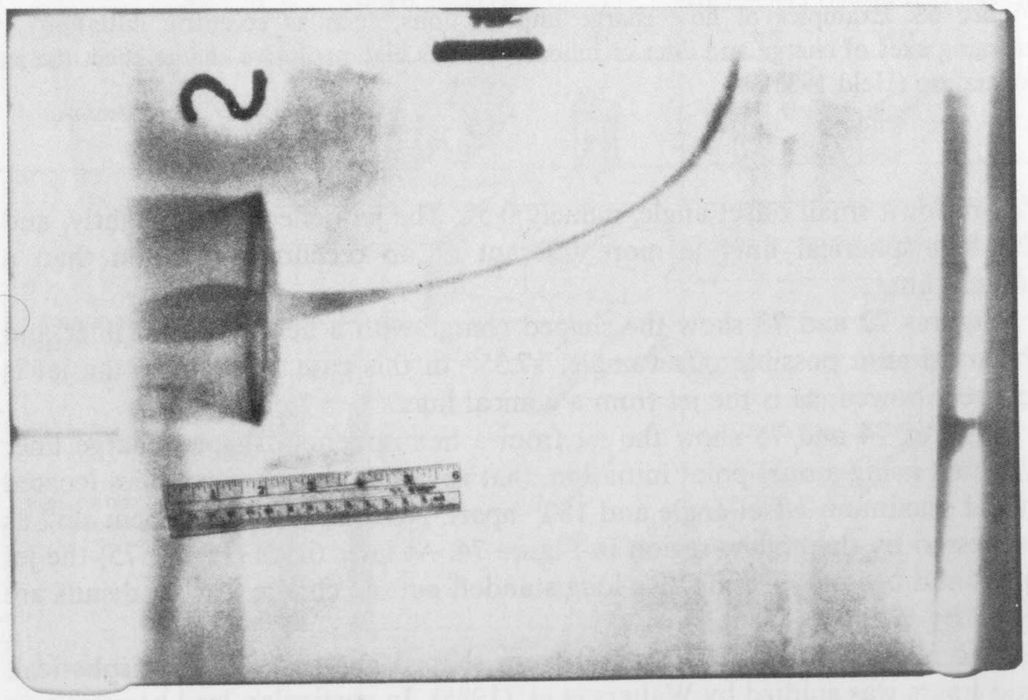

Figure 67. The jet formed from the collapse of a shaped charge with a conical liner. The flash time was 60.3 μs and the offset angle was 11.4° (Walters 1986).

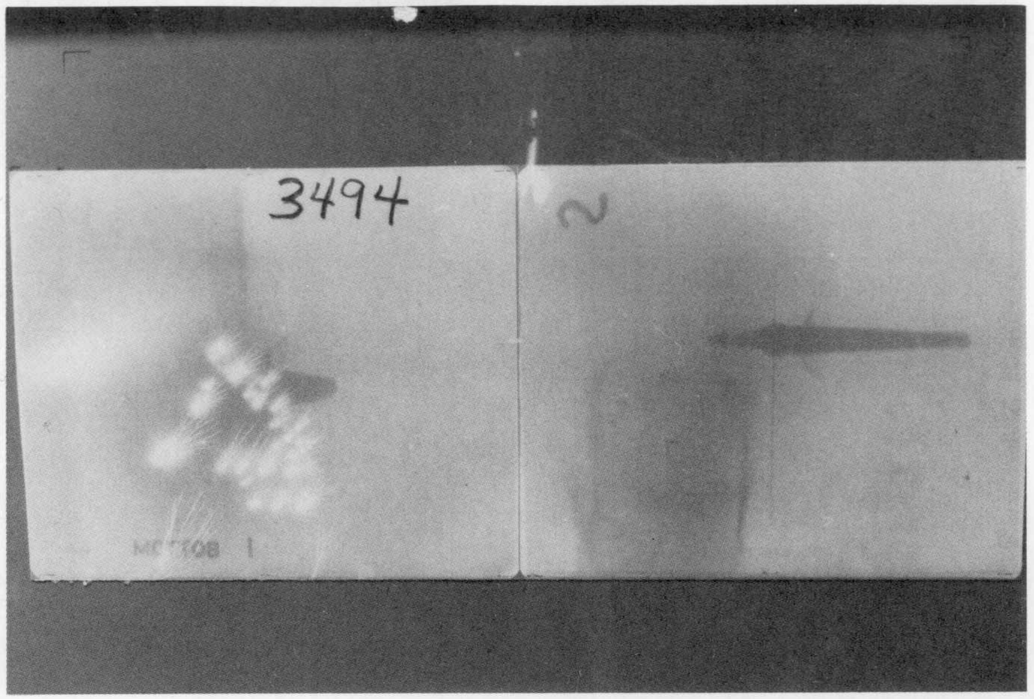

Figure 68. The jet formed from the collapse of a shaped charge with a hemispherical liner, reference case, or 0° offset angle. Flash times were 39.8 and 55.5 μs (Walters 1986).

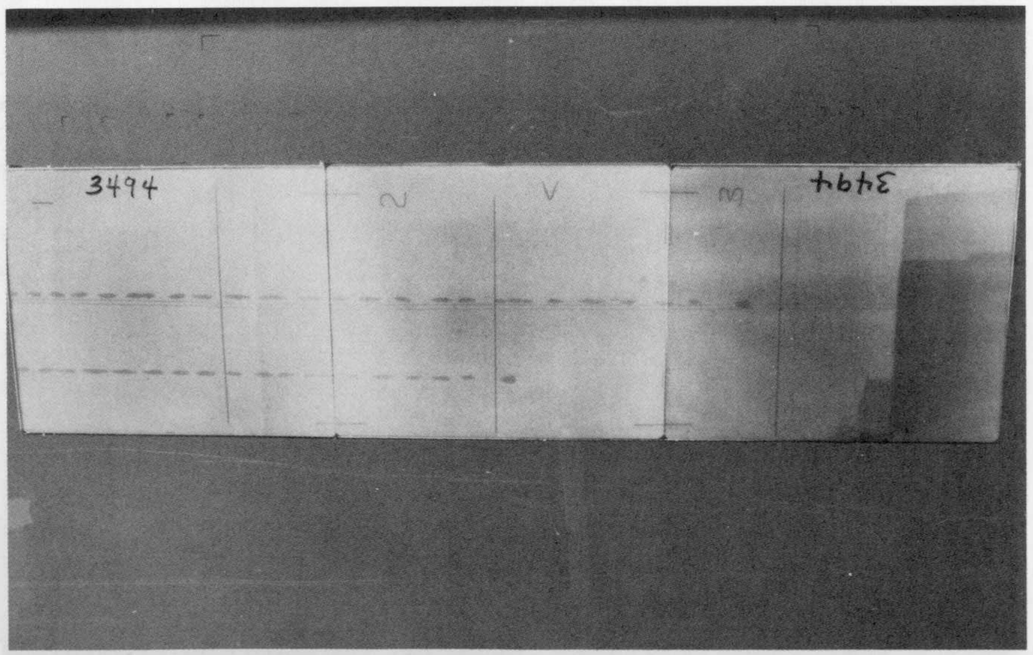

Figure 69. The jet formed from the collapse of a shaped charge with a hemispherical liner, reference case, or 0° offset angle. Flash times were 309.7 and 361.6 μs (Walters 1986).

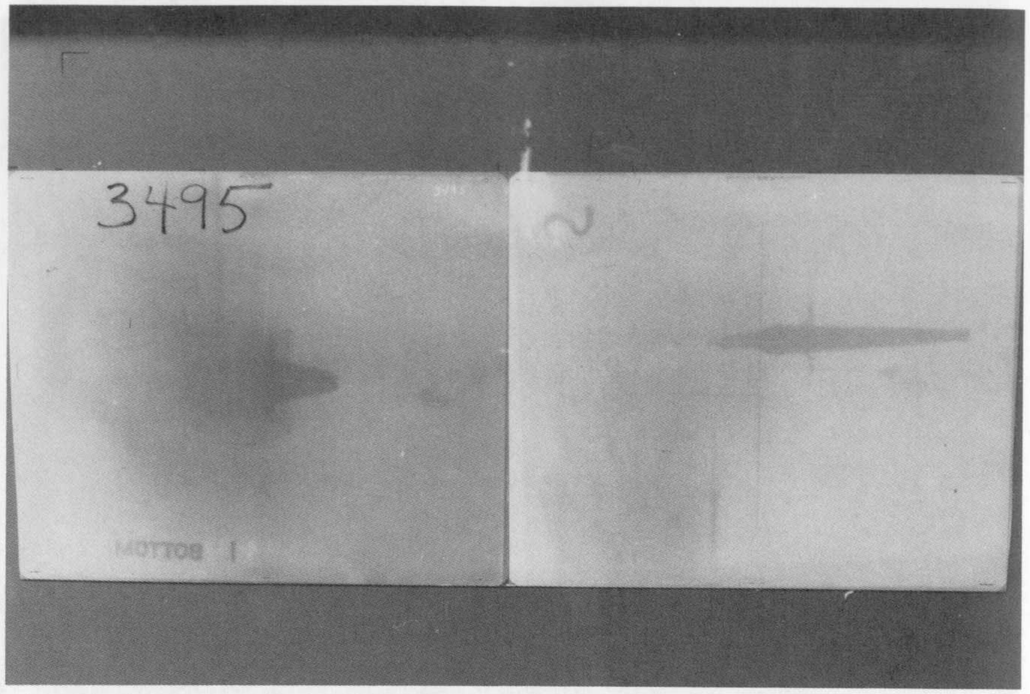

Figure 70. The jet formed from the collapse of a shaped charge with a hemispherical liner. The flash times were 39.9 and 55.5 μs. The offset angle was 0.5° (Walters 1986).

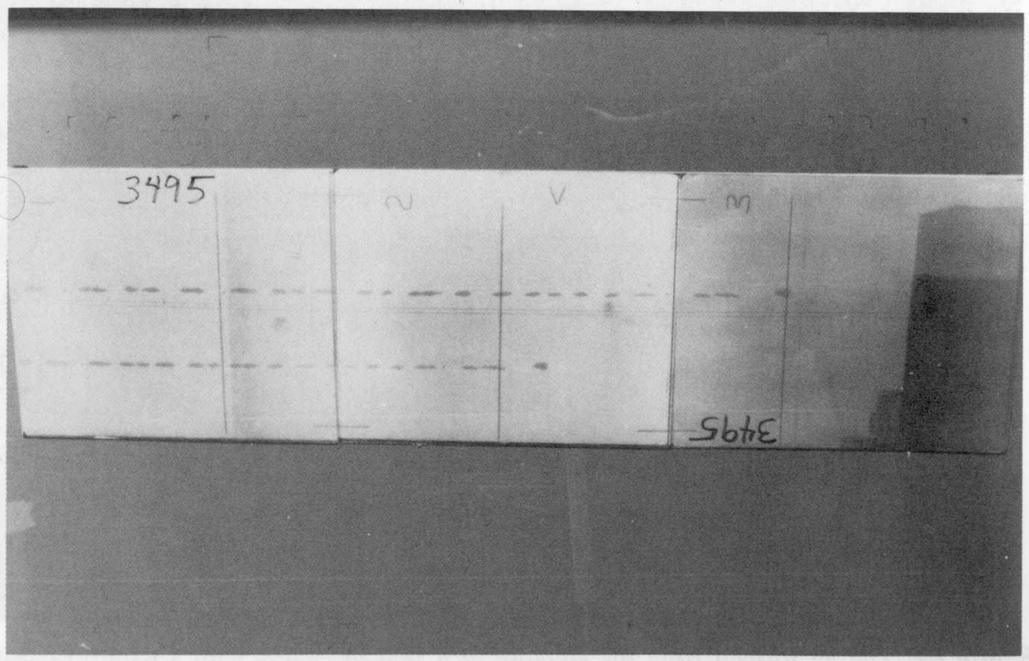

Figure 71. The jet formed from the collapse of a shaped charge with a hemispherical liner. The flash times were 309.3 and 361.6 μs. The offset angle was 0.5° (Walters 1986).

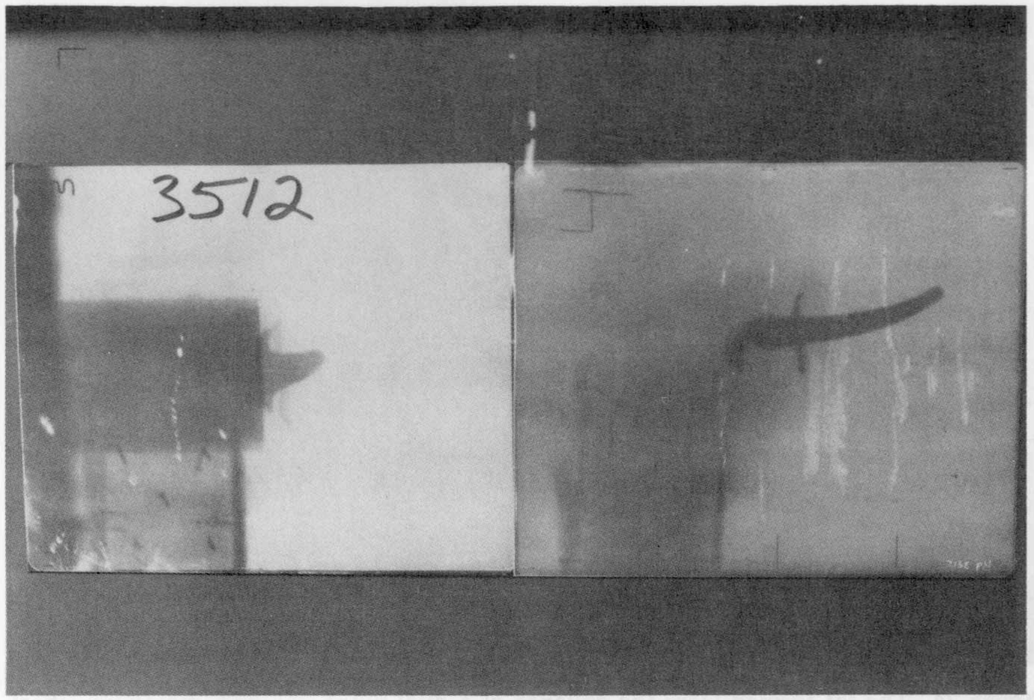

Figure 72. The jet formed from the collapse of a shaped charge with a hemispherical liner. The flash times were 39.4 and 54.4 μs. The offset angle was 17.35° (Walters 1986).

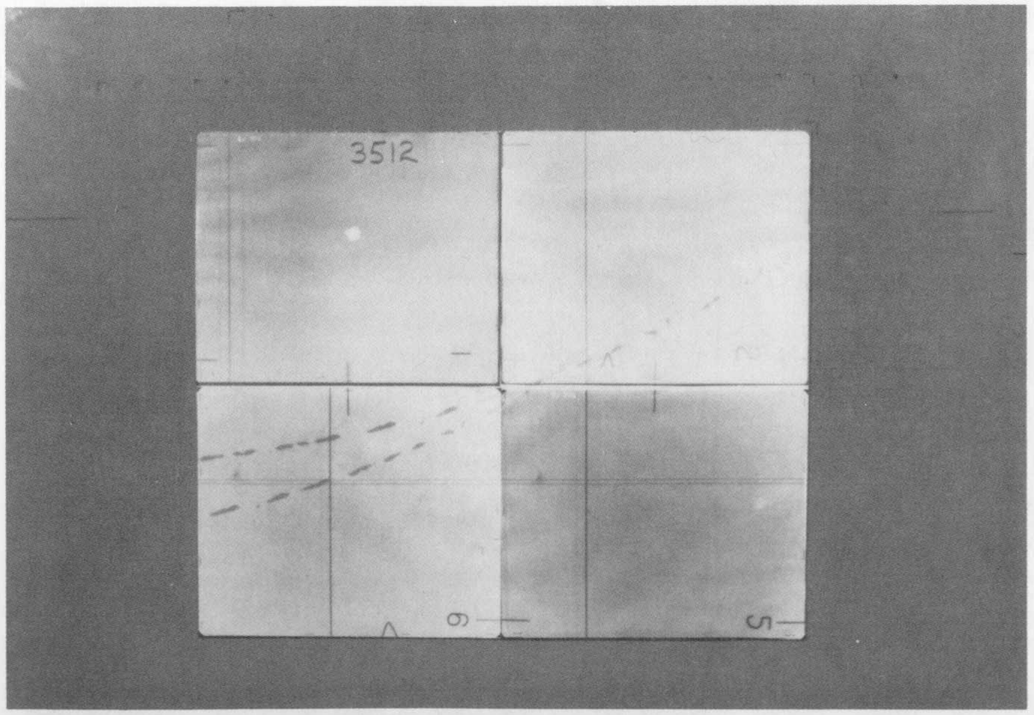

Figure 73. The jet formed from the collapse of a shaped charge with a hemispherical liner. The flash times were 310.1 and 368.1 μs. The offset angle was 17.35° (Walters 1986).

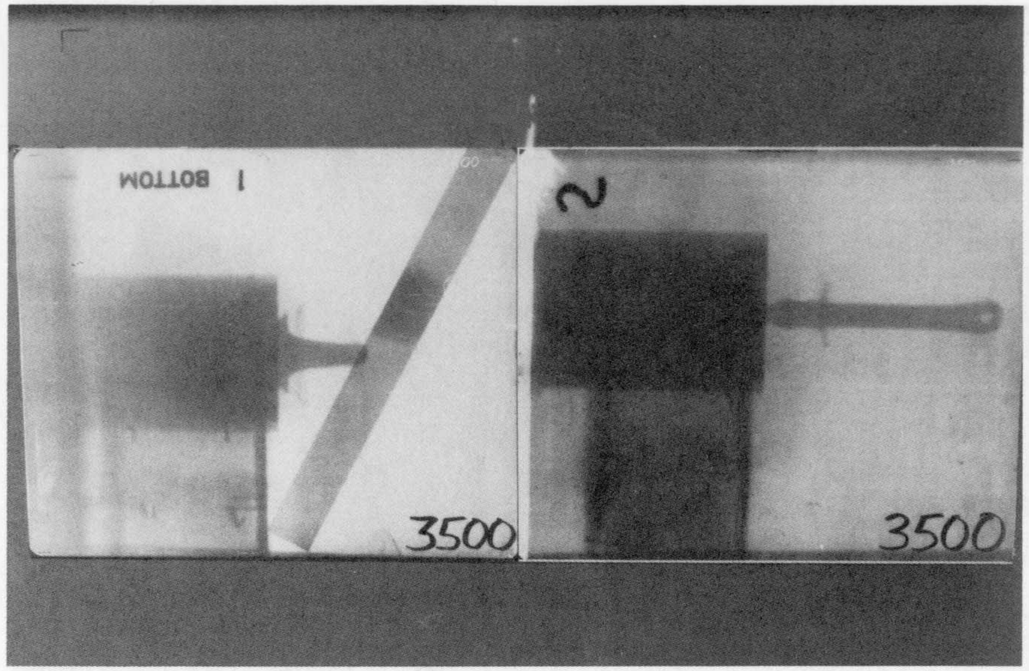

Figure 74. The jet formed from the collapse of a dual-point initiated, maximum offset angle, shaped charge with a hemispherical liner. The flash times were 39.9 and 55.7 μs (Walters 1986).

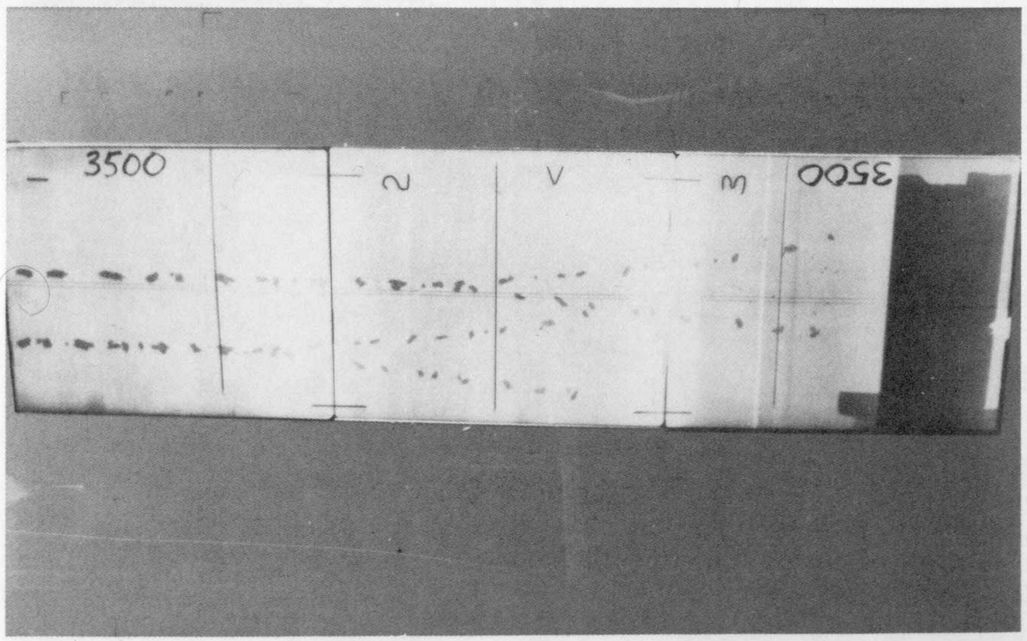

Figure 75. The jet formed from the collapse of a dual-point initiated, maximum offset angle, shaped charge with a hemispherical liner. The flash times were 309.6 and 361.6 μs (Walters 1986).

TABLE 1. Results of the Lead Hemispherical Liner Tests

Round Number	Liner	X-ray Flash Times (s)	Penetration (CD)	Jet Tip Velocity (km/s)
2950	127 mm diameter	408	0.81[a]	4.63
	2.97 mm	433		
	wall thickness	457.9		
	(2.34% wall)			
2951	127 mm diameter	418	3.13[a]	4.57
	3.81 mm wall	443		
	thickness (3% wall)	467.9		
2952	127 mm diameter	418.1	2.03[a]	4.0
	5.08 mm wall	442.9		
	thickness (4% wall)	467.9		
3157	50.8 mm diameter	483.2	0.07[b]	
	1.9 mm wall	505.3		
	thickness (3.75% wall)	524.6		

[a]At a 17.15 CD standoff into 50 mm stacked RHA plates.
[b]At a 31 CD standoff into 50 mm stacked RHA plates.

together with the liner diameter, resulting penetration depths, and the jet tip velocities. Flash radiographs depicting jets from the three configurations are shown in Figures 76 to 78. The associated wall thicknesses and flash times are listed in Table 1. Table 1 also lists the characteristics of a small-diameter lead hemispherical liner as scaled from the 127 mm liner, except that the wall thickness was 1.9 mm. This liner was tested to provide data regarding the rear of the jet. The delay times were altered to allow the tip of the jet to leave the field of view covered by the film in order to provide coverage of the jet tail. Radiographic data for this jet are shown in Figure 79. Details were given in Chapter 12.

Figures 76–78 indicate several interesting features. The same piece of film on the first channel (designated as 1 1, 1 11, and 1 111) was inadvertently used for both rounds 2951 and 2952 (Figures 77 and 78, respectively). Thus, the jets from both these rounds were superimposed on the first channel. Round 2951 has the longest jet, round 2952 the shortest. From the figures, it is evident that jet quality improves as the wall thickness increases (that is, the jet becomes less fluid, more solid in appearance as wall thickness increases). Correspondingly, the jet tip velocity decreases as wall thickness increases (Table 1) since the liner becomes more massive.

Note the obvious transition of the fluid characteristics of the jet as the wall thickness increases. The thin wall liner yields a jet with considerable amounts of vapor present. The vapor content of jets from thicker lines is markedly reduced. Most probably they are in a solid or liquid phase. Information regarding liquefaction of the jet can be obtained by firing the jet into a target

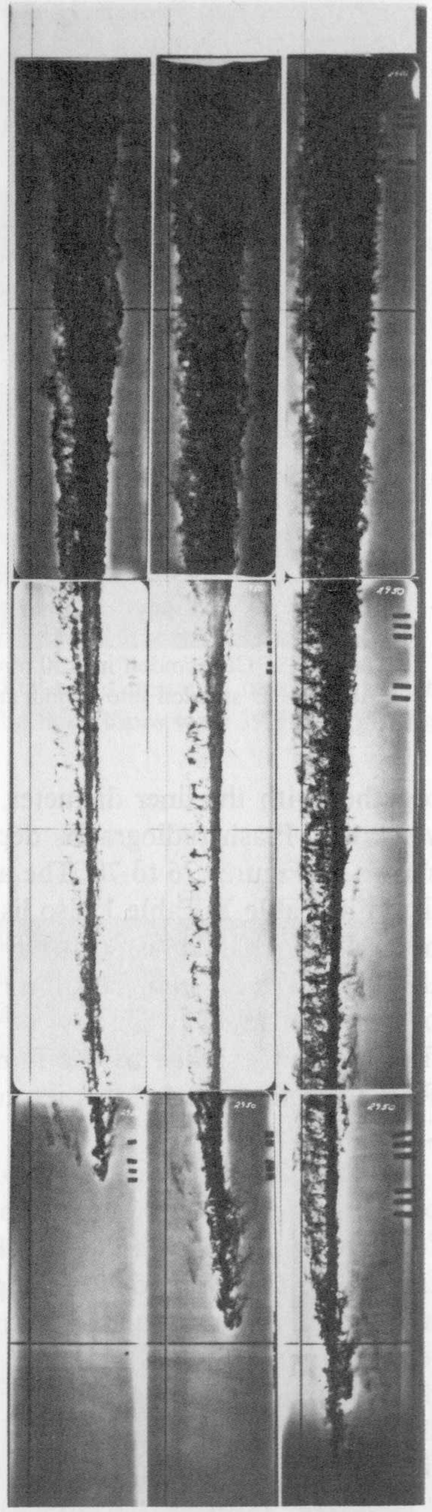

Figure 76. Free-flight flash radiograph of round 2950 of Table 1 (Walters et al. 1985).

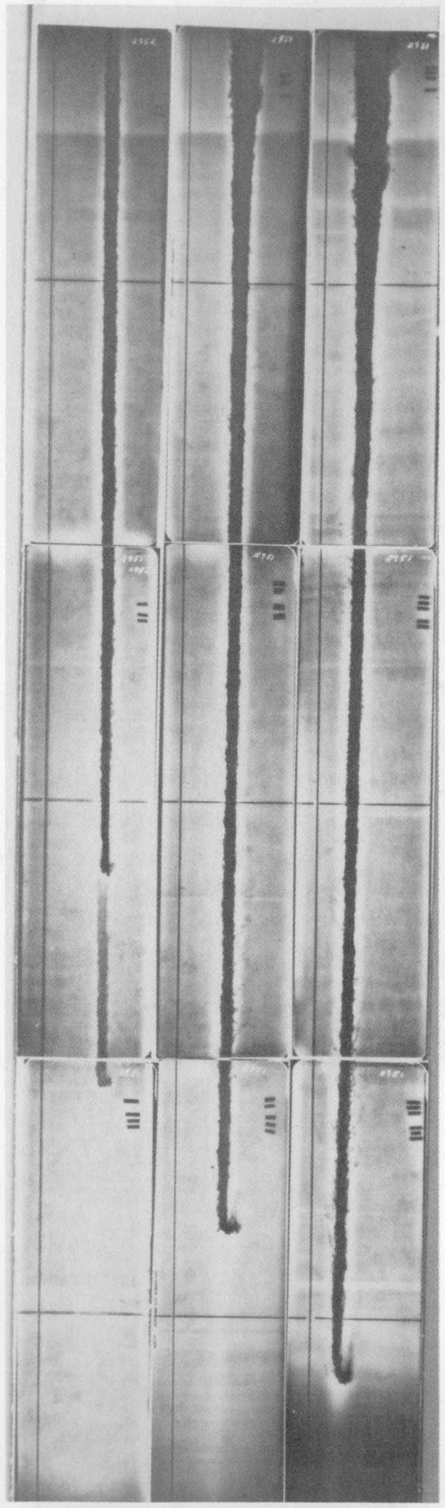

Figure 77. Free-flight flash radiograph of round 2951 of Table 1 (Walters et al. 1985).

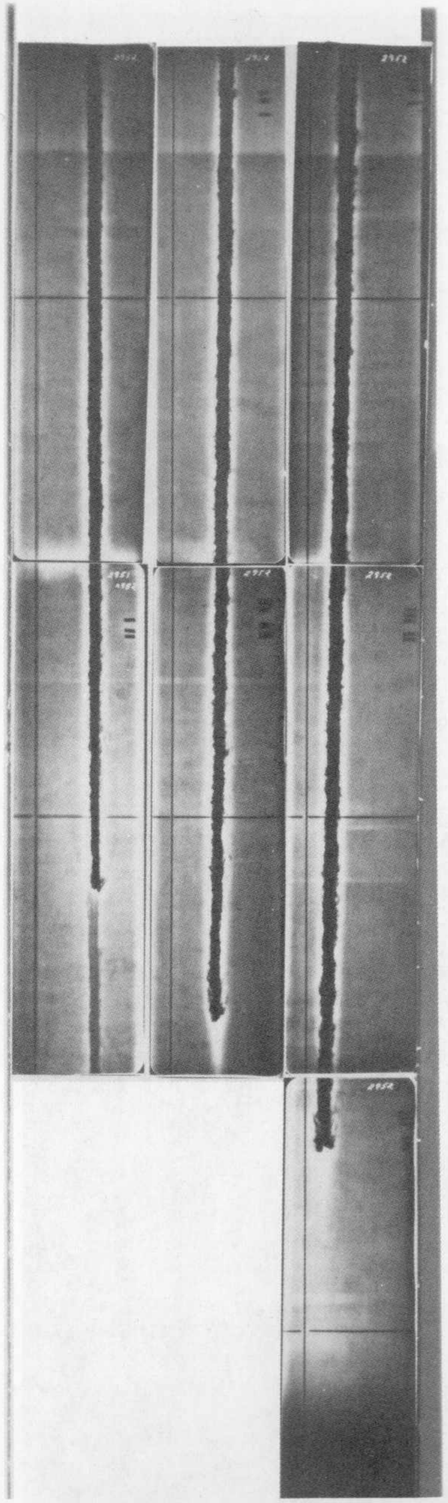

Figure 78. Free-flight flash radiograph of round 2952 of Table 1 (Walters et al. 1985).

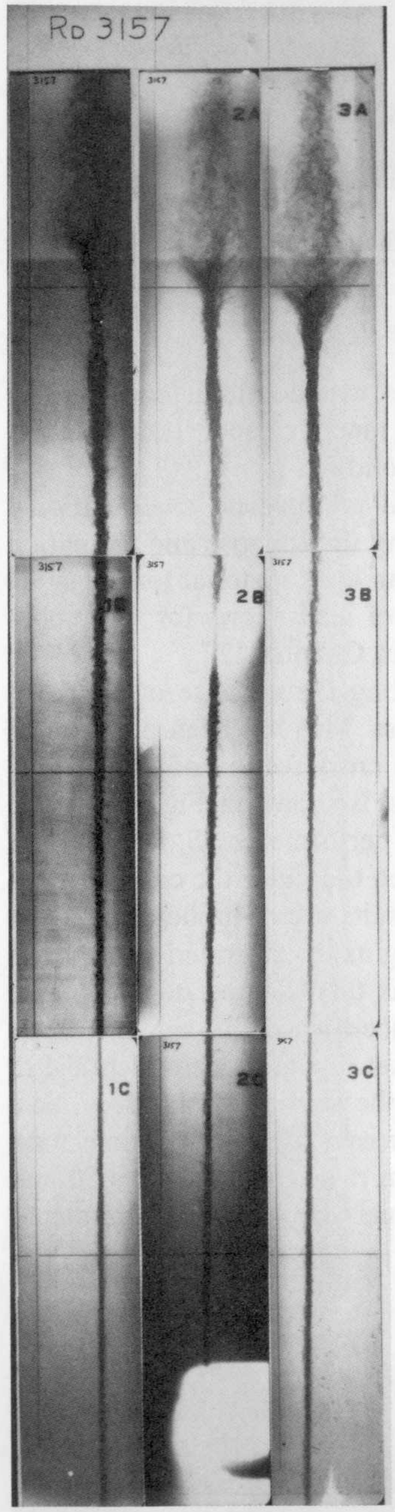

Figure 79. Free-flight flash radiograph of round 3157 of Table 1 (Walters et al. 1985).

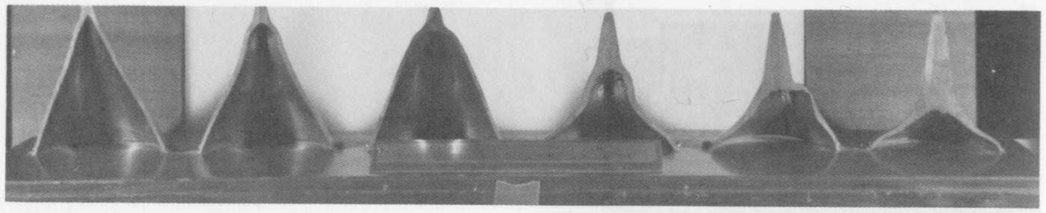

Figure 80. The partial collapse of a conical shaped charge liner, front view (courtesy BRL).

at an oblique angle to the jet axis. A liquid jet would exhibit considerable splatter against an oblique plate, whereas a much cleaner (and deeper) penetration channel would be obtained from a solid jet.

Walters et al. (1985) provide additional detail and present computational results that show the temperature gradients during the collapse and formation of the jets from the lead liners. Note that lead is an ideal material for the study of jet temperatures since the low melting point of lead allows for thermodynamic phase changes. Again, details were given in Chapter 12.

Earlier chapters described methods of inhibiting the collapse of a shaped charge liner in order to study the collapse process. This has been done, using various techniques, as discussed previously. The cross section of a recovered liner, with the collapse arrested at various stages, is shown in Figures 80 and 81. These liners were recovered in an experiment performed by S. Kronman of BRL many years ago. The exact procedure he used to inhibit the collapse is no longer known. However, these experimental results were duplicated by the authors by using a water column (of various heights) to surround the liner in lieu of a high explosive. An explosive pellet was then floated on top of the water column and detonated to propagate a shock wave through the water column. The recovered liners (captured in a bucket of water) were identical to those shown in Figures 80 and 81. Note that the partially collapsed liners agree with the computational pictures of jet formation and early time flash radiographs. Also note that the second liner from the right in Figures 80 and 81 was damaged during the recovery process, which explains its unsymmetric appearance.

Figure 81. The partial collapse of a conical shaped charge liner, rear view (courtesy BRL).

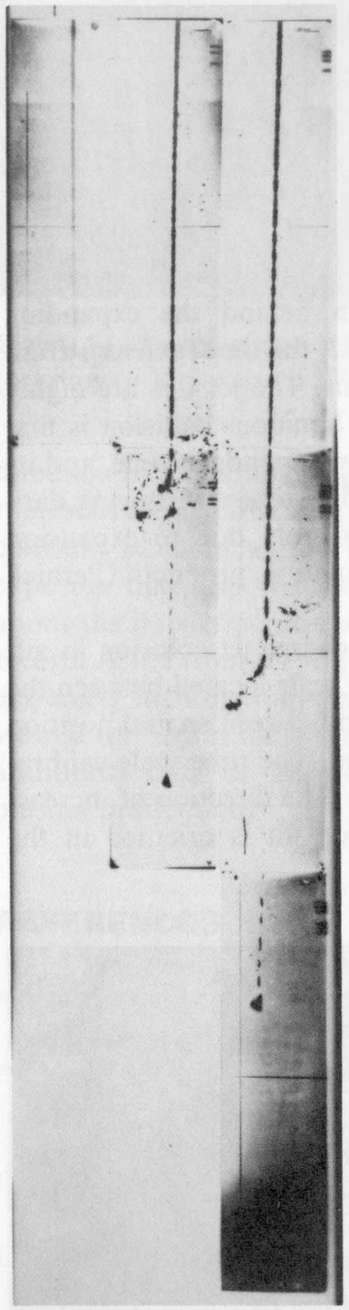

Figure 82. A shaped charge jet overtaking and colliding with another jet.

Hallquist, J. O. (1980), "User's Manual for DYNA2D—An Explicit Two-Dimensional Hydrodynamic Finite Element Code with Interactive Rezoning," Report UCID-18756, Lawrence Livermore National Laboratory.

Held, M. (1980), "Cutting Charges," *Proc. 5th Int. Symp. on Ballistics*, Toulouse, France, 16–18 April.

Held, M. (1983), "Characterizing Shaped Charge Performance by Stand-Off Behavior," *7th Int. Symp. on Ballistics*, The Hague, Netherlands, 19–21 April.

Held, M. (1986), "The Orthogonal-Synchro-Streak Technique as a Diagnostic Tool, Particularly for Shaped Charge Jets," *Propell. Explos. Pyrotech.*, *11*:170–175.

Hermann, J. W., Jr., Randers-Pehrson, G., and Berus, E. R. (1977), "Experimental and Analytical Investigation of Self-Forging Fragments for the Defeat of Armor at Extremely Long Standoff," *3rd Int. Symp. on Ballistics*, Karlsruhe, West Germany, 23–25 March.

Lukasik, S. J., and Pernick, B. J. (1965), "Plasma Production by Kinetic Impact," Davidson Laboratory Report 850, February.

Pernick, B. J. (1965), "Plasma Production by Kinetic Impact," Ph.D. Dissertation, Stevens Institute of Technology, Hoboken, NJ.

PI (1979), "SFF Design Technology," Physics International, California, January.

Simon, J., and DiPersio, R. (1972), "Jet Formation and Utilization," in *Proc. 12th Annual Symp. on Behavior and Utilization of Explosives in Engineering Design*, L. Davison and J. E. Kennedy (eds.), New Mexico Section of the ASME, March.

Walters, W. P. (1986), "Asymmetric Initiation of Shaped Charges," *Proc. of SECTAM XIII, The Southeastern Conference on Theoretical and Applied Mechanics*, Columbia, South Carolina, April.

Walters, W. P., Jonas, G. H., and Zukas, J. A. (1985), "Explosive Loading of Lead Hemispherical Liners," *Comput. Struct. 20*(1–3):615–621.

Walters, W. P., and Golaski, S. K. (1987), "Hemispherical and Conical Shaped Charge Liner Collapse and Jet Formation," Ballistic Research Laboratory Technical Report, ARBRL-TR-2781, February.

Weickert, C. A. (1986), "Spinning Self-Forging Fragments and Shaped Charges," Ph.D. Dissertation, Drexel University, Philadelphia, June.

INDEX